REGULATION OF PROTEIN TRANSLATION AND CELL CYCLE PROCESSES BY REVERSIBLE PROTEIN PHOSPHOYRYLATION IN RESPONSE TO DEHYDRATION IN THE AFRICAN CLAWED FROG

by

BRYAN EDWARD-DINH LUU

B. Sc Honours – Carleton University, 2011

A THESIS SUBMITTED TO THE FACULTY OF GRADUATE STUDIES AND RESEARCH IN PARTIAL FUFILLMENT OF THE REQUIREMENTS FOR THE DEGREE OF

MASTER OF SCIENCE

DEPARTMENT OF BIOLOGY

CARLETON UNIVERSITY

OTTAWA, ONTARIO, CANADA

The undersigned hereby recommend to the
Faculty of Graduate Studies and Research acceptance of the thesis entitled:

"Regulation of protein translation and cell cycle processes by reversible protein phosphorylation in response to dehydration in the African clawed frog"

Submitted by

BRYAN E. LUU

B.Sc. Honours – Carleton University, 2011

In partial fulfillment of the requirements for the degree of Master of Science

_____

Chair, Biology Department

_____

Thesis Supervisor

Carleton University, 2013

ABSTRACT

The primarily aquatic African clawed frog, *Xenopus laevis*, has adapted to endure substantial dehydration, partly by entering a state of hypometabolism. This thesis focuses on two processes targeted by the central protein kinase Akt (that is inhibited during dehydration) – protein translation and the cell cycle. Results suggest that dehydration leads to mTORC1 inhibition via PRAS40 activation in both liver and skeletal muscle, thereby suppressing protein synthesis. Suppression of Akt also allows activation of p21 and p27 cell cycle inhibitors to promote cell cycle arrest in liver. Analysis of multiple protein components shows that cell cycle arrest is actively facilitated in liver, but not in muscle. Regulation of liver kinases and phosphatases led to hypophosphorylation of Rb which inhibits E2F1-induced transcription of genes required for cell cycle progression. Overall, during dehydration, frogs suppress protein translation in liver and muscle, and show regulated cell cycle arrest in liver, a proliferative tissue.

ACKNOWLEDGEMENTS

I thank Dr. Ken Storey for allowing me to work and grow throughout the years in his lab. I thank him for his guidance when I needed it, but also opportunity he gave me to learn how to work independently. His lab has given me much more than I could have ever imagined while joining his research team back in 2009. During my time here, the opportunity to work with him has not only given me more opportunities as a science student, but also many successes outside the lab also. I truly believe that by giving me the opportunity to work with him, he has helped me more than he knows. I also thank Jan Storey for her endless time and energy which has went through to editing my papers and manuscripts. Working with her has gradually taught me how to become a better writer. I thank both Ken and Jan for the great conversations throughout the years that will help me not only in science, but in life. Also, I thank you both for being unbelievably patient for when I test your patience with deadlines. I don't think I would've been as patient if I were in your positions.

Thank you to the members of the Storey lab, past and present. I particularly thank Shannon Tessier and Kyle Biggar for their training and tutelage when I started out in the lab. I thank Jing, Mike, Anastasia, Amal, Ben, Oscar and Craig for answering questions I had while we worked together. I thank all Storey lab members for the memorable conversations we had and hope everyone succeeds as they get in there with their life goals.

Lastly, I thank my parents for their love which has allowed me to succeed in the past, present and future.

TABLE OF CONTENTS

LIST OF ABBREVIATIONS

4EBP	eIF4E binding protein
Akt	protein kinase B
APS	ammonium persulphate
ATP	adenosine triphosphate
BLAST	basic local alignment search tool
Cdc	cell division cycle protein
Cdk	cyclin dependent kinase
cDNA	complementary deoxyribonucleic acid
Chk	checkpoint kinase
Cip/kip	CDK interacting protein / kinase inhibitory protein
DEPC	diethylpyrocarbonate
dNTP	deoxynucleotide triphosphate
DTT	dithiolthreitol
E2F	E2 promoter binding factor
ECL	enhanced chemiluminescense
EDTA	ethylenediamine tetraacetic acid
eIF4E	eukaryotic translation initiation factor 4E
ELISA	enzyme-linked immunosorbent assay
EMSA	electrophoretic mobility shift assay
ERK	extracellular signal-regulated kinase
FOXO	forkhead box
G1	Gap phase 1

G2	Gap phase 2
GβL	G protein beta subunit like protein
GSK-3β	glycogen synthase kinase – 3 beta
GTP/GDP	guanosine tri-/diphosphate
HEPES	N-(2-hydroxyethyl) piperazine-(2-ethanesulfonic acid)
HRP	horseradish peroxidase
kDa	kiloDaltons
M	mitosis
MAPK	mitogen-activated protein kinase
MEK	MAPK kinase
miRNA	micro RNA
MRD	metabolic rate depression
mRNA	messenger RNA
mTOR	mechanistic/mammalian target of rapamycin
mTORC1/2	mTOR complex 1 or 2
MW	molecular weight
NCBI	National Center for Biotechnology Information
P70S6K	p70 s6 kinase
PAGE	polyacrylamide gel electrophoresis
PBS	phosphate-buffered saline
PCNA	proliferating cell nuclear antigen
PCR	polymerase chain reaction

PDK1	phosphoinositide-dependent kinase
PIP_3	phosphatidylinositol trisphosphate
PMSF	phenylmethanesulfonyl fluoride
PRAS40	Proline-rich Akt substrate of 40 kDa
PTEN	phosphatase and tensin homolog
PTM	post-translational modification
PVDF	polyvinylidine fluoride
Raptor	regulatory associated protein of mTOR
Ras	Rat sarcoma
Rb	retinoblastoma protein
Rheb	Ras homolog enriched in brain
RPP	reversible protein phosphorylation
RPTK	receptor protein tyrosine kinase
RT	reverse transcriptase
S	DNA synthesis phase/DNA replication phase
S6	ribosomal protein s6
SDS	sodium dodecyl sulphate
TAE	tris-acetate-ethylenediamine tetraacidic acid buffer
TBST	tris-buffered saline with Tween-20
TEMED	N,N,N',N'-tetra methylethylenediamine
TMB	3,3',5,5'-Tetramethylbenzidine
TRIS	tris (hydroxymethyl) aminomethane
TSC1/2	tuberous sclerosis 1 or 2

LIST OF TABLES AND FIGURES

threonine 308 in *X. laevis* liver. Histograms show mean values standardized to controls, with error bars showing standard error of the mean derived from n = 4 independent biological replicates. Statistically significant differences were determined by one-way ANOVA and Tukey's post-hoc test, and denoted by different letters above each bar, where $p < 0.05$.

Figure 3.4. Western blot analysis demonstrating the effect of medium and high dehydration on Akt protein expression, nuclear localization, and phosphorylation at serine 473 and threonine 308 in *X. laevis* skeletal muscle. Other information as in Figure 3.3.

Figure 3.5. Western blot analysis demonstrating the effect of medium and high dehydration on PDK1 and PTEN protein expression, PDK1 phosphorylation at serine 241, PTEN phosphorylation serine 380/threonine 382/383, and non-phosphorylated PTEN in *Xenopus laevis* liver. Other information as in Figure 3.3.

Figure 3.6. Western blot analysis demonstrating the effect of medium and high dehydration on PDK1 and PTEN protein expression, PDK1 phosphorylation at serine 241, PTEN phosphorylation serine 380/threonine 382/383, and non-phosphorylated PTEN in *Xenopus laevis* skeletal muscle. Other information as in Figure 3.3.

Figure 3.7. Western blot analysis demonstrating the effect of medium and high dehydration on protein expression and phosphorylation of mTOR, PRAS40, Raptor and GβL in *X. laevis* liver. Phosphorylation sites were serine 2448 for mTOR, threonine 246 for PRAS40, and serine 863 for Raptor. Other information as in Figure 3.3.

Figure 3.8. Western blot analysis demonstrating the effect of medium and high dehydration on protein expression and phosphorylation of mTOR, PRAS40, Raptor and GβL in *Xenopus laevis* skeletal muscle. Phosphorylation sites were serine 2448 for mTOR, threonine 246 for PRAS40, and serine 863 for Raptor. Other information as in Figure 3.3.

Figure 3.9. Western blot analysis demonstrating the effect of medium and high dehydration on protein expression and phosphorylation of 4EBP, eIF4E, p70 s6k and ribosomal s6 protein in *X. laevis* liver. Phosphorylation sites were threonine 37/46 for 4EBP, threonine 389 for PRAS40, and serine 235/236 for ribosomal protein s6. Other information as in Figure 3.3.

Figure 3.10. Western blot analysis demonstrating the effect of medium and high dehydration on protein expression and phosphorylation of 4EBP, eIF4E, p70 s6k and ribosomal s6 protein in *X. laevis* skeletal muscle. Phosphorylation sites were threonine 37/46 for 4EBP, threonine 389 for PRAS40, and serine 235/236 for ribosomal protein s6. Other information as in Figure 3.3.

Figure 3.11. Western blot analysis demonstrating the effect of medium and high dehydration on p21 and p27 protein expression and phosphorylation at threonine 145 (p-p21) and serine 187 (p-p27) in *.X. laevis* liver. Other information as in Figure 3.3.

Figure 3.12. Western blot analysis demonstrating the effect of medium and high dehydration on p21 and p27 protein expression and phosphorylation at threonine 145 (p-p21) and serine 187 (p-p27) in *Xenopus laevis* skeletal muscle. Other information as in Figure 3.3.

Figure 3.13. Western blot analysis demonstrating the effect of medium and high dehydration on GSK-3β protein expression and phosphorylation at serine 9 in *X. laevis* liver and skeletal muscle. Other information as in Figure 3.3.

Figure 3.14. Western blot analysis demonstrating the effect of medium and high dehydration on FoxO1 and FoxO4 protein expression and phosphorylation at serine 319, 256 (FoxO1) and serine 193 (FoxO4) in *Xenopus laevis* liver. Other information as in Figure 3.3.

Figure 3.15. Western blot analysis demonstrating the effect of medium and high dehydration on FoxO1 and FoxO4 protein expression and phosphorylation at serine 319, 256 (FoxO1) and serine 193 (FoxO4) in *Xenopus laevis* skeletal muscle. Other information as in Figure 3.3.

Figure 3.16. Amino acid sequence alignment analysis between *X. laevis*, *X. tropicalis, H. sapiens and R. norvegicus* for proteins TSC2, Akt and 4EBP done on EMBL-EBI's Clustal Omega program. Of interest are the phosphorylated sites threonine 1462 in TSC2, serine 473 in Akt, and threonine 37/46 in 4EBP (boxed in red). These residues, when phosphorylated, are detected by antibodies listed in Table 3.2. However, threonine 1462 in *Xenopus* TSC2 does not appear to be conserved when compared to the human TSC2 protein, which explains why it failed to cross-react with an anti-phospho-TSC2 (T1462) antibody designed for humans and mice.

Figure 4.1a. Current understanding of the events during the G1 to S phase of the mammalian cell cycle in the literature. E2F1 is permitted to induce gene expression of targets required for cell cycle progression only when CDKs are capable of forming active complexes with their respective cyclin protein targets and then hyperphosphorylate and suppress Rb allowing E2F1 to be released.

Figure 4.1b. Summary of the accepted pathway by which cell cycle progression occurs in mammalian models. Kinase activity by CDKs and phosphatase activity by cdc25s play key roles in allowing E2F1 to signal for expression of genes required for cell cycle progression.

Figure 4.2. Western blot analysis demonstrating the effect of medium and high dehydration on the protein expression of E2F1 and E2F4 in *Xenopus laevis* liver and skeletal muscle. Histograms show mean values standardized to controls, where error bars

represent the standard error of the mean derived from n = 4 independent biological replicates. Statistically significant differences were assessed by one-way ANOVA with Tukey's post-hoc test, and are denoted by different letters above each bar, where $p < 0.05$.

Figure 4.3. Western blot analysis demonstrating the effect of medium and high dehydration on the nuclear localization of E2F1 and E2F4 in *Xenopus laevis* liver and skeletal muscle. Other information as in Figure 4.2.

Figure 4.4. Electrophoretic mobility shift assay validating the binding of the DNA probe to protein. Negative controls (no DNA probe, no protein) were run and resulted in no visible protein/DNA shift. Reactions run with higher protein amounts resulted in larger shift bands. Antibody (anti-E2F1) shift reaction theoretically increases the size of the complex to validate that the DNA probe indeed targets *X. laevis* E2F protein.

Figure 4.5. A modified TF/DNA ELISA was used to determine relative binding of E2F1 and E2F4 (from *Xenopus laevis* nuclear extracts) to the E2F binding domain. Analysis was performed to demonstrate the effects of medium and high dehydration on DNA binding in both liver and skeletal muscle. Other information as in Figure 4.2.

Figure 4.6. Western blot analysis demonstrating the effect of medium and high dehydration on posttranslational modifications of Rb and protein expression of p130 (Rb2) in *Xenopus laevis* liver. Other information as in Figure 4.2.

Figure 4.7. Western blot analysis demonstrating the effect of medium and high dehydration on posttranslational modifications of Rb and protein expression of p130 (Rb2) in *Xenopus laevis* skeletal muscle. Other information as in Figure 4.2.

Figure 4.8. Western blot analysis demonstrating the effect of medium and high dehydration on the nuclear localization of posttranslationally modified Rb levels and p130 (Rb2) protein levels in *Xenopus laevis* liver. Other information as in Figure 4.2.

Figure 4.9. Western blot analysis demonstrating the effect of medium and high dehydration on the nuclear localization of posttranslationally modified Rb levels and p130 (Rb2) protein levels in *Xenopus laevis* skeletal muscle. Other information as in Figure 4.2.

Figure 4.10. Western blot analysis demonstrating the effect of medium and high dehydration on the protein expression of Cyclins A, B, D and E as well as phospho-cyclin D (Thr 286) in *Xenopus laevis* liver. Other information as in Figure 4.2.

Figure 4.11. Western blot analysis demonstrating the effect of medium and high dehydration on the protein expression of Cyclins A, B, D and E as well as phospho-cyclin D (Thr 286) in *Xenopus laevis* skeletal muscle. Other information as in Figure 4.2.

Figure 4.12. Western blot analysis demonstrating the effect of medium and high dehydration on the nuclear localization of cyclins A, B, D and E as well as phosphorylated cyclin D (Thr 286) in *Xenopus laevis* liver. Other information as in Figure 4.2.

Figure 4.13. Western blot analysis demonstrating the effect of medium and high dehydration on the nuclear localization of cyclins A, B, D and E as well as phosphorylated cyclin D (Thr 286) in *Xenopus laevis* skeletal muscle. Other information as in Figure 4.2.

Figure 4.14. Western blot analysis demonstrating the effect of medium and high dehydration on the protein expression of CDK1/CDC2, CDK2, CDK4, and CDK6 in *Xenopus laevis* liver. Other information as in Figure 4.2.

Figure 4.15. Western blot analysis demonstrating the effect of medium and high dehydration on the protein expression of CDK1/CDC2, CDK2, CDK4, and CDK6 in *Xenopus laevis* skeletal muscle. Other information as in Figure 4.2.

Figure 4.16. Western blot analysis demonstrating the effect of medium and high dehydration on the nuclear localization of CDK1/CDC2, CDK2, CDK4, and CDK6 in *Xenopus laevis* liver. Other information as in Figure 4.2.

Figure 4.17. Western blot analysis demonstrating the effect of medium and high dehydration on the nuclear localization of CDK1/CDC2, CDK2, CDK4, and CDK6 in *Xenopus laevis* skeletal muscle. Other information as in Figure 4.2.

Figure 4.18. Western blot analysis demonstrating the effect of medium and high dehydration on the protein expression and phosphorylation of cdc25a (serine 76) and cdc25c (serine 216) in *Xenopus laevis* liver. Other information as in Figure 4.2.

Figure 4.19. Western blot analysis demonstrating the effect of medium and high dehydration on the protein expression and phosphorylation of cdc25a (serine 76) and cdc25c (serine 216) in *Xenopus laevis* muscle. Other information as in Figure 4.2.

Figure 4.20. Western blot analysis demonstrating the effect of medium and high dehydration on the nuclear localization of total cdc25a, phospho-cdc25a (serine 76), total cdc25c and phospho-cdc25c (serine 216) in *Xenopus laevis* liver. Other information as in Figure 4.2.

Figure 4.21. Western blot analysis demonstrating the effect of medium and high dehydration on the nuclear localization of total cdc25a, phospho-cdc25a (serine 76), total cdc25c and phospho-cdc25c (serine 216) in *Xenopus laevis* skeletal muscle. Other information as in Figure 4.2. **Figure 4.22.** Western blot and PCR analysis demonstrating the effect of medium and high dehydration on relative PCNA protein levels and *pcna* mRNA transcript levels in *Xenopus laevis* liver and skeletal muscle. Band densities for *pcna* transcripts were normalized against bands for alpha-tubulin amplified from the same RNA samples. Other information as in Figure 4.2.

CHAPTER 1

GENERAL INTRODUCTION

1.1 Animal adaptations to environmental stress

Each animal species has evolved to optimally thrive and reproduce in the habitat in which it lives. However, many animals live in environments that can change suddenly, either randomly or on a seasonal basis, creating conditions that can be detrimentally stressful or even lethal to the animal. Through evolution, animals have developed various adaptations which may increase their chances of survival through periods of extreme environmental stress. This thesis is focused on amphibian estivation. Estivation is a survival strategy involving dormancy to withstand periods of drought, high temperatures and low food availability (Secor and Lignot, 2010). Certain anurans have developed the ability to survive extreme summer climates. The spade-foot toad, *Scaphiopus couchii*, is found in the Californian desert (Carvalho *et al*., 2010). However, researchers have noted that these anurans are found in environments that appear to be "entirely too hot and dry for any species of amphibian to survive successfully" (Mayhew, 1965). Specifically, these amphibians were found to withstand scant rain, several consecutive days with air temperatures above 40ºC, and peak temperatures of 50ºC. During periods of estivation, spade-foot toads do not estivate in random locations, but bury themselves in moist areas where temperature is more moderate and humidity lasts longer (Carvalho *et al*., 2010). Throughout these periods of estivation, anurans encounter various problems. One obvious problem is that while inactive, the animals are subjected to lack of food (Secor and Lignot, 2010). However, they have adapted accordingly to meet the challenges of disuse atrophy (Hudson and Franklin, 2002). Furthermore, when buried in drying mud, oxygen intake through the skin becomes problematic as skin exposure to the air is reduced

(Carvalho *et al.*, 2010). Therefore, studies have made it clear that estivating anurans make key animal models for studying adaptations to extreme environmental stresses.

1.2 The dehydration-resistant African clawed frog *Xenopus laevis*

The African clawed frog, *Xenopus laevis*, is a primarily aquatic frog that was described in 1803 by Daudin. Wagler and Daudin both named the frog *Xenopus* for its peculiar clawed foot and *laevis* for its smooth body (Deuchar, 1975). This frog evolved a flat body which is advantageous for swimming, but its hind legs which extend sideways are not ideal for supporting its body weight on land. Its eyes are present dorsally, which suggests that attention is paid above for potential prey/predators while they dwell at the bottom of bodies of water. African clawed frogs have no tongue, and have well-developed ears which are protected by a layer of skin (Cannatella and De Sa, 1993; Deuchar, 1975). However, biologists believe the cartilaginous discs present underneath the skin behind the eyes may be used to receive vibrations carried through the water as they are more robust than eardrums (Deuchar, 1975). These physiological traits support the argument that these frogs are most comfortable in aquatic environments.

Despite preferring aquatic environments, the African clawed frog lives in the sub-Saharan areas where their swamps, lakes, and rivers are subject to seasonal drought (Tinsley and Kobel, 1996). Being aquatic animals, dehydration stress is a major stress factor that impacts their survival chances in the dry season. Two main options are available to the frogs as their ponds dry out. Noctural migration to other bodies of water can occur, but as noted above, the frogs are poor at terrestrial locomotion. The alternative

is to burrow down into the wet mud of drying ponds to reduce the amount of water lost through their skin. Dehydrating *Xenopus* also excrete mucous over their skin in order to help retard water loss across their permeable skin (Hillman, 1978). In addition to increasing soil-skin contact, these frogs also elevate the concentrations of low molecular weight osmolytes in their tissues to reduce their water potential (Feder and Burggren, 1992). Water potential is a measure of the tendency of water to move from one area to another due to osmosis. By increasing the amount of osmolytes in their bodies, they will be losing water at a slower rate. The main osmolyte used by amphibians to reduce water loss during estivation is urea (Grundy and Storey, 1994). The dehydrating frog increases urea by reducing the excretion of ammonia (the nitrogenous waste that they produce in water) and instead converting ammonia to urea, supported by up-regulating the enzymes of the urea cycle (Balinsky *et al*., 1961; Janssens, 1964; Seiter *et al*., 1978). Previous studies of *Xenopus* naturally dehydrating for 2-3 months revealed that plasma amino acid levels tripled, along with a 15-20 fold increase in plasma urea concentration (Balinsky *et al*., 1967). Researchers also noted that carbamoyl phosphate synthase (CPS), the rate-limiting enzyme in the urea cycle, had its activity increase 6-fold in the liver of dehydrating frogs (Balinsky *et al*., 1967). Ultimately, under dessicating conditions, African clawed frogs increase their urea concentrations as an adaptation to prevent dehydration. As an aquatic animal with resilient coping strategies to dehydration, *X. laevis* is a key animal model to study signal transduction pathways related to dehydration stress.

1.3 Introduction to metabolic rate depression

Metabolic rate depression (MRD) is a coping strategy used by many organisms to extend survival time under harsh environmental conditions. MRD is common to animal survival phenomena including torpor, hibernation, anaerobiosis, diapause, freeze tolerance, and estivation (Storey and Storey, 2010). Estivation is generally characterized as a state of torpor used by animals responding to arid conditions, often also accompanied by high temperatures and low food availability. A variety of frogs and toads living in seasonally arid environments are well known to estivate, often for 9-10 months of the year (Feder and Burggren, 1992, Carvalho *et al*., 2010; Secor and Lignot, 2010). All of these animals decrease their metabolic demands over extended periods of time when the environment presents harsh conditions. Numerous aspects of the biochemical regulation of MRD have been thoroughly studied and are triggered/coordinated by signal transduction pathways. One major mechanism of controlling transitions to/from the hypometabolic state is by altering the activity states of key enzymes in cellular pathways by reversible protein phosphorylation (RPP; Storey and Storey, 2004). The process of RPP is facilitated by protein kinases which phosphorylate target proteins, and protein phosphatases, which remove phosphate groups. For example, RPP plays a key role in facilitating signal transduction during MRD via the mitogen-activated protein kinase (MAPK) signaling cascade (Cowan and Storey, 2003). This signal transduction cascade begins at the cell membrane where an external signal triggers a receptor protein tyrosine kinase (RPTK) to active a three-stage cascade. The RPTK then activates a MAPK kinase kinase (MAPKKK), which activates a MAPK kinase (MAPKK), and then finally a MAPK in a serial fashion. This serial cascade allows for a signal amplification of about

1000-fold (Cowen and Storey, 2003). RPP has since been shown to play a key role in regulating stress-induced signal responses in multiple tissues and animals (Greenway and Storey, 2000a; Greenway and Storey, 2000b; MacDonald and Storey, 2005; Larade and Storey, 2006). Facilitation of MRD by RPP has also been explored in *X. laevis* (Malik and Storey, 2009).

Recent reviews suggest that another key theme across animals that undergo MRD is the global suppression of gene expression and protein translation. Transcription and translation are energy expensive processes that can take up to 10% and 40% of cellular ATP, respectively (Storey and Storey, 2004). As a result, RPP has been shown to shut down the majority of gene expression and protein translation when organisms enter hypometabolism with the exception of some key genes which improve the animal's chances of survival (Storey and Storey, 2004). For example, in animal models of MRD, studies have demonstrated that animals continue to express and/or up-regulate chaperone proteins which help stabilize proteins and lower protein turnover rate (Zhang and Storey, 2011; Krivoruchko and Storey, 2010a; Mamady and Storey, 2006). This is particularly important to conserve protein structural integrity during MRD, where ATP expenditure on protein degradation and resynthesis needs to be minimized. Antioxidant enzymes are also produced in various animal models of MRD to help minimize oxidative damage to proteins and other cellular macromolecules over the course of long periods of environmental stress (Kubrak *et al*., 2010; Storey, 2012; Krivoruchko and Storey, 2010b; Hermes-Lima and Storey, 1993a; Hermes-Lima and Storey, 1993b; Hermes-Lima and Storey, 1996; Willmore and Storey, 1997a; Willmore and Storey, 1997b; Joanisse and Storey, 1996). Recently, RPP has also been implicated in the expression of antioxidants

in *X. laevis* under dehydration stress (Malik and Storey, 2011). Since RPP plays such an important role in regulating key metabolic processes during MRD, I proposed to study the pivotal protein kinase Akt (also known as protein kinase B) in the dehydrating African clawed frog, which has been shown to regulate energy expensive processes such as gene expression, protein translation, glucose metabolism and the cell cycle.

In addition to gene expression, protein translation, and glucose metabolism, analysis of cell cycle arrest has been a key target in animals that undergo MRD. The cell cycle is an energy expensive process which can be reversibly arrested by RPP. Recently, cell cycle arrest has been shown to occur during anaerobiosis in turtles, hibernation in ground squirrels, and freezing survival in wood frogs (Biggar and Storey, 2012; Wu and Storey, 2012; Zhang and Storey 2012). In this thesis, I will explore how dehydration-induced RPP will facilitate MRD and control expression of key genes in order to reversibly induce cell cycle arrest.

1.4 Objectives and Hypotheses

Objective 1: The role of Akt/protein kinase B in dehydration tolerance by *X. laevis*

The protein kinase Akt has been studied in various animal models of hypometabolism and adaptation to environmental stress. Research on Akt primarily highlights its pivotal role in regulation of cellular metabolism (involvement in insulin signaling, glucose metabolism, protein translation, gene expression; Altomare and Khaled, 2012; Vadlakonda *et al*., 2013). Disruptions to regular Akt functionality have resulted in improper regulation of glucose levels as observed in diabetes, and also

incorrect cell cycle control – which leads to cancers (Altomare and Khaled, 2012; Vadlakonda *et al*., 2013). Furthermore, Akt has been highly established as a regulator of protein translation via the mTOR pathway (Haar *et al*., 2007). Akt also plays a role in regulating key transcription factors by phosphorylation (Zhang *et al*., 2002). These characteristics suggest that Akt is a feasible target which is regulated during dehydration stress. It potentially plays a role in mediating the success of estivating animals where all of these metabolic cellular processes are regulated. Various stressors have been shown to facilitate Akt-mediated RPP in order to regulate cellular processes. It is therefore feasible to speculate that stress can signal for Akt to play roles in mediating MRD as a coping strategy to environmental stressors which ultimately promotes the chances of survival. Again, this kinase in particular has been well characterized to regulate many processes such as gene regulation, protein translation, glucose metabolism, and cell cycle arrest. Although Akt has been studied in mammalian and invertebrate models of MRD, it has yet to be studied in a non-mammalian vertebrate model of MRD. Recent reviews have pointed out that although Akt appears to play a key role in general MRD in all animals, there are significant differences to the mechanisms by which Akt is increasing the animal's chances of survival. For example, Akt appears to play a role in the regulation of protein translation in mammals via the Akt/TSC2/Rheb/mTOR/Raptor pathway, but studies with invertebrates suggest that Akt plays a less important role in stress-induced depression of protein translation. Studying Akt in a non-mammalian vertebrate model of MRD will not only increase our knowledge of how hypometabolism is facilitated, but it will reveal the molecular similarities and differences by which animals achieve hypometabolism.

Hypothesis 1: Akt is deactivated in response to dehydration stress in the estivating African clawed frog. As a result, energy expensive processes such as gene expression, protein translation, and glucose metabolism are down-regulated, and cell cycle inhibitors are activated.

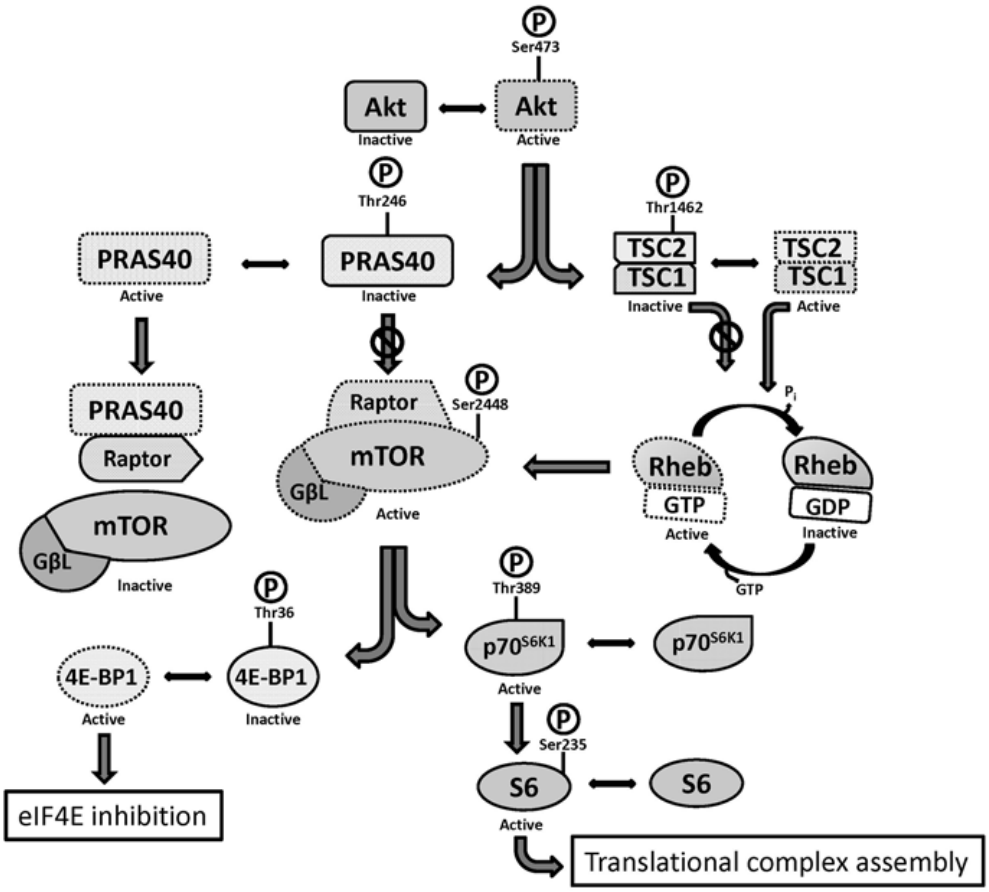

Figure 1.1. The protein kinase Akt has been previously shown to regulate the mTOR pathway which resulted in protein translation suppression in mammalian models of hypometabolism (Wu and Storey, 2012).

Chapter 3 of this thesis tests this hypothesis by quantifying the protein levels and activation status (phosphorylation of key residues) of Akt, its upstream regulators and its crucial downstream targets which play key roles in regulating the processes previously

mentioned. Akt and some of its major targets were studied in both liver and muscle under dehydration stress. Upstream regulators of Akt, PTEN and PDK1 were also studied in hopes of shedding light on how Akt itself is regulated during dehydration. These upstream regulators may play a role in suppressing Akt activity during dehydration, but another upstream regulator of Akt, mTORC2, warrants further investigation. Next, Akt has been shown to regulate glucose levels by regulating glycogen synthase via via GSK-3β phosphorylation. The role of Akt in glucose metabolism (via GSK-3β phosphorylation) was investigated in both liver and muscle in response to dehydration. As previously stated, Akt has been implicated in improper cell cycle regulation which leads to cancers. In this thesis, cell cycle inhibitors previously shown to be under Akt control will be investigated. A suppression of Akt would promote cell cycle arrest by allowing dephosphorylation (and activation) of cell cycle inhibitors – which ultimately result in cell cycle arrest. Lastly, Akt is known to play an important role in the regulation of protein translation. Akt regulates protein translation by activating or suppressing mTORC1 kinase activity. However, there is more than one route by which Akt regulates mTOR. Akt can potentially influence mTORC1 via the Akt/TSC2/Rheb/mTOR/Raptor pathway. Akt can also directly regulate PRAS40, which ultimately interacts with mTOR to facilitate the dissociation of the mTORC1 kinase. If mTORC1 is suppressed, it can cause decreases to relative 4EBP phosphorylation levels. This activates 4EBP to bind to eIF4E – causing the inhibition of protein translation.

Objective 2: Cell cycle arrest in dehydration tolerance of *X. laevis*

Cell cycle processes are a large consumer of cellular energy. Like many cellular processes, the cell cycle is controlled by various types of molecular machinery ranging

from transcription factors which regulate the expression of genes required for cell cycle progression, to kinases which facilitate RPP to signal the cell to proceed from one stage of the cell cycle to the next. As previously discussed, one method for an animal to save energy during bouts with environmental stressors is to suppress energy expensive processes which involve gene expression and protein translation. During periods of MRD where the animal becomes relatively inactive, one strategy it can employ is entering a state of cell cycle arrest. Cell cycle arrest means that not only is energy saved through suppression of key regulatory genes which control the cell cycle, but significant amounts of energy is saved from reduced cell proliferation. This thesis investigated cell cycle regulators in both liver and muscle to understand how this process is regulated in response to dehydration.

> **Hypothesis 2:** Cell cycle arrest occurs in the dehydrating African clawed frog by the dephosphorylation of Rb which ultimately inhibits E2F1 from binding to DNA and facilitating the expression of pro-cell cycling genes.

Cell cycle progression from the G1 to the S phase (preparing to enter the Synthesis phase where DNA replication will occur) is regulated by the transcription factor E2F1, and is suppressed by E2F4. E2F1 regulates crucial genes including cyclin A, cyclin B, cyclin E, and PCNA (proliferative cell nuclear antigen). Furthermore, E2F1 is regulated by RPP of Rb (Retinoblastoma protein). This thesis investigated these transcription factors and its regulators, and target genes in order to understand the roles they may play in response to dehydration stress. Phosphorylation of Rb is facilitated by cyclin dependent kinases (CDKs) 2, 4 and 6. These kinases were also studied in order to understand how they may be regulated to control the cell cycle in the estivating frog.

Similarly to the cell cycle inhibitors under Akt control which were studied in this thesis, the regulation of cell cycle promoters (cdc25a and cdc25c phosphatases) was studied in response to dehydration stress. This thesis performed various analyses on these cell cycle machinery targets, which allowed for a deeper understanding of differing levels of regulation – from protein expression, cellular localization, post-translational modifications, transcription factor/DNA binding, and mRNA expression in order to shed light on the state of the cell cycle in the dehydrating frog.

CHAPTER 2

GENERAL MATERIALS AND METHODS

2.1 Animal treatment and tissue preparation

Adult African clawed frogs (*Xenopus laevis*) were obtained from the Department of Zoology at the University of Toronto. Prior to experimentation, frogs were held at 22°C ± 1°C in tanks with dechloraminated water with aeration for 1-2 weeks. Frogs were then divided into control, medium and high dehydration groups. Controls were maintained in the same conditions as above. To induce dehydration, frogs were removed from water, quickly weighed and placed into dry containers at 22°C. Animals were allowed to lose water over time, as determined by body mass measurements at various time intervals until target levels of water loss were reached. The percentage of total body water lost was calculated as follows:

$$\% \text{ water lost} = [m_i - m_d / (m_i - BWC_i)] \times 100\%,$$

where m_i, m_d, and BWC_i are initial mass, dehydrated mass, and initial body water content of *X. laevis* frogs, respectively. Mean initial body water content was 0.74 ± 0.02 g H_2O g^{-1} body mass (Malik and Storey, 2009). Frogs were sampled when mean total body water loss was 16.4 ± 0.33 % SEM (medium dehydration) or 31.2 ± 0.83 % SEM (high dehydration). Previous work suggested that the mortality limit was reached at 32.4% ± 1.5 SEM of total body water loss (Malik and Storey, 2009). All frogs were killed by pithing, and then tissue samples were quickly dissected, immediately frozen in liquid nitrogen and transferred to -80°C until use. Liver and hind leg skeletal muscle were used in this study. Animals were cared for in accordance with the guidelines of the Canadian Council on Animal Care and all experimental procedures had the prior approval of the Carleton University Animal Care Committee.

2.2 Total soluble protein extraction

Samples of frozen tissue were quickly weighed, crushed under liquid nitrogen, and then mixed 1:2.5 w:v in ice-cold homogenizing buffer (20 mM Hepes, pH 7.5, 200 mM NaCl, 0.1 mM EDTA, 10 mM NaF, 1 mM Na_3VO_4, 10 mM β-glycerophosphate) with a few crystals of phenylmethylsulfonyl fluoride and 1 µl Protease Inhibitor Cocktail (BioShop; 0.15 units/ml Apoprotinin, 5 µg/ml Leupeptin, 1 µg/ml Pepstatin) added immediately before homogenization using a Polytron PT10. Samples were centrifuged at 10,000 × g at 4°C for 15 min. The supernatant containing soluble protein was removed and used for all remaining steps. Soluble protein concentration of samples was determined using the Coomassie blue dye-binding method and the BioRad prepared reagent with bovine serum albumin as the protein standard. All sample concentrations were subsequently standardized to 10 µg/µl by addition of small measured aliquots of homogenization buffer. Samples were then mixed 1:1 v:v in 2 x SDS sample buffer (100 mM Tris-base, 4% w/v SDS, 20% v/v glycerol, 0.2% w/v bromophenol blue, 10% v/v 2-mercaptoethanol, pH 6.8) to give a final protein concentration of 5 µg/µL. Samples were boiled for 5 min and chilled on ice prior to loading onto gels.

2.3 Nuclear soluble protein extraction

To prepare nuclear extracts, samples of frozen liver (0.5 g) or skeletal muscle (1.0 g) were broken up and homogenized by hand using a Dounce homogenizer. Homogenization was in 1:2 w:v ratio of homogenization buffer (10 mM HEPES, pH 7.9, 10 mM KCl, 10 mM EDTA, 1 mM DTT, 20 mM 2-glycerophosphate) with the addition of 10 µl Protease Inhibitor Cocktail (Bio-Rad, Hercules, CA, USA) just prior to

homogenization. Samples were centrifuged at 10,000 × g for 10 min at 4°C. The supernatant (cytoplasmic extract) for each sample was removed to a separate tube. The pellet was then resuspended in 150 µL of extraction buffer (20 mM Hepes, pH 7.9; 400 mM NaCl; 1 mM EDTA, 10% v/v glycerol, 10 mM 2-glycerophosphate 1 mM DTT) with 1.5 µl of Protease Inhibitor Cocktail added just prior to the addition of the buffer to the pellet. Samples were incubated on ice horizontally on a rocking platform for 1 h. After the incubation, samples were centrifuged at 10,000 × g for 10 min at 4°C. The supernatant was collected (nuclear extract) and placed into a separate tube. As described for total soluble protein extraction, the protein concentrations of nuclear extracts were determined with the Bio-Rad protein assay and concentrations were adjusted to constant values with extraction buffer. At this point, nuclear protein extractions were used for electrophoretic mobility shift assays and transcription factor DNA-binding ELISAs. For immunoblotting analysis of nuclear proteins, 2 × SDS sample buffer was added to aliquots of the samples as described in total soluble protein extraction. The integrity of the nuclei was confirmed by immunoblotting of nuclear fractions and probing with a highly conserved eukaryotic protein found exclusively in the nucleus (anti-histone H3 antibody; Cell Signaling; diluted 1:1000 in TBST).

2.4 Western blotting

SDS-PAGE was carried out with a 4% stacking gel and a 6-12% resolving gels (depending on target molecular weight) in a Bio-Rad Mini-Protean III apparatus filled with running buffer (25 mM Tris, 190 mM glycine, 0.1% w/v SDS) at 180 V for 45 min. Pre-stained molecular weight standards (Bio-Rad, Hercules, CA, USA) and 20 µg of total soluble protein extracts or nuclear protein extracts (n = 4 biological replicates of each

tissue or experimental condition) loaded onto gels. Proteins were then transferred from the polyacrylamide gels onto polyvinylidene fluoride (PVDF; Biotrace, PALL Life Sciences) membranes using a BioRad mini Trans-Blot cell with transfer buffer (25 mM Tris, 192 mM glycine, and 20% v/v methanol). The transfer process was run for 90-180 min (depending on target molecular weight) at 70V at 4°C. After protein transfer, all membranes were equilibrated in fresh TBST (10 mM Tris, pH 7.5, 150 mM NaCl, 0.05% v/v Tween-20) for 10 min. Membranes were then blocked with milk by equilibrating in a 2.5% w/v non-fat milk solution (20 mL TBST, 0.5 g dried non-fat skim milk powder) for 20 min. After incubation with blocking solution, membranes were washed with fresh TBST for 3×5 min.

Membranes were incubated with primary antibody (1:1000 v/v in TBST) overnight at 4 °C with gentle rocking. Primary antibodies were purchased from Cell Signalling Technologies, Genscript, and Santa Cruz Biotechnology. After washing with fresh TBST for another 3 ×5 minute, the membranes were incubated with anti-mouse or anti-rabbit secondary antibody (1:8000 v/v) for 30 min at room temperature with gentle rocking. Fresh TBST was used again to wash the membrane for 4 ×5 min at room temperature with gentle rocking. Enhanced chemiluminescent reagents were used to expose each immunoblot and band densities were visualized and quantified. The PVDF membrane was then stained with Coomassie Blue dye (0.25% w/v Coomassie brilliant blue, 7.5% v/v acetic acid, 50% v/v methanol). Protocol conditions differed for each target and are specified in detail in their respective chapters.

2.5 Electrophoretic Mobility Shift Assay (EMSA)

Using nuclear protein extracts, biotinylated oligonucleotides were designed and purchased from Sigma Genosys. The oligonucleotide sequences were designed based on the DNA binding element of the E2F transcription factor family, and were as follows: biotinylated probe (E2F 5′-Biotin- ATTTAAGTTTCGCGCCCTTTCTCAA-3′) and complement probe (E2F 5′-c- TTGAGAAAGGGCGCGAAACTTAAAT -3′). Oligonucleotides were diluted to a concentration of 500 pmol/µL, and biotinylated and complement strands were combined 1:1 (v/v) for a total volume of 20 µL. Probes were then incubated in a PCR machine for 10 min at 95°C, and then left at room temperature to cool. Transcription factor-DNA complexes were formed by adding 10 ng of double stranded probe, 50 µg of nuclear extract, 1 µg of poly d(I-C) (Sigma-Aldrich, Oakville, ON), 2 µL of EMSA binding buffer (10 mM Tris, 50 mM NaCl, 1 mM EDTA, 5% glycerol, 2.5 uM DTT, pH 7.8), and adding water to a total volume of 10 µL. Complexes were incubated in a thermocycler for 10 min at 94°C, before adding 1 µL of 6x DNA loading dye (BioShop, Burlington, ON), and running samples on a 6% native polyacrylamide gel at 4°C. Complexes were transferred to a Pall Biodyne B nylon membrane, before being fixed to the membrane for 1 h at 80°C, and blocked in 1x blocking buffer (Affymetrix, Santa Clara, CA) for 15 min. Streptavidin-HRP (BioShop, Burlington, ON) diluted 1:1000 in 1x blocking buffer was used to probe the transferred nucleic acid probes, and 1X wash buffer (Affymetrix, Santa Clara, CA) was used to wash the membrane prior to exposure with enhanced chemiluminescence using the ChemiGenius Bioimaging System.

2.6 Transcription factor-DNA binding ELISA

After biotin-labelled probes were verified with the EMSA, probe functionality was further validated by running a TF-ELISA assay with three negative controls (no probe, no protein, no primary antibody) as well as a full sample time point. Transcription factor binding was quantitatively evaluated for all three experimental conditions in skeletal muscle and liver (control, medium dehydration, high dehydration). Double stranded probes were diluted in phosphate-buffered saline (PBS) (137mM NaCl, 2.7 mM KCl, 10 mM Na_2HPO_4, 2 mM $KHPO_4$, pH 7.4). To every streptavidin coated well used, 50 µL of diluted DNA probe was added (40 pmol DNA/well). Following a 1 h incubation, unbound probe was discarded and wells were rinsed three times in wash buffer (1X PBS containing 0.1% Tween-20), and a fourth time with 1X PBS. Equal amounts of protein from nuclear extractions were vortexed with transcription factor binding buffer (10 mM HEPES, 50 mM KCl, 0.5 mM EDTA, 3 mM $MgCl_2$, 10% glycerol, 0.5 mg/ml bovine serum albumin, 0.05% NP-40, 20 mM DTT, pH 7.9). In each well containing DNA probe, 50 µL of protein mixture was added, with the exception of negative control wells which contained transcription factor binding buffer without protein. Following 1 h incubation with gentle shaking, protein mixtures were discarded and the wells were washed three times with wash buffer.

Diluted primary antibody was then added (60 µL/well) and allowed to incubate for 1 h. Excess primary antibody was discarded, and the wells were rinsed three times with wash buffer before being incubated with diluted secondary antibody (60 µL/well) for 1 h. Diluted secondary antibody was discarded and wells were rinsed four times with wash buffer. Primary and secondary antibodies were the same as those in the Western

Blot protocol. The quantitative run for E2F1 utilized the following conditions: 50 µg of protein/well, 1 µg of salmon sperm/well, 30 mM NaCl, 1:1000 v:v E2F1 primary antibody in TBST, 1:2000 v:v anti-rabbit secondary antibody in TBST. The quantitative run for E2F4 utilized the following conditions: 30 µg protein/well, 1 µg of salmon sperm/well, 30 mM NaCl, 1:1000 v:v E2F4 primary antibody in TBST, 1:2000 v:vanti-rabbit secondary antibody in TBST. After secondary antibody incubation and washing, bound antibody was detected using tetramethylbenzidine (TMB) purchased from BioShop. A 60 µL aliquot of TMB was dispensed into each well, and 60 µL of 1 M HCl was added to each well to inactivate the TMB once colour was developed. At this point, absorbance was measured at 450 nm (reference wavelength of 655 nm) using a Multiskan spectrophotometer.

Following the quantification run, a competitive run was performed to determine the specificity of the probes. A competitive run compares the relative binding of the biotin-labelled probe to frog E2F to two other interactions: 1. the same reaction in the quantitative run with the addition of competing wild-type double stranded oligos (the same sequence as the biotin-labelled probes, without biotin labelling) and, 2. The same reaction in the quantitative run with the addition of a competing double stranded oligo with a mutated sequence (5'- ATTTAAGTAACGCGCCCTTTCT-3'; compliment 5'-TTGAGAAAGGGCGCGATTCTTAAAT-3').

2.7 Total RNA extraction

All equipment and solutions were treated with 0.1% v/v diethylpyrocarbonate (DEPC) and autoclaved prior to use. Total RNA was extracted from skeletal muscle and liver under control, medium dehydration, and high dehydration experimental conditions.

In general, 0.1-0.2 g of frozen tissue was homogenized in 1.5 mL of Trizol (Invitrogen) using a Polytron PT10 homogenizer. Next, 300 µL of chloroform was added, and samples were vortexed prior to centrifugation at 10,000 x g for 15 min at 4°C. The upper aqueous phase, which contained total RNA, was displaced to a new tube without disturbing the other layers of the solution. Each sample was combined with 750 µL 2-propanol, prior to allowing RNA precipitation to occur at room temperature over 15 min. The samples were then centrifuged at 12,000 x g for 15 min at 4°C, washed with 1 mL 70% ethanol, before re-centrifugation at 12,000 x g for 5 min. The supernatants were removed and pellets were allowed to air dry over 20 min at room temperature before being resuspended in 30 µL DEPC-treated water. Purity and concentration of RNA was assessed by measuring the 260/280 nm ratio. RNA quality was also assessed by the appearance of two sharp bands representing 28S and 18S ribosomal RNA on a 1% agarose gel with SybrGreen staining. Normalization of RNA concentrations was done by adjusting samples to a final concentration of 1 µg/µL with DEPC-treated water.

2.8 cDNA synthesis and PCR amplification

Complementary DNA (cDNA) was synthesized from each RNA sample. In each reaction, 15 µg of RNA was combined with 1 µL of 200 ng/µL oligo-dT (5'-TTTTTTTTTTTTTTTTTTTTTTV-3'; where V= A, G, or C; Sigma Genosys) in a total volume of 10 µL DEPC-treated water. Samples were incubated at 65°C in a water bath for 5 min and then placed on ice to hybridize the oligo-dTs with the poly-A-tails of RNA transcripts. Then, 4 µL of 5X first strand buffer, 2 µL of 10 mM DTT, 1 µL of 10 mM dNTPs, and 1 µL reverse transcriptase enzyme Superscript II (all Invitrogen) were added

into each sample, and cDNA synthesis was allowed to proceed by incubating samples at 42°C for 45 min in an Eppendorf thermocycler.

The polymerase chain reaction (PCR) was used to amplify selected genes from the cDNA samples. Each 25 µL reaction contained 15 µL DEPC-treated water, 5 µL of cDNA dilution, 0.5 µL 10X PCR buffer, 1.75 µL 50 mM $MgCl_2$ (Invitrogen), 1.25 µL *X. laevis* specific primer dilution (0.5 µM forward and 0.5 µM reverse; designed from the *X. laevis* genome using NCBI BLAST and ordered from IDT Technologies), 0.5 µL 10 mM dNTPs, and 1 µL *Taq* polymerase (Invitrogen). The PCR protocol began with 10 min of secondary structure denaturing at 94ºC, followed by 37 cycles of 94ºC for 1 minute, primer-specific annealing temperature for 1 minute, and elongation at 75ºC for 1 minute. The protocol was concluded with one final step of 75ºC for 10 min. For every gene studied, the optimal cDNA dilution (10^{-1} or 10^{-2}) and annealing temperature was determined. Further details are included in appropriate data chapters of this thesis.

After cDNA amplification, PCR products were resolved on a 1-2% w/v agarose gel. Agarose gels were produced by dissolving agarose in 200 mL of hot 1X TAE buffer (40 mM Tris, 20 mM glacial acetic acid, 1 mM EDTA, pH 8.5). To each sample of amplified cDNA, 3 µL of 1:2 v/v SybrGreen / 1X DNA loading Dye (Bioshop) was added. Samples were then loaded onto the agarose gels and electrophoresis was carried out at 130 V in 1X TAE buffer.

Amplified PCR products were excised from agarose gels,isolated using the freeze/squeeze method and then sent for sequencing (BioBasic, Markham, ON). To do this, excised gel samples were frozen in liquid nitrogen for at least 5 min, thawed and transferred into 0.5 mL Eppendorf tubes with punctured bottoms that were filtered with

glass wool. Samples were centrifuged at 12,000 x g for 5 min into 1.5 mL Eppendorf tubes and each filtrate was treated with 0.1 volume of 3 M sodium acetate and 3 volumes of 90% ethanol. Nucleic acid precipitation was allowed to occur at room temperature for 15 min before samples were centrifuged at 12,000 x g for 15 min. Nucleic acid pellets were then rinsed with 0.5 mL of 70% ethanol before pellets were dried and resuspended in 40 µL of DEPC-treated water.

2.9 Primer design

To design primers for gene-specific amplification from cDNA samples, the *Xenopus laevis* genome was accessed on the NCBI database (www.ncbi.nlm.nih.gov). NCBI has several accessible annotated cDNA libraries for the *Xenopus laevis* genome that have been cross-referenced with other sequenced animals to identify conserved genes. After accessing the mRNA sequence for the genes of interest, NCBI Primer-BLAST (http://www.ncbi.nlm.nih.gov/tools/primer-blast/) was used to produce potential primers which would not amplify any other region of the *X. laevis* genome. To identify the ideal primer pairs out of those produced from NCBI Primer-BLAST, the IDT OligoAnalyzer (http://www.idtdna.com/analyzer/applications/oligoanalyzer) site was used to analyze physical properties, homo- and heterozygous dimerization.

2.10 Data quantification and statistics

Imaging of immunoblots and agarose gels was done using a Chemi-Genius Bio-imager (Syngene, Frederick, MD) and band intensities were quantified using the accompanying GeneTools software. For Western blots, membranes were subsequently

stained with Coomassie blue and densities of a group of protein bands that did not change with experimental condition were quantified and used to standardize the intensities of the immunoreactive bands to correct for any minor differences in protein loading. Use of these Coomassie stained bands for standardization was previously validated for all experimental conditions with immunoblots detecting two housekeeping proteins, α-tubulin and β-actin, that showed constant expression across all samples both on their own and when expressed relative to the corresponding Coomassie blue stained bands. Both the quantified intensity of the bands and the density of the protein loaded were corrected against the background of the membrane.

For agarose gel quantification, the band densities of amplified target genes were standardized against the band densities of α-tubulin amplified from the same sample. Statistically significant differences between the three experimental groups were assessed using one way ANOVA with Tukey's test on SigmaPlot 11.

CHAPTER 3

FACILITATION OF METABOLIC DEPRESSION BY KINASE REGULATION IN THE ESTIVATING AFRICAN CLAWED FROG

3.1. INTRODUCTION

When encountering environmental stresses such as drought, many animal species adapt by entering a hypometabolic state. Energy expensive processes such as translational machinery are tightly regulated, and protein turnover rates have been found to decrease (Storey and Storey, 2010, 2012). Although certain protein targets can be degraded and re-expressed to control biochemical pathways, a significant part of metabolic regulation relies on post-translational modifications such as phosphorylation, acetylation, methylation, ubiquitination, sumoylation, etc. which are more energetically conservative. Reversible protein phosphorylation (RPP) has been shown to be a major regulatory mechanism involved in the hypometabolic response to environmental stresses and controls many facets of metabolism, notably the activity of transcription factors to depress gene expression, and the activities of enzymes involved in energy metabolism (Storey and Storey, 2012). Phosphorylation of proteins is facilitated by protein kinases and their roles in facilitating stress-induced metabolic depression have been previously studied in various animals, including the estivating African clawed-frog (Storey and Storey, 2012). The present chapter focuses on the Akt (also known as protein kinase B) and the mechanistic target of rapamycin (mTOR) pathways, including some key phosphorylation targets which play major roles in gene transcription, glucose metabolism, cell cycle control, and protein translation.

3.1.1 Akt/Protein kinase B

Akt is a serine-threonine specific protein kinase. Its targets include proteins involved in regulating glucose metabolism, apoptosis, cell proliferation, gene

transcription and protein synthesis (Figure 3.1). Thus, I hypothesized that it plays a significant role in the reorganization of metabolism during the adaptation of the African clawed frog to dry conditions. Studies suggest that Akt is regulated in several ways. Firstly, the phosphatase and tumour suppressor, PTEN, regulates Akt by suppressing intracellular phosphatidylinositol trisphosphate levels (PIP_3) which are required for phosphorylation and activation of Akt (Stambolic *et al*., 1998). When appropriate PIP_3 levels are present, phosphoinositide-dependent kinase 1 (PDK1) phosphorylates and activates Akt at threonine 308 (Hofler *et al*., 2011; Sarbassov *et al*., 2005). However, PDK1 phosphorylation of Akt cannot proceed before Akt is first phosphorylated by mTORC2 (mTOR complex 2 kinase) at serine 473 (Sarbassov *et al*., 2005). Regulation of Akt in response to dehydration by modifications of its phosphorylation states, potentially by its upstream regulators PTEN and PDK1, will be assessed in this study.

3.1.2 Mechanistic / Mammalian Target of Rapamycin (mTOR)

One heavily studied target of Akt is the mTOR serine/threonine kinase. It was discovered due to its sensitivity to the drug rapamycin, but has since been found to play central roles in the regulation of protein translation (Figure 3.2). Akt does not directly phosphorylate mTOR. Activation of mTOR kinase is regulated by Akt due to its action on TSC2/Rheb (Inoki *et al*., 2003). By phosphorylating TSC2, this kinase is no longer able to inhibit shuttling between Rheb:GTP / Rheb:GDP which is required for mTOR phosphorylation at Serine 2448 and mTOR Complex 1 (mTORC1) assembly (Inoki *et al*., 2003). The regulatory protein of mTOR (Raptor) is a member of mTORC1 that is also regulated by TSC2 phosphorylation (at serine 863; Foster *et al*., 2009). When active, one

role of mTORC1 is to phosphorylate and inhibit 4E-BP (eukaryotic translation initiation factor [eIF4E] binding protein), which allows eIF4E to initiate translation by directing ribosomes to the cap structures of mRNA (Tomoo *et al*., 2005). Active mTORC1 will also phosphorylate protein kinase p70 s6k whose best characterized target is ribosomal protein s6 (Zhou *et al*., 2004). There is conflicting evidence that suggests that phosphorylation of ribosomal protein s6 has regulatory implications in protein translation (Storey and Storey, 2012). Lastly, another negative regulator of the mTORC1 complex is the proline-rich Akt substrate of 40 kDa (PRAS40). PRAS40, which normally binds to Raptor to prevent mTORC1 formation, is inhibited when Akt phosphorylation occurs at threonine 246 (Haar *et al*., 2007). To elucidate the roles played by the Akt-dependent mTOR pathway in regulating protein translation with respect to dehydration stress and hypometabolism, multiple elements of the mTOR1 downstream pathway are also characterized in this chapter.

Akt-regulated hypometabolism has been studied in animal models ranging from mammalian hibernation to *C. elegans* dauer (Storey and Storey, 2012). In the thirteen-lined ground squirrel, the data indicated that the Akt/TSC2/mTOR pathway shuts down during torpor (Wu and Storey, 2012). Other studies with an estivating land snail (*Otala lactea*) have suggested that Akt is active during estivation – elevating phospho-BAD levels to prevent mitochondrial apoptosis, and deactivating FoxO3-mediated transcription of pro-apoptotic genes (Ramnanan *et al*., 2007; Storey and Storey, 2012). Furthermore, studies have suggested that mTOR phosphorylation state is not changed during estivation in these snails (Ramnanan *et al*., 2007; Storey and Storey, 2012). Due to this uncoupling of the Akt/mTOR pathway, it was suggested that Akt may not be important for the

dissociation of mTORC1 and inhibition of 4EBP, which depresses protein translation in estivating animals (Storey and Storey, 2012). Thus, current literature suggests that mammalian models of metabolic depression rely on the Akt/TSC2/mTOR pathway to regulate and suppress protein translation, whereas estivating invertebrates halt protein translation machinery by other means. The present study seeks to understand the mechanisms by which estivation-induced protein translation is regulated in a non-mammalian vertebrate animal model.

3.1.3 Cell cycle inhibitors p21/p27 Cip/Kip, GSK-3β, and FoxO transcription factors

Other targets of Akt include the cell cycle inhibitors p21 and p27 Cip/Kip (cyclin dependent kinase interacting protein/kinase inhibitory protein), glycogen synthase kinase 3β (GSK-3β), and the Forkhead box transcription factors (FoxO). Akt has been previously shown to phosphorylate and inhibit p21 and p27 at threonine 145 and serine 187, respectively (Xu *et al*., 2011). By phosphorylating these residues, Akt inhibits their action, ultimately allowing cell cycle progression. The p21 and p27 proteins are cyclin-dependent kinase inhibitors and prevent these kinases from facilitating cell cycle progression. The mechanism by which cyclin-dependent kinases regulate the cell cycle will be reviewed in Chapter 4. Analysis of p21 and p27 protein levels and their respective phosphorylation sites targeted by Akt will reveal if these targets play a role in facilitating hypometabolism by arresting the cell cycle during estivation. Akt is also known to stimulate glycogen synthesis by inhibiting GSK-3β via phosphorylation at serine 9 (Acevedo *et al*., 2007; Cross *et al*., 1995). Phosphorylation at this site stimulates GSK-3β kinase activity and subsequently results in glycogen synthase inhibition. Investigation of

GSK-3β is of interest because not only is it known to be regulated by Akt, but has been shown to regulate cell cycle arrest and glucose metabolism which are target mechanisms for facilitating hypometabolism (Yang *et al*., 2006a; Yang *et al*., 2006b; Cross *et al*., 1995). Lastly, FoxO1 and FoxO4 transcription factors are known to regulate a diverse range of downstream targets ranging from antioxidants to cell cycle regulation (Peck *et al*., 2013; Araujo *et* al., 2011; Malik and Storey, 2011). Akt has been well documented to regulate the phosphorylation of these transcription factors at serine 256 and 319 for FoxO1 and serine 193 for FoxO4 (Obsil *et al*., 2003; Zhang *et al*., 2002). Recent studies demonstrated that FoxO1 plays an active role in regulating antioxidant proteins in *Xenopus laevis* in response to dehydration stress (Malik and Storey, 2011). Phosphorylation of FoxO transcription factors signal for nuclear exclusion via 14-3-3 mediated protein transport. In this chapter, links between Akt and the regulation of FoxO activity will be analyzed by examining the phosphorylation states of FoxO1 and FoxO4 in response to dehydration and changes in Akt activity.

The present study seeks to reveal the role of RPP in the responses of African clawed frogs to whole body dehydration, a core stress experienced during estivation. Previous studies with animal models ranging from invertebrates to mammals have shown that suppression of protein translation by means of differential phosphorylation occurs widely under stress. The mechanism by which protein translation is depressed (ie. the mechanism by which the mTOR pathway is regulated) has been shown to differ between different species and different environmental stressors. Also of interest in estivators are pathways that regulate glucose metabolism (GSK-3β), cell cycle arrest (p21/p27 Cip/Kip), and gene expression (FoxO). By studying Akt, a major protein kinase known to

regulate all of these cell processes, a broader understanding of the roles played by RPP in regulating energy expensive cell functions will be achieved for the estivating African clawed frog, and further the understanding of vertebrate estivation.

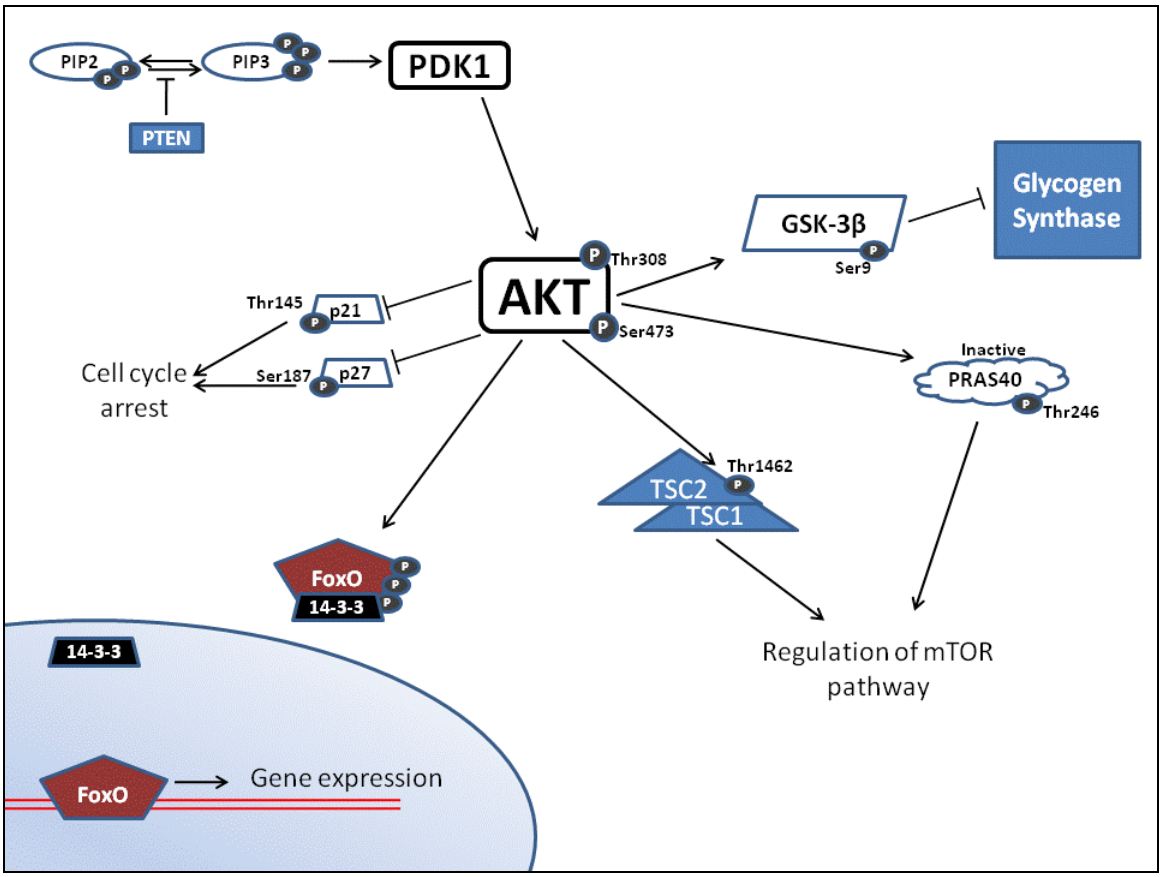

Figure 3.1. The Akt pathway has the potential to regulate glucose metabolism via the GSK-3β kinase, the cell cycle via p21/p27 (Cip/Kip), gene transcription via the FoxO transcription factors, and protein translation via TSC2 and PRAS40.

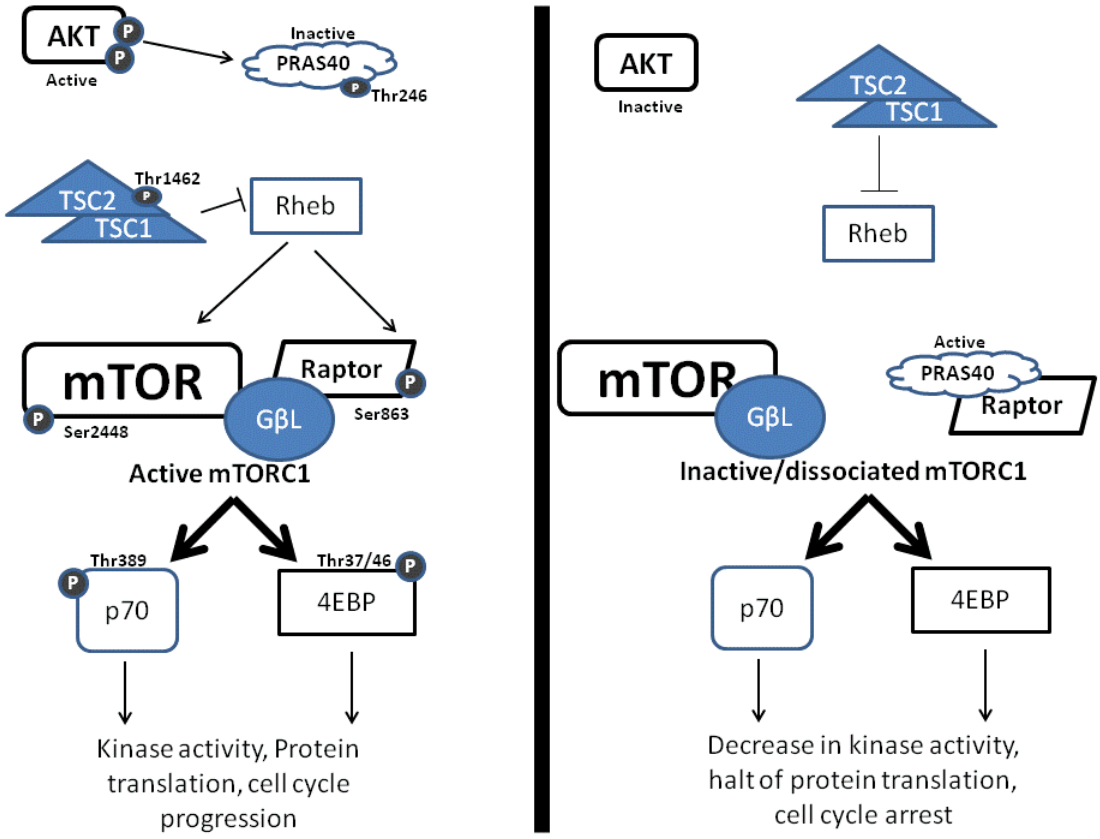

Figure 3.2. Akt-regulated mTORC1 targets 4EBP which is responsible for regulating protein translation by binding to eIF4E. Active mTORC1 also phosphorylates p70 s6 kinase which can regulate protein translation and cell cycle progression.

3.2. MATERIALS AND METHODS

3.2.1 Animals and tissue collection

Adult African clawed frogs were treated, sacrificed, and dissected as in Chapter 2.

3.2.2 Soluble protein isolation and Western Blotting

Relative total protein and phosphorylated protein levels were determined using Western blotting as described in Chapter 2. Tables 3.1-3.3 summarize the antibodies and

conditions used for detecting protein and phospho-protein levels of Akt and its downstream targets.

3.2.3 Analysis of selected gene sequences between X. laevis and other species

Conservation of nucleotide coding sequence (cds) from mRNA and protein sequences of selected genes of interest in *X. laevis* was assessed by sequence alignment in EMBL-EMI's Clustal Omega. These selected sequences from *X.* laevis were compared with the respective sequences from *Danio rerio, Mus musculus,* and *Xenopus tropicalis* obtained from the appropriate databases available on NCBI, Ensembl and Xenbase. This was done in response to a lack of cross-reactivity from two primary antibodies used to detect TSC2 in western blotting. The Raptor, 4E-BP, and Akt genes were analyzed as controls to demonstrate that other key targets are conserved in *X. laevis*.

3.2.4 Statistics

Statistical analysis was performed as described in Chapter 2. Data in figures are presented relative to control data which were standardized to 1. Error bars represent standard error of the mean (SEM). Statistical analysis used one-way ANOVA and Tukey's post-hoc test with $p < 0.05$ accepted as significant.

Table 3.1. Summary of Akt-related antibodies and Western blot experimental conditions.

Primary Antibody	**Size**	**Blocking Condition**	**Probing Conditions (dilution)**	**Secondary Antibody (dilution)**	**Source of Primary Antibody**
Rabbit anti-Akt	~ 60 kDa	2.5% w/v milk for 20 minutes	Overnight Incubation (1: 1000)	Anti-Rabbit IgG-HRP (1:8000)	GenScript Corp. A00275

Rabbit anti-p-Akt^{Ser473}	~ 60 kDa	2.5% w/v milk for 20 minutes	Overnight Incubation (1: 1000)	Anti-Rabbit IgG-HRP (1:8000)	Cell Signaling #9271
Rabbit anti-p-Akt^{Thr308}	~ 60 kDa	2.5% w/v milk for 20 minutes	Overnight Incubation (1: 1000)	Anti-Rabbit IgG-HRP (1:8000)	Cell Signaling #4056
Rabbit anti-PTEN	~ 57 kDa	2.5% w/v milk for 20 minutes	Overnight Incubation (1: 1000)	Anti-Rabbit IgG-HRP (1:8000)	Cell Signaling #9559
Rabbit anti-p-PTEN$^{Ser380/Thr382/383}$	~ 57 kDa	2.5% w/v milk for 20 minutes	Overnight Incubation (1: 1000)	Anti-Rabbit IgG-HRP (1:8000)	GenScript Corp. A00302
Rabbit anti-non-p-PTEN	~ 57 kDa	2.5% w/v milk for 20 minutes	Overnight Incubation (1: 1000)	Anti-Rabbit IgG-HRP (1:8000)	Cell Signaling #7960
Rabbit anti-PDK1	~ 63 kDa	2.5% w/v milk for 20 minutes	Overnight Incubation (1: 1000)	Anti-Rabbit IgG-HRP (1:8000)	GenScript Corp. A00208
Rabbit anti-p-PDK1^{Ser241}	~ 63 kDa	2.5% w/v milk for 20 minutes	Overnight Incubation (1: 1000)	Anti-Rabbit IgG-HRP (1:8000)	GenScript Corp. A00207

Table 3.2. Summary of mTOR-related antibodies and Western blot conditions.

Primary Antibody	**Size**	**Blocking Condition**	**Probing Conditions (dilution)**	**Secondary Antibody (dilution)**	**Source of Primary Antibody**
Rabbit anti-mTOR	~ 290 kDa	2.0% w/v milk for 10 minutes	Overnight Incubation (1: 1000)	Anti-Rabbit IgG-HRP (1:8000)	GenScript Corp. A01154

Rabbit anti-p-mTOR^{Ser2448}	~ 290 kDa	2.0% w/v milk for 10 minutes	Overnight Incubation (1: 1000)	Anti-Rabbit IgG-HRP (1:8000)	GenScript Corp. A00643
Rabbit anti-p-PRAS40^{Thr246}	~ 40 kDa	2.5% w/v milk for 20 minutes	Overnight Incubation (1: 1000)	Anti-Goat IgG-HRP (1:8000)	SantaCruz Biotechnology sc-32629
Rabbit anti-Raptor	~ 150 kDa	2.5% w/v milk for 20 minutes	Overnight Incubation (1: 1000)	Anti-Rabbit IgG-HRP (1:8000)	SantaCruz Biotechnology
Rabbit anti-p-Raptor^{Ser863}	~ 150 kDa	2.5% w/v milk for 20 minutes	Overnight Incubation (1: 1000)	Anti-Rabbit IgG-HRP (1:8000)	Abgent AP3495a
Rabbit anti-GβL	~ 36 kDa	2.5% w/v milk for 20 minutes	Overnight Incubation (1: 1000)	Anti-Rabbit IgG-HRP (1:8000)	Cell Signaling #3274
Rabbit anti-p70	~ 70 kDa	2.5% w/v milk for 20 minutes	Overnight Incubation (1: 1000)	Anti-Rabbit IgG-HRP (1:8000)	GenScript Corp. A00516
Rabbit anti-p-p70^{Thr389}	~ 70 kDa	5.0% w/v milk for 30 minutes	Overnight Incubation (1: 1000)	Anti-Goat IgG-HRP (1:8000)	SantaCruz Biotechnology sc-11759
Rabbit anti-p-s6$^{Ser235/236}$	~ 30 kDa	2.5% w/v milk for 20 minutes	Overnight Incubation (1: 1000)	Anti-Rabbit IgG-HRP (1:8000)	GenScript Corp. A00315
Rabbit anti-4EBP	~ 17 kDa	2.5% w/v milk for 20 minutes	Overnight Incubation (1: 1000)	Anti-Rabbit IgG-HRP (1:8000)	GeneTex GTX77626
Rabbit anti-p-4EBP$^{Thr37/46}$	~ 17 kDa	2.5% w/v milk for 20 minutes	Overnight Incubation (1: 1000)	Anti-Rabbit IgG-HRP (1:8000)	GenScript Corp. A00328

Rabbit anti-eIF4E	~ 28 kDa	2.5% w/v milk for 20 minutes	Overnight Incubation (1: 1000)	Anti-Rabbit IgG-HRP (1:8000)	GeneTex GTX50553
Rabbit anti p-TSC2^{Thr1462}	N/A				Abgent AP3471A

Table 3.3.Summary of antibodies for other Akt targets and their Western blot conditions.

Primary Antibody	**Size**	**Blocking Condition**	**Probing Conditions (dilution)**	**2º Antibody (dilution)**	**Source of Primary Antibody**
Rabbit anti-GSK-3β	~ 47 kDa	2.5% w/v milk for 20 minutes	Overnight Incubation (1: 1000)	Anti-Rabbit IgG-HRP (1:8000)	SantaCruz Biotechnology sc-7291
Rabbit anti-GSK-3β^{Ser9}	~ 47 kDa	2.5% w/v milk for 20 minutes	Overnight Incubation (1: 1000)	Anti-Rabbit IgG-HRP (1:8000)	SantaCruz Biotechnology sc-11757
Rabbit anti-p21	~ 21 kDa	2.5% w/v milk for 20 minutes	Overnight Incubation (1: 1000)	Anti-Rabbit IgG-HRP (1:8000)	SantaCruz Biotechnology sc-397
Rabbit anti-p-p21^{Thr145}	~ 21 kDa	2.5% w/v milk for 20 minutes	Overnight Incubation (1: 1000)	Anti-Rabbit IgG-HRP (1:8000)	SantaCruz Biotechnology sc-12902
Rabbit anti-p27	~ 27 kDa	2.5% w/v milk for 20 minutes	Overnight Incubation (1: 1000)	Anti-Rabbit IgG-HRP (1:8000)	GenScript Corp. A00436
Rabbit anti-p-p27^{Ser187}	~ 27 kDa	2.5% w/v milk for 20 minutes	Overnight Incubation (1: 1000)	Anti-Rabbit IgG-HRP (1:8000)	GenScript Corp. A00333

Rabbit anti-FoxO4	~ 60 kDa	2.5% w/v milk for 20 minutes	Overnight Incubation (1: 1000)	Anti-Rabbit IgG-HRP (1:8000)	Cell Signaling #9454
Rabbit anti-FoxO1	~ 80 kDa	2.5% w/v milk for 20 minutes	Overnight Incubation (1: 1000)	Anti-Rabbit IgG-HRP (1:8000)	Cell Signaling #9454
Rabbit anti-p-FoxO1^{Ser319}	~ 80 kDa	2.5% w/v milk for 20 minutes	Overnight Incubation (1: 1000)	Anti-Rabbit IgG-HRP (1:8000)	GenScript Corp. A00373
Rabbit anti-p-FoxO4^{Ser193} FoxO4^{Ser193}	FoxO1/4 80/60 kDa	2.5% w/v milk for 20 minutes	Overnight Incubation (1: 1000)	Anti-Rabbit IgG-HRP (1:8000)	Cell Signaling #9471

3.3. Results

3.3.1 Relative Akt protein expression and phosphorylation state in response to dehydration in X. laevis liver and skeletal muscle

Regulation of the protein kinase Akt during dehydration in the African clawed frog was assessed in liver and skeletal muscle tissues. Relative changes in protein expression, post-translational phosphorylation, and nuclear localization (to determine roles in transcription factor phosphorylation/regulation) were assessed between control, medium dehydration (16.4% total body water lost), and high dehydration (31.2% total body water lost), conditions. This was done by performing SDS-PAGE and immunoblotting on protein extracts of liver and muscle utilizing selected specific antibodies. The anti-rabbit Akt antibodies recognizing total Akt, Akt phosphorylated at serine 473, and Akt phosphorylated at threonine 308 all cross-reacted with frog Akt showing a single band at approximately 60 kDa (Figures 3.3 and 3.4).

Total Akt and phosphorylated Akt (Thr 308) levels in liver remained constant

throughout medium and high dehydration, with respect to corresponding controls. However, relative Akt phosphorylation at serine 473 dropped to 77% and 76% of control levels during medium and high dehydration, respectively (Figure 3.3). In addition, a decrease to 68% of control levels in nuclear Akt content was observed during high dehydration in liver.

In skeletal muscle, total Akt, phosphorylated Akt (both Ser 473 and Thr 308), and nuclear Akt levels all decreased with dehydration stress. Total Akt decreased to 34% and 37% of relative control levels in medium and high dehydration stress, respectively (Figure 3.4). The phosphorylation state of muscle Akt at serine 473 dropped to 61% of control values during medium dehydration and then to 43% of control under high dehydration. Phosphorylation at threonine 308 showed the same pattern dropping significantly to 58% and 45% of controls under medium and high dehydration, respectively. In liver, nuclear levels of Akt decreased to 67% of control levels in high dehydration. Akt in muscle nuclear extracts also decreased significantly to 76% and 68% in response to medium and high dehydration.

3.3.2 Effects of dehydration on Akt upstream regulators, PDK1 and PTEN, in X. laevis liver and skeletal muscle

Regulation of protein kinase PDK1 and protein phosphatase PTEN during dehydration in the African clawed frog was assessed in liver and skeletal muscle. Western blotting showed that the anti-rabbit PDK1 antibodies (total and phosphorylated serine 241) cross-reacted with frog PDK1 with a single band at approximately 63 kDa (Figures 3.5, 3.6). Anti-rabbit PTEN antibodies (total, phosphorylated serine

380/threonine 282/283, non-phosphorylated) cross-reacted with frog PTEN with a single band at approximately 57 kDa (Figures 3.5, 3.6).

Total and phosphorylated PDK1 remained constant in liver over all experimental conditions (Figure 3.5). However, total muscle PDK1 dropped to 77% of control under high dehydration, and phosphorylated muscle PDK1 (Ser 241) dropped to 49% of control in medium dehydration but rebounded under high dehydration conditions (Figure 3.6). In both liver and skeletal muscle, total PTEN protein expression did not change significantly with experimental dehydration exposure. However, phosphorylation of liver PTEN increased by 1.38-fold over controls in high dehydration (Figure 3.5). Unlike in liver, phosphorylated muscle PTEN decreased to 46% of control values under high dehydration (Figure 3.6). Whereas non-phosphorylated PTEN levels remained unchanged in liver (Figure 3.5), muscle levels decreased to 67% and 56% of control levels in medium and high stress, respectively (Figure 3.6). The anti-non-p-PTEN antibody detects levels of PTEN when not phosphorylated on Ser380/Thr382/Thr383.

3.3.3 Effects of dehydration on mTORC1 components in X. laevis liver and muscle

Regulation of mTORC1 was studied during dehydration of the African clawed frog by assessing liver and skeletal muscle protein expression and post-translational phosphorylation for mTOR, PRAS40, Raptor and GβL. The mTOR (total and phosphorylated serine 2448), PRAS40 (threonine 246 phosphorylation), Raptor (total and phosphorylated serine 863), and GβL antibodies cross-reacted with the corresponding frog proteins showing single bands at respective molecular weights of approximately 290, 40, 150, 36 kDa (Figures 3.7, 3.8).

In liver, total and phosphorylated mTOR increased 2.04-fold and 1.65-fold, respectively, after medium dehydration compared to controls, but both returned to control levels under high dehydration conditions (Figure 3.7). Total muscle mTOR decreased to 59% of control during high dehydration and phosphorylated (Ser 2448) mTOR also decreased to 72% and 76% of control values during medium and high dehydration, respectively (Figure 3.8). In both liver and muscle, reduced phosphorylation of PRAS40 was observed with dehydration stress. Liver PRAS40 (Thr 246) content decreased to 69% of control under high dehydration conditions, whereas muscle PRAS40 (Thr 246) fell to 82% and 71% of control during medium and high dehydration exposure, respectively (Figures 3.7, 3.8). Although liver Raptor phosphorylation state remained unchanged, total Raptor levels decreased to 74% and 62% of control values under medium and high dehydration conditions, respectively (Figure 3.7). In muscle, total Raptor levels rose by 1.62-fold increase over controls under high dehydration, but corresponding Raptor phosphorylation (Ser 863) dropped to 67% of control (Figure 3.8). In both liver and muscle, total GβL levels dropped during high dehydration to 74% and 77% respectively, of control values (Figures 3.7, 3.8).

3.3.4 Relative protein and phospho-protein expression of mTORC1 downstream targets

The effects of dehydration on downstream targets of mTORC1 were also analyzed in liver and skeletal muscle of African clawed frogs. Relative changes in protein expression and post-translational phosphorylation for 4EBP, eIF4E, p70 and s6 were assessed between control, medium dehydration, and high dehydration conditions. The antibodies detecting 4EBP (total and phosphorylated threonine 37/46), eIF4E (total),

p70 (total and phosphorylated threonine 389), and s6 (phosphorylated serine 235/236) antibodies cross-reacted with frog proteins showing single bands at the expected molecular weights of approximately 17, 28, 70, 30 kDa, respectively (Figures 3.9, 3.10).

Liver 4EBP levels remained constant during dehydration but phosphorylated 4EBP (Thr 37/46) content decreased to 57% and 65% of control values in medium and high dehydration conditions, respectively (Figure 3.9). In skeletal muscle, total 4EBP dropped to 67% of control under high dehydration conditions, and relative phosphorylation dropped to 63% of control (Figure 3.10). In both liver and skeletal muscle, total eIF4E levels did not change. Liver p70 kinase levels increased under medium dehydration by 1.51-fold, but returned to control levels in high dehydration (Figure 3.9). However, liver p70 kinase phosphorylation (Thr 389) decreased to 86 % and 73% in medium and high dehydration, respectively, as compared with the phosphorylation state of controls (Figure 3.9). Although total skeletal muscle p70 kinase remained unchanged, p70 phosphorylation (Thr 389) decreased to 75% of control values in high dehydration (Figure 3.10). Phosphorylation of liver s6 protein (Ser 235/236) increased remarkably by 5.89 and 5.98-fold, respectively, under medium and high dehydration conditions, and also increased by 2.25-fold under high dehydration in skeletal muscle (Figures 3.9, 3.10).

3.3.5. Relative protein and phospho-protein expression of p21/p27 (Cip/Kip)

Regulation of the Akt-targeted cell cycle regulators p21 and p27 during dehydration was studied in liver and skeletal muscle of African clawed frogs. The antibodies detecting p21 (total and threonine 145 phosphorylation) and p27 (total and

serine 187) cross-reacted with frog proteins with single bands at 21 and 27 kDa, respectively (Figures 3.11 and 3.12).

Total protein levels of p21 in liver remained constant throughout dehydration exposure, but the relative phosphorylation state of the protein (Thr 145) decreased to 42% of control values during medium dehydration and remained suppressed at 46% under high dehydration (Figure 3.11). In skeletal muscle, total p21 levels decreased to 30% and 37% of corresponding control in medium and high dehydration, respectively (Figure 3.12). However, p21 phosphorylation decrease to 54% of control values during medium dehydration but rebounded under high dehydration conditions (Figure 3.12). Both total protein and phosphorylation state of p27 (Ser 127) decreased in liver during high dehydration by 73% and 61%, respectively, when compared to control levels (Figure 3.11). In skeletal muscle, total p27 levels increased by 1.32-fold in high dehydration, but phosphorylation decreased to 44% when compared to controls (Figure 3.12).

3.3.6 Relative protein and phospho-protein expression of GSK-3β

Regulation of the Akt-target, GSK-3β, was also assessed in liver and muscle of frogs during dehydration. The antibodies detecting total GSK-3β and phosphorylated GSK-3β (Ser 9) cross-reacted with frog proteins showing single bands at approximately 47 kDa, the expected molecular mass of the protein from other species (Figure 3.13).

Total protein levels of GSK-3β were unchanged over the course of dehydration in both liver and skeletal muscle. Phosphorylation of GSK-3β in liver increased by 1.29-fold during medium dehydration, but returned to control levels under high dehydration

(Figure 3.13). In skeletal muscle, phosphorylation of GSK-3β did not change in response to dehydration.

3.3.7 Effects of dehydration on relative protein and phospho-protein expression of FoxO1 and FoxO4 in X. laevis liver and skeletal muscle

Regulation of the Akt-targeted FoxO transcription factors was studied during dehydration of the African clawed frog by assessing liver and skeletal muscle tissues. The antibodies detecting FoxO1 (total, serine 319 phosphorylation, and serine 256 phosphorylation) and FoxO4 (total and serine 194 phosphorylation) cross-reacted with frog proteins with single bands at 80 and 60 kDa, respectively (Figures 3.14, 3.15).

In both liver and skeletal muscle, total protein levels for FoxO1 and FoxO4 were unchanged over the course of dehydration exposure (Figures 3.14, 3.15). With respect to their relative controls, liver FoxO1 phosphorylation at serine 319 decreased to 56% in high dehydration, but serine 256 phosphorylation increased by 1.56-fold in medium dehydration (Figure 3.14). Liver FoxO4 phosphorylation at serine 193 also increased by 1.38-fold in medium dehydration, compared to controls, but decreased again under high dehydration. Although muscle FoxO1 phosphorylation at serine 256 did not change with dehydration, serine 319 phosphorylation decreased to 49% of control values under medium dehydration and remained suppressed at 50% under high dehydration (Figure 3.15). Skeletal muscle FoxO4 phosphorylation (Ser 193) also decreased in high dehydration to 65% of relative control levels (Figure 3.15).

3.3.8 Conservation of TSC2 in the African clawed frog

Western blots using African clawed frog tissue extracts failed to produce a signal for TSC2 protein when using an anti-rabbit TSC2 antibody. To determine whether a sequence change in *X. laevis* TSC2 could be responsible for this outcome, a cross-species analysis of mRNA and protein sequences was performed. Nucleotide and protein sequences for the Akt, TSC2, Raptor, and 4EBP genes were obtained from *Xenopus tropicalis*, *Danio rerio*, and *Mus musculus* databases (NCBI, Xenbase, and Ensembl). These sequences were then used to identify similar nucleotide and protein sequences in *X. laevis* which closely matched or had conserved regions. To do this, known sequences from other animals were aligned with respective *X. laevis* sequences using EMBL-EBI's Clustal Omega program (http://www.ebi.ac.uk/Tools/msa/clustalo/) for comparison of both nucleotide and amino acid sequences.

A summary of sequence comparisons and identified conserved domains is compiled in Table 3.4. Comparison of Akt mRNA coding sequence from *X. tropicalis*, *D. rerio*, and *M. musculus* showed sequence conservation ranging from 74-97% with *X. laevis*. The respective Akt protein sequence comparison showed sequence conservation ranging from 81-93%. Comparison for TSC2 mRNA resulted in 65-92% conservation in *X. laevis*, and appropriately resulted in lower 54-95% protein sequence conservation (Table 3.4). There was strong conservation for the protein Raptor as mRNA coding sequence matching ranged from 76-92%, whereas protein sequences were highly similar at 88-98% (Table 3.4). Lastly, coding sequences from 4EBP mRNA from other animals matched closely in *X. laevis* (74-96%), and protein sequences for 4EBP were similarly conserved (72-96 % identity) for *X. tropicalis*, *D. rerio*, and *M. musculus*. In summary,

major proteins such as Akt, Raptor and 4EBP are highly conserved in *X. laevis*, whereas TSC2 from the *Xenopus* genus appears to have relatively lower conservation compared to *D. rerio* and *M. musculus*. Further alignments have shown that the Thr1462 equivalent in human TSC2 is not conserved in the respective *X. laevis* protein. This explains why antibodies currently available failed to cross-react with frog TSC2 during immunoblotting. More importantly, since Thr1462 in TSC2 is a target of Akt, regulation of TSC2 in *X. laevis* warrants further study.

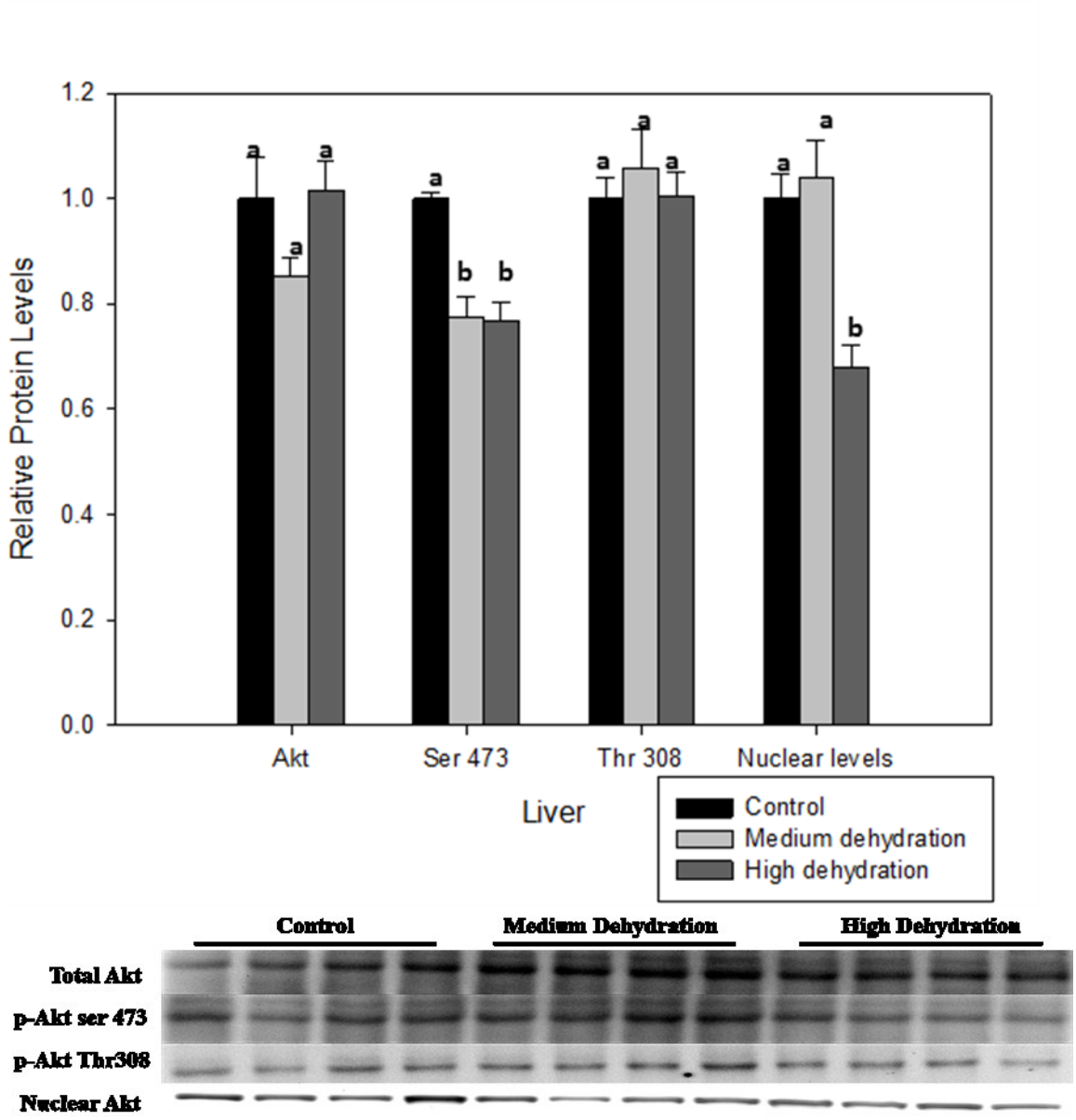

Figure 3.3. Western blot analysis showing the effect of medium and high dehydration on Akt protein expression, nuclear localization, and phosphorylation at serine 473 and threonine 308 in *X. laevis* liver. Histograms show mean values standardized to controls, with error bars showing standard error of the mean derived from n = 4 independent biological replicates. Statistically significant differences were determined by one-way ANOVA and Tukey's post-hoc test, and denoted by different letters above each bar, where $p < 0.05$.

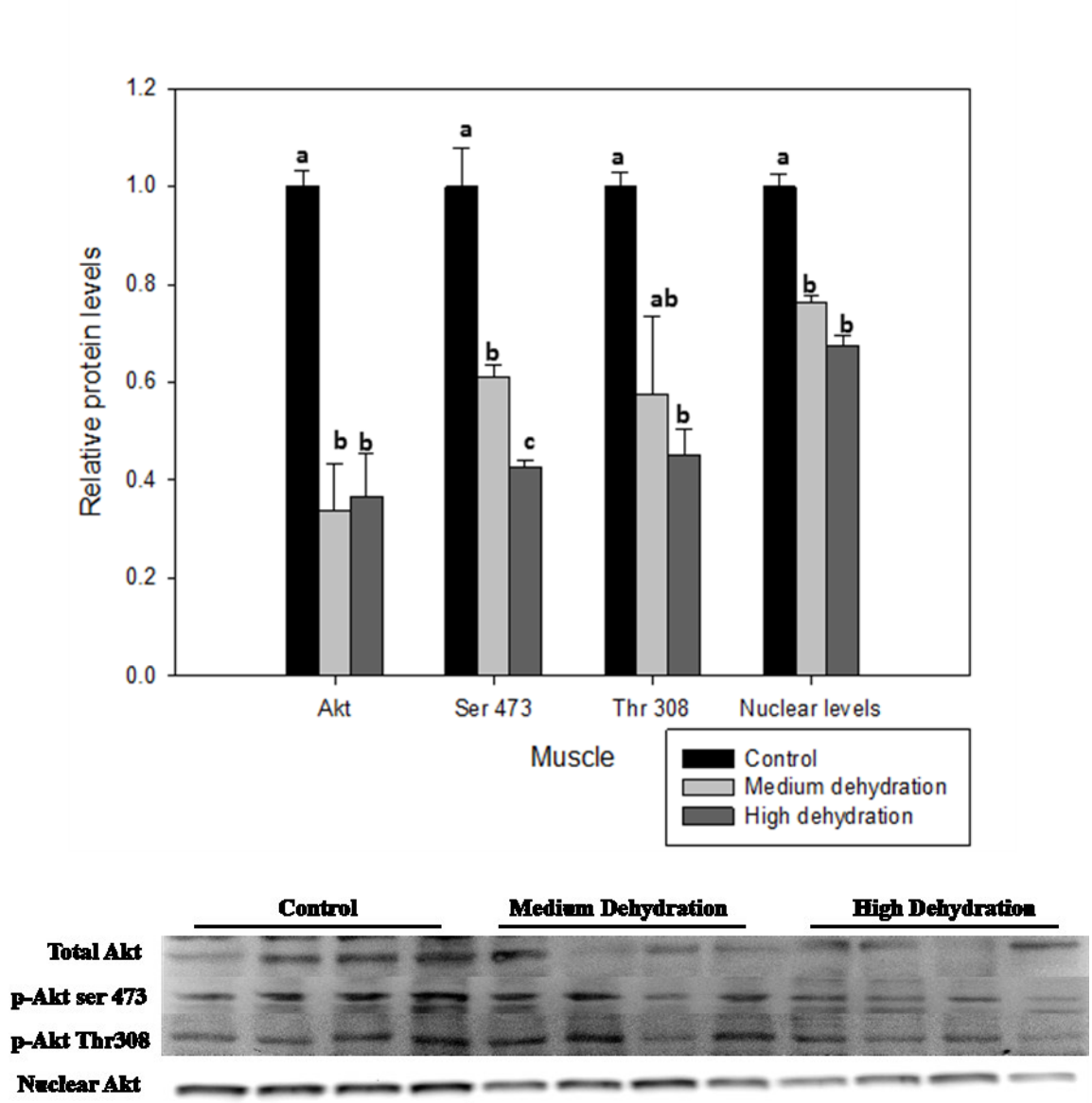

Figure 3.4. Western blot analysis demonstrating the effect of medium and high dehydration on Akt protein expression, nuclear localization, and phosphorylation at serine 473 and threonine 308 in *X. laevis* skeletal muscle. Statistically significant differences were determined by one-way ANOVA and Tukey's post-hoc test, and denoted by different letters above each bar, where $p < 0.05$. Other information as in Figure 3.3.

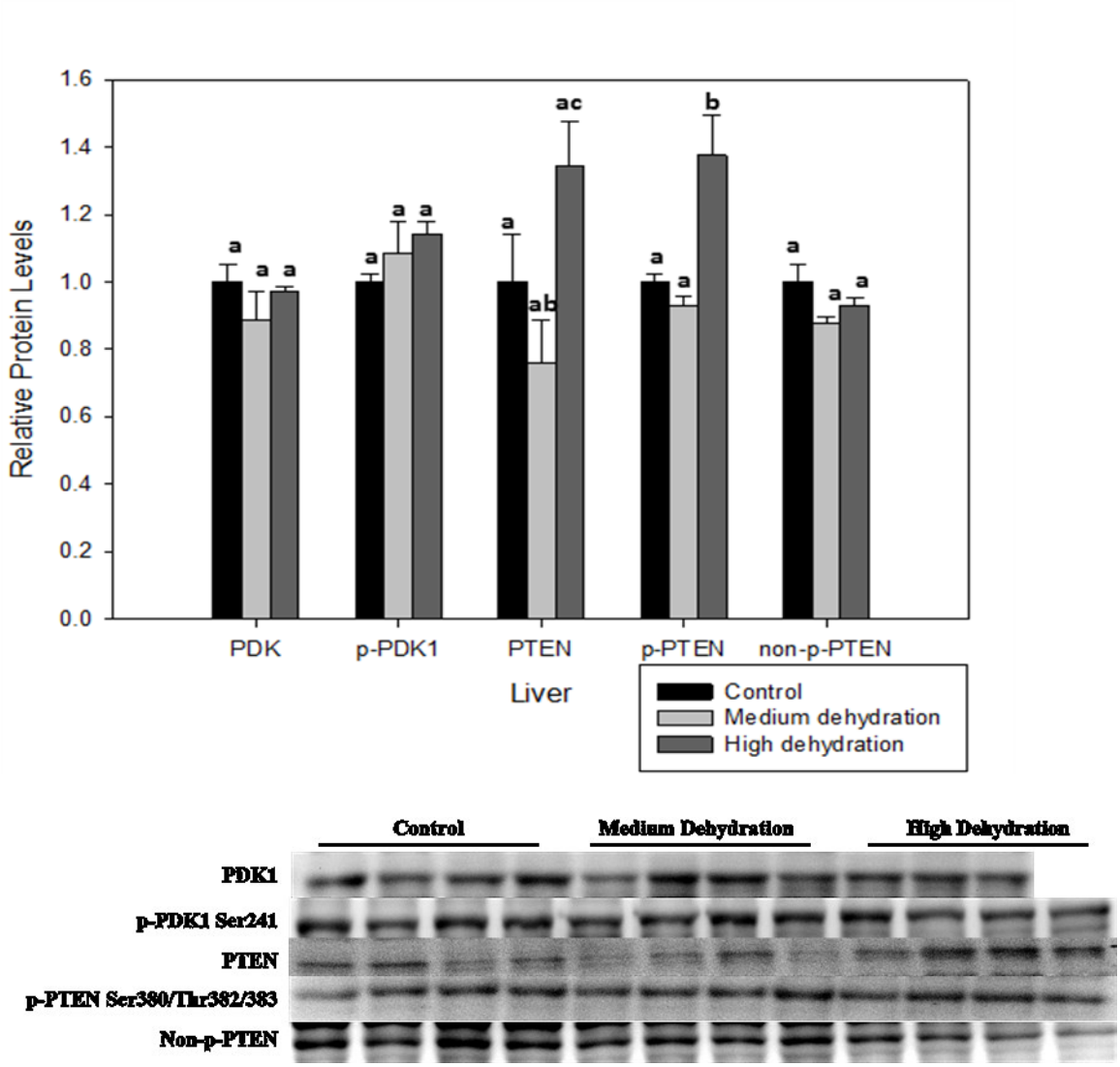

Figure 3.5. Western blot analysis demonstrating the effect of medium and high dehydration on PDK1 and PTEN protein expression, PDK1 phosphorylation at serine 241, PTEN phosphorylation serine 380/threonine 382/383, and non-phosphorylated PTEN in *Xenopus laevis* liver. Statistically significant differences were determined by one-way ANOVA and Tukey's post-hoc test, and denoted by different letters above each bar, where $p < 0.05$. Other information as in Figure 3.3.

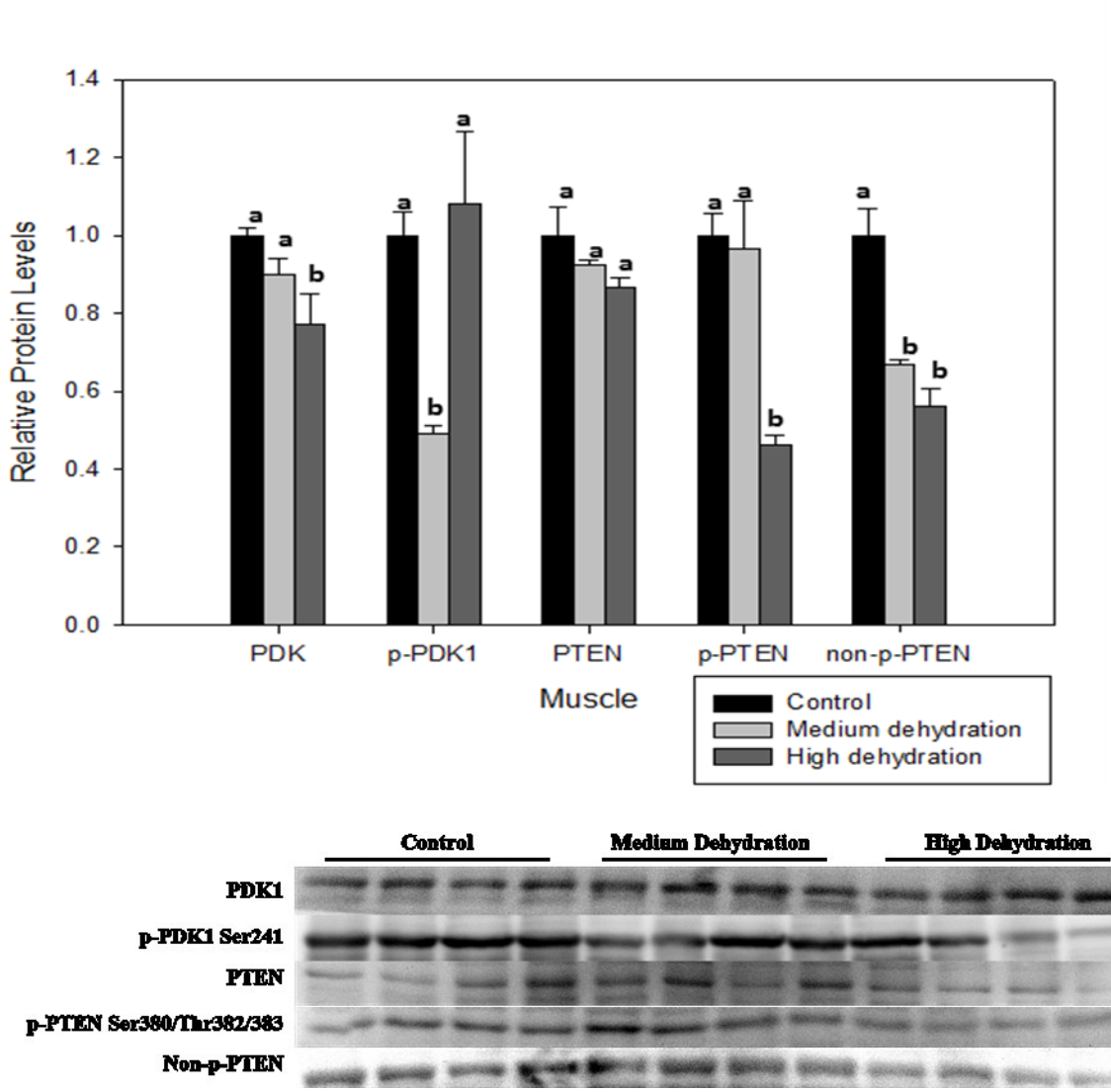

Figure 3.6. Western blot analysis demonstrating the effect of medium and high dehydration on PDK1 and PTEN protein expression, PDK1 phosphorylation at serine 241, PTEN phosphorylation serine 380/threonine 382/383, and non-phosphorylated PTEN in *Xenopus laevis* skeletal muscle. Statistically significant differences were determined by one-way ANOVA and Tukey's post-hoc test, and denoted by different letters above each bar, where $p < 0.05$. Other information as in Figure 3.3.

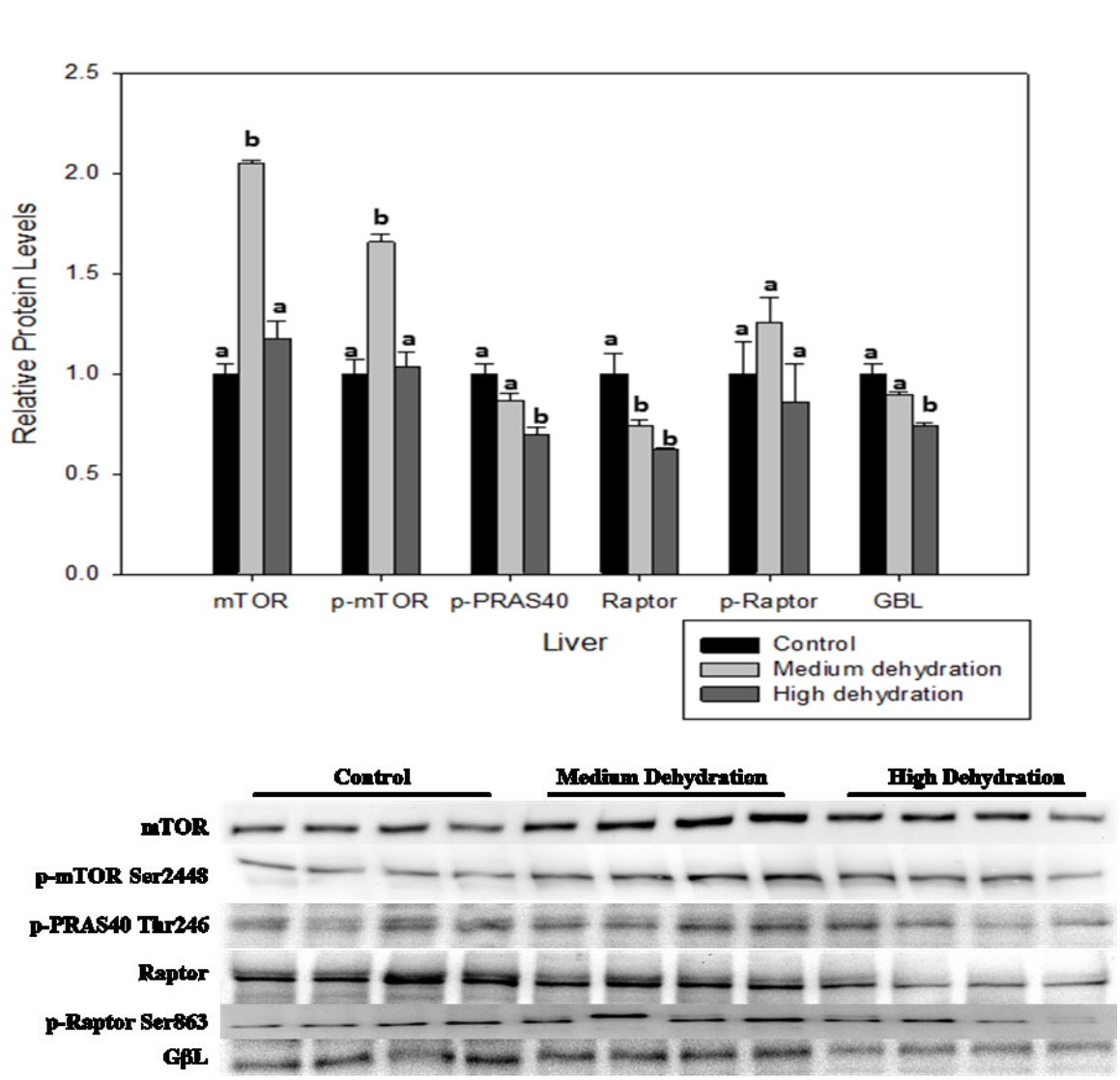

Figure 3.7. Western blot analysis demonstrating the effect of medium and high dehydration on protein expression and phosphorylation of mTOR, PRAS40, Raptor and GβL in *Xenopus laevis* liver. Phosphorylation sites were serine 2448 for mTOR, threonine 246 for PRAS40, and serine 863 for Raptor. Statistically significant differences were determined by one-way ANOVA and Tukey's post-hoc test, and denoted by different letters above each bar, where $p < 0.05$. Other information as in Figure 3.3.

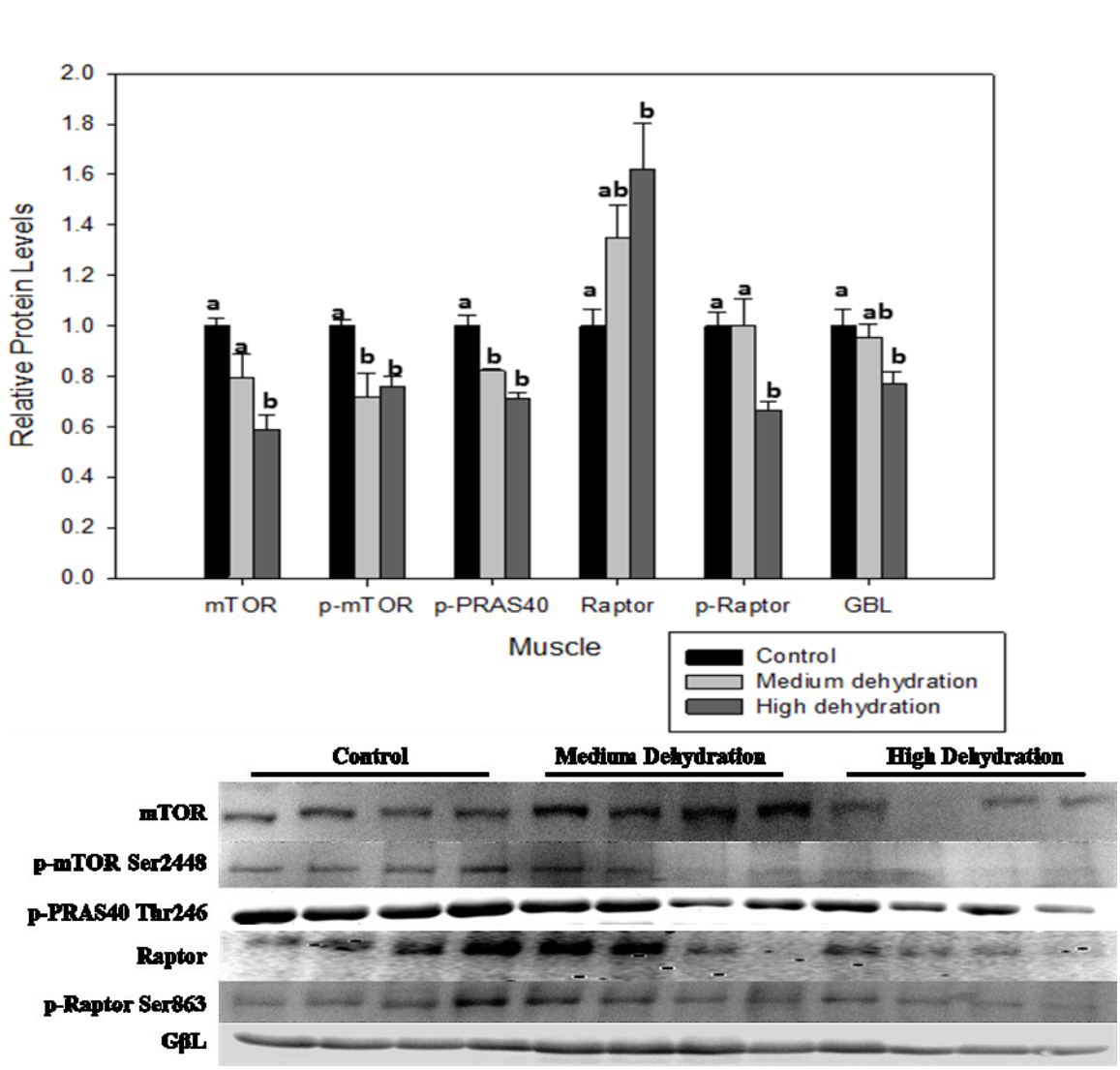

Figure 3.8. Western blot analysis demonstrating the effect of medium and high dehydration on protein expression and phosphorylation of mTOR, PRAS40, Raptor and GβL in *Xenopus laevis* skeletal muscle. Phosphorylation sites were serine 2448 for mTOR, threonine 246 for PRAS40, and serine 863 for Raptor. Statistically significant differences were determined by one-way ANOVA and Tukey's post-hoc test, and denoted by different letters above each bar, where $p < 0.05$. Other information as in Figure 3.3.

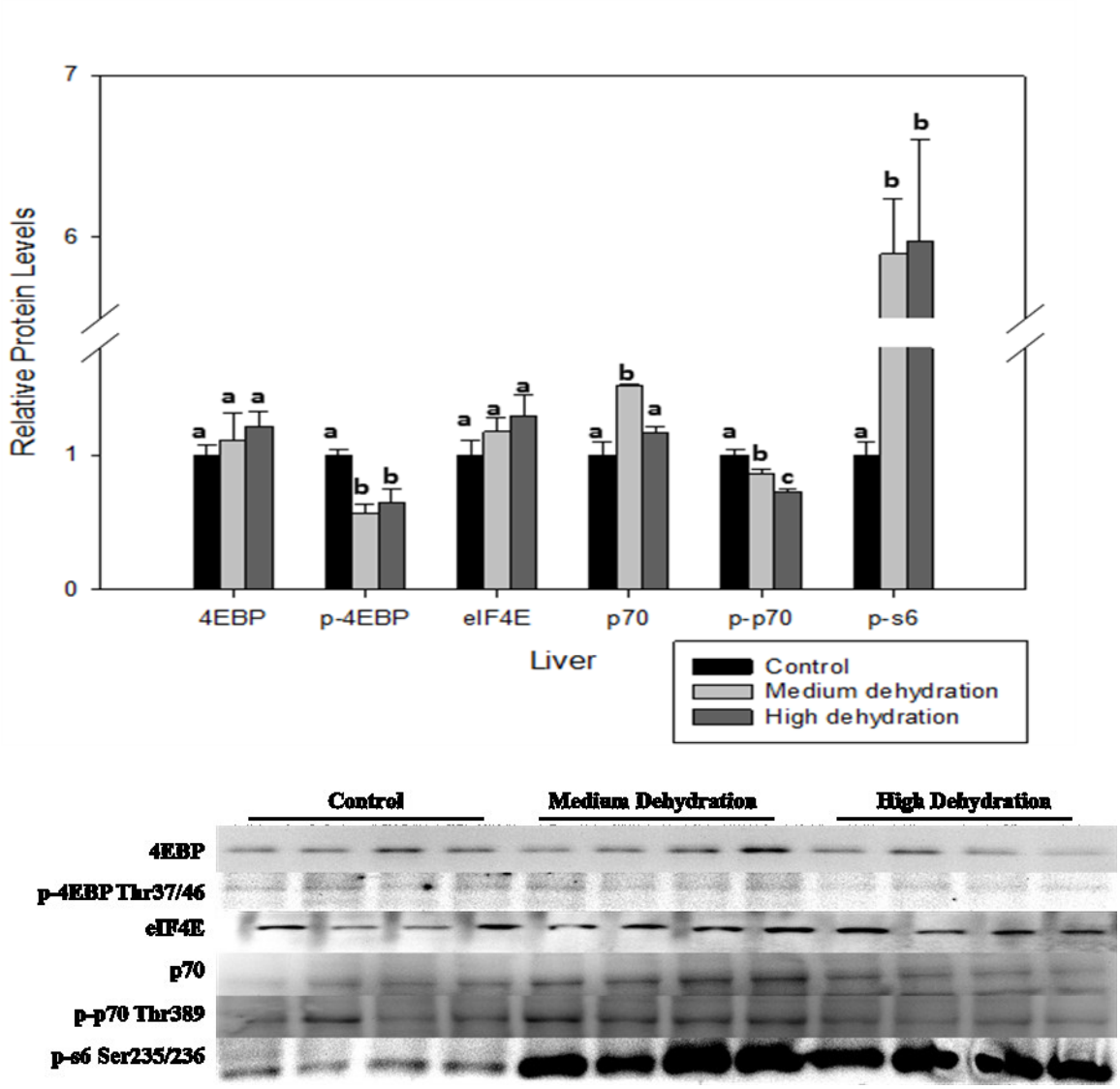

Figure 3.9. Western blot analysis demonstrating the effect of medium and high dehydration on protein expression and phosphorylation of 4EBP, eIF4E, p70 s6k and ribosomal s6 protein in *Xenopus laevis* liver. Phosphorylation sites were threonine 37/46 for 4EBP, threonine 389 for PRAS40, and serine 235/236 for ribosomal protein s6. Statistically significant differences were determined by one-way ANOVA and Tukey's post-hoc test, and denoted by different letters above each bar, where $p < 0.05$. Other information as in Figure 3.3.

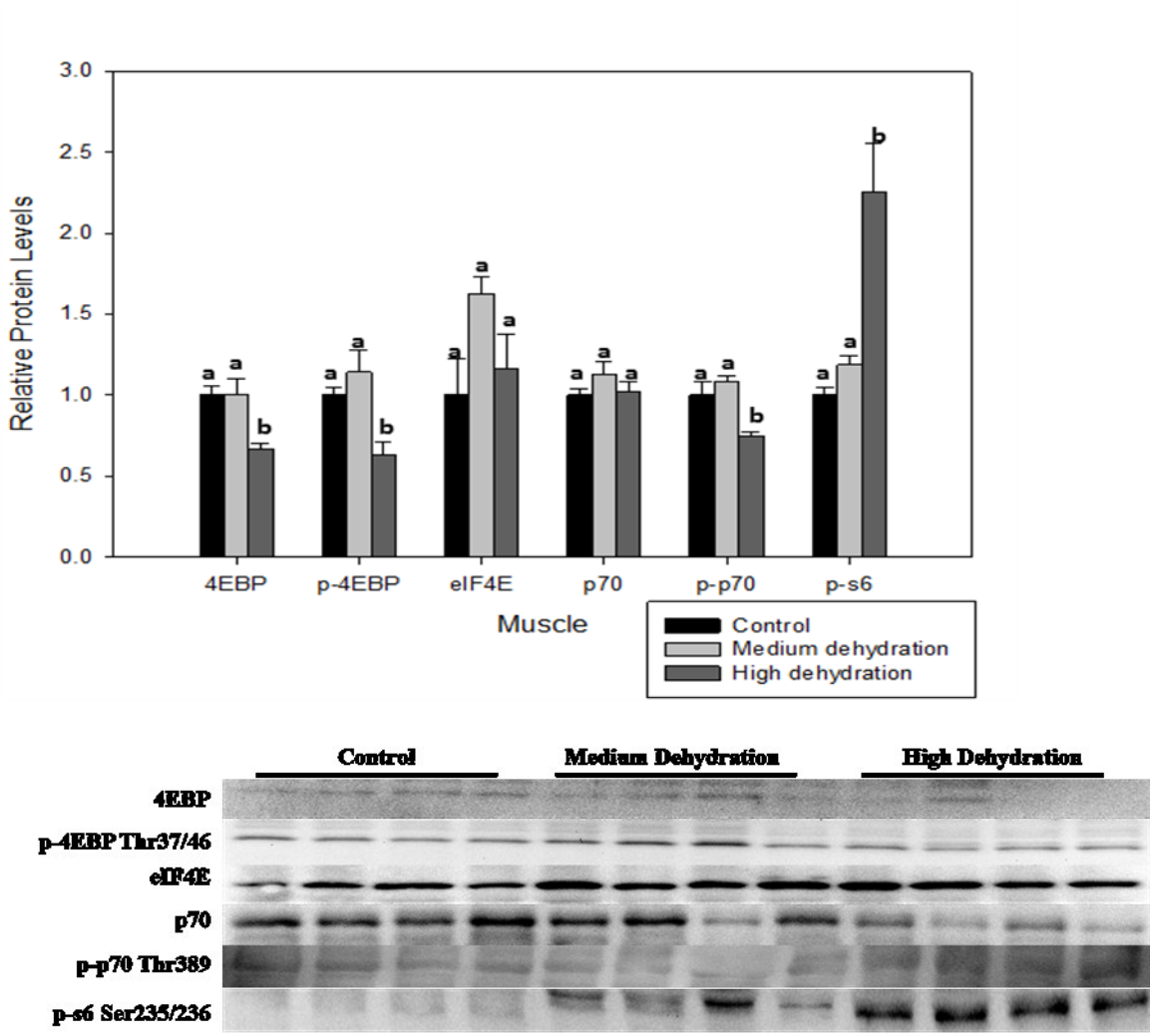

Figure 3.10. Western blot analysis demonstrating the effect of medium and high dehydration on protein expression and phosphorylation of 4EBP, eIF4E, p70 s6k and ribosomal s6 protein in *Xenopus laevis* skeletal muscle. Phosphorylation sites were threonine 37/46 for 4EBP, threonine 389 for PRAS40, and serine 235/236 for ribosomal protein s6. Statistically significant differences were determined by one-way ANOVA and Tukey's post-hoc test, and denoted by different letters above each bar, where $p < 0.05$.Other information as in Figure 3.3.

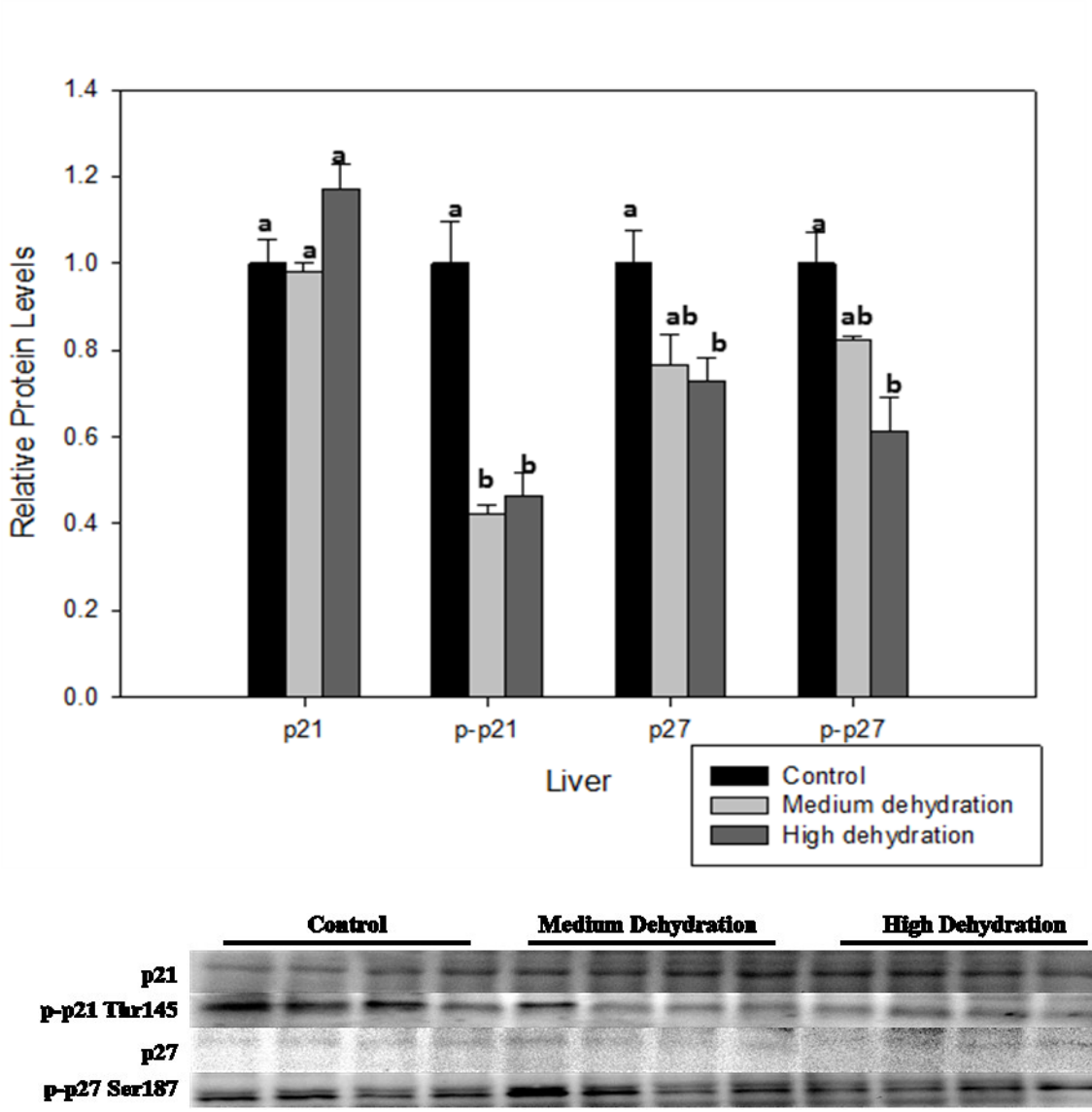

Figure 3.11. Western blot analysis demonstrating the effect of medium and high dehydration on p21 and p27 protein expression and phosphorylation at threonine 145 (p-p21) and serine 187 (p-p27) in *.Xenopus laevis* liver. Statistically significant differences were determined by one-way ANOVA and Tukey's post-hoc test, and denoted by different letters above each bar, where $p < 0.05$. Other information as in Figure 3.3.

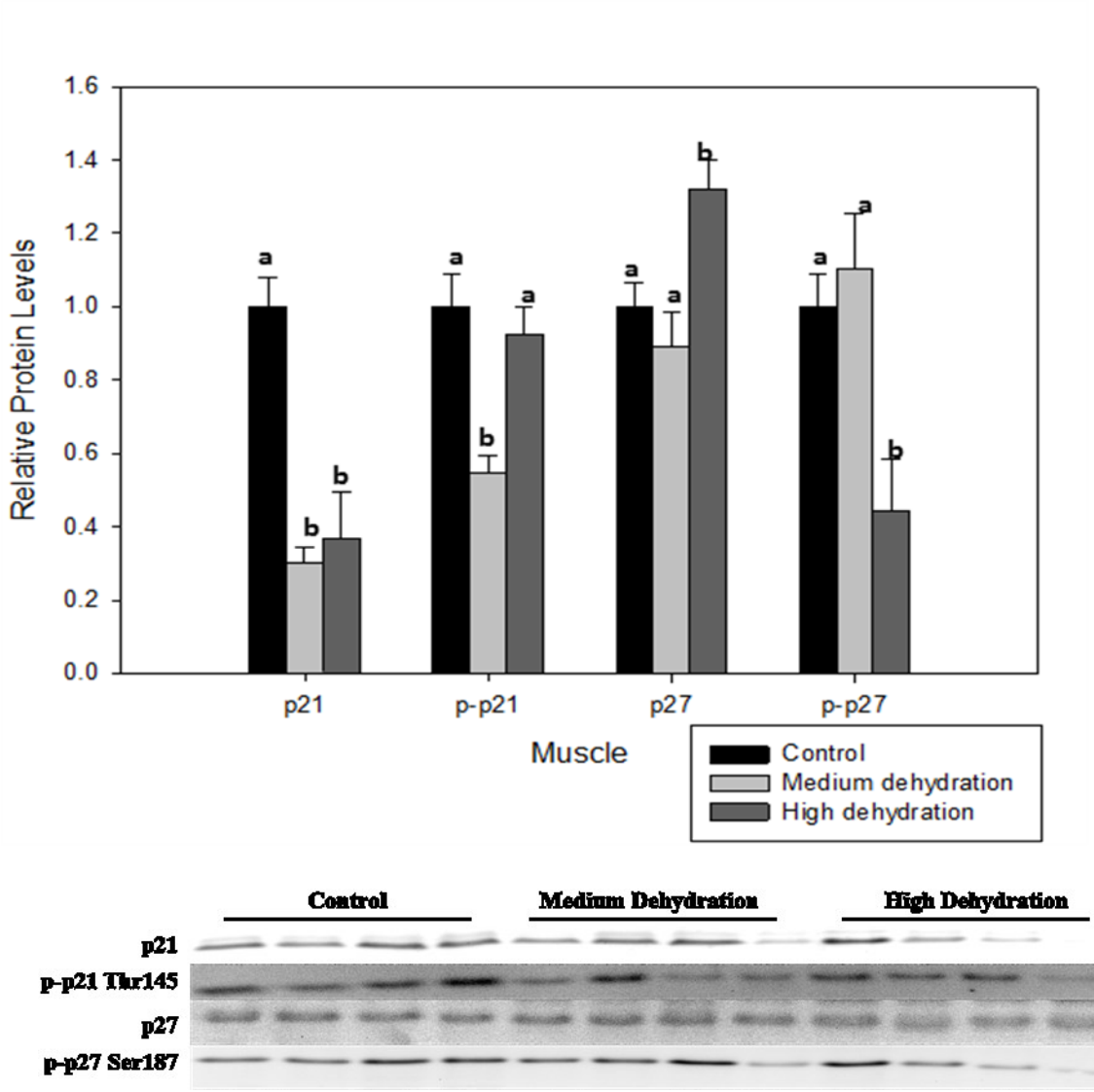

Figure 3.12. Western blot analysis demonstrating the effect of medium and high dehydration on p21 and p27 protein expression and phosphorylation at threonine 145 (p-p21) and serine 187 (p-p27) in *Xenopus laevis* skeletal muscle. Statistically significant differences were determined by one-way ANOVA and Tukey's post-hoc test, and denoted by different letters above each bar, where $p < 0.05$. Other information as in Figure 3.3.

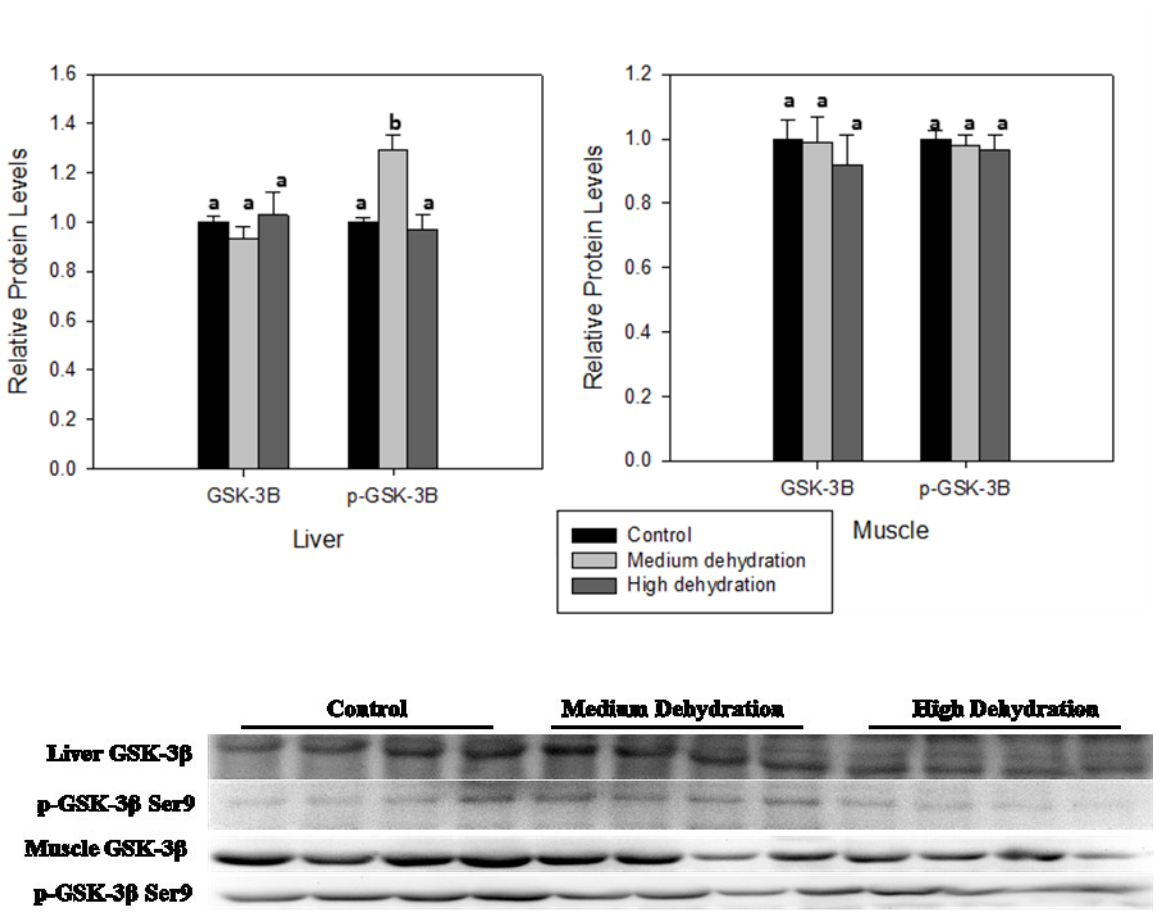

Figure 3.13. Western blot analysis demonstrating the effect of medium and high dehydration on GSK-3β protein expression and phosphorylation at serine 9 in *Xenopus laevis* liver and skeletal muscle. Statistically significant differences were determined by one-way ANOVA and Tukey's post-hoc test, and denoted by different letters above each bar, where $p < 0.05$. Other information as in Figure 3.3.

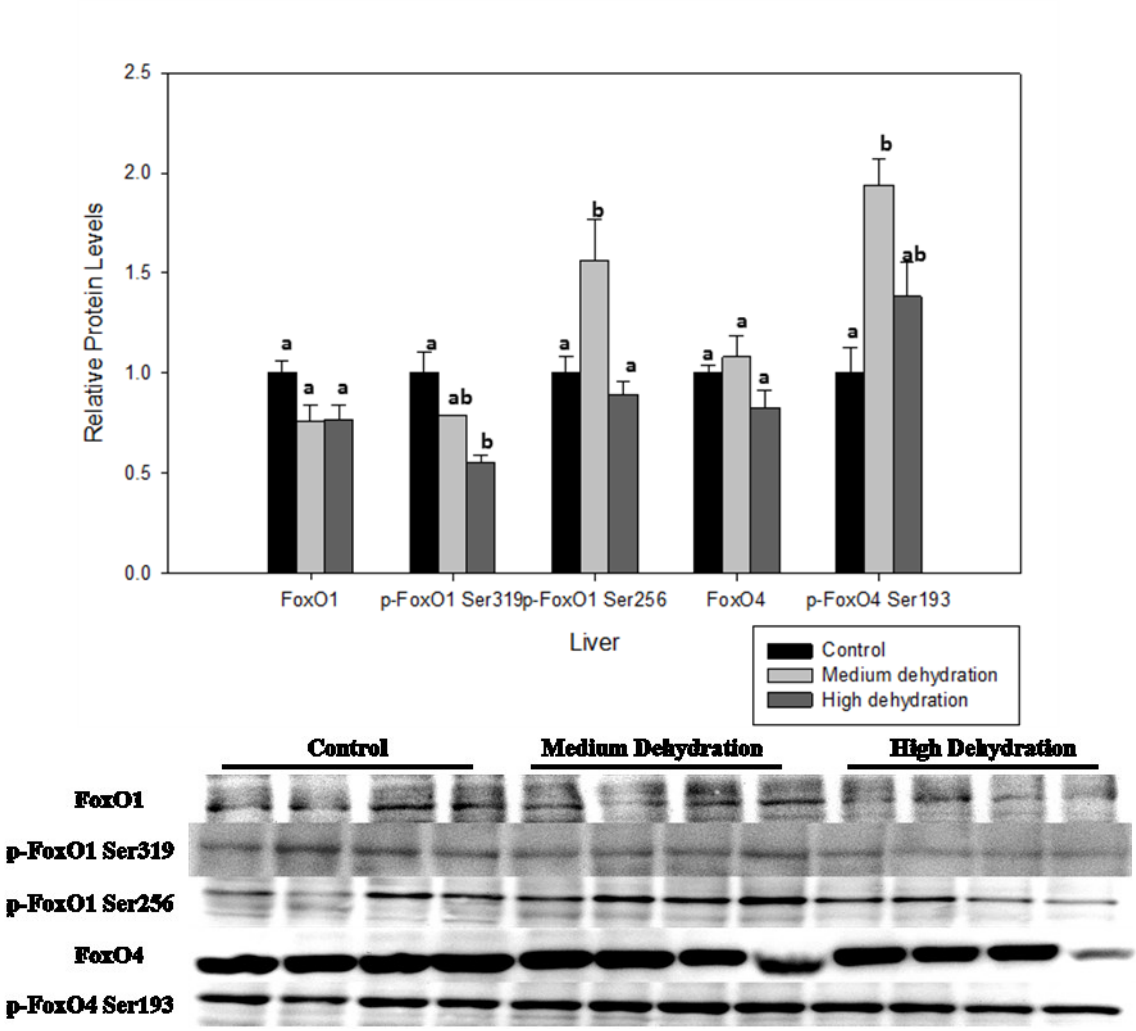

Figure 3.14. Western blot analysis demonstrating the effect of medium and high dehydration on FoxO1 and FoxO4 protein expression and phosphorylation at serine 319, 256 (FoxO1) and serine 193 (FoxO4) in *Xenopus laevis* liver. Statistically significant differences were determined by one-way ANOVA and Tukey's post-hoc test, and denoted by different letters above each bar, where $p < 0.05$. Other information as in Figure 3.3.

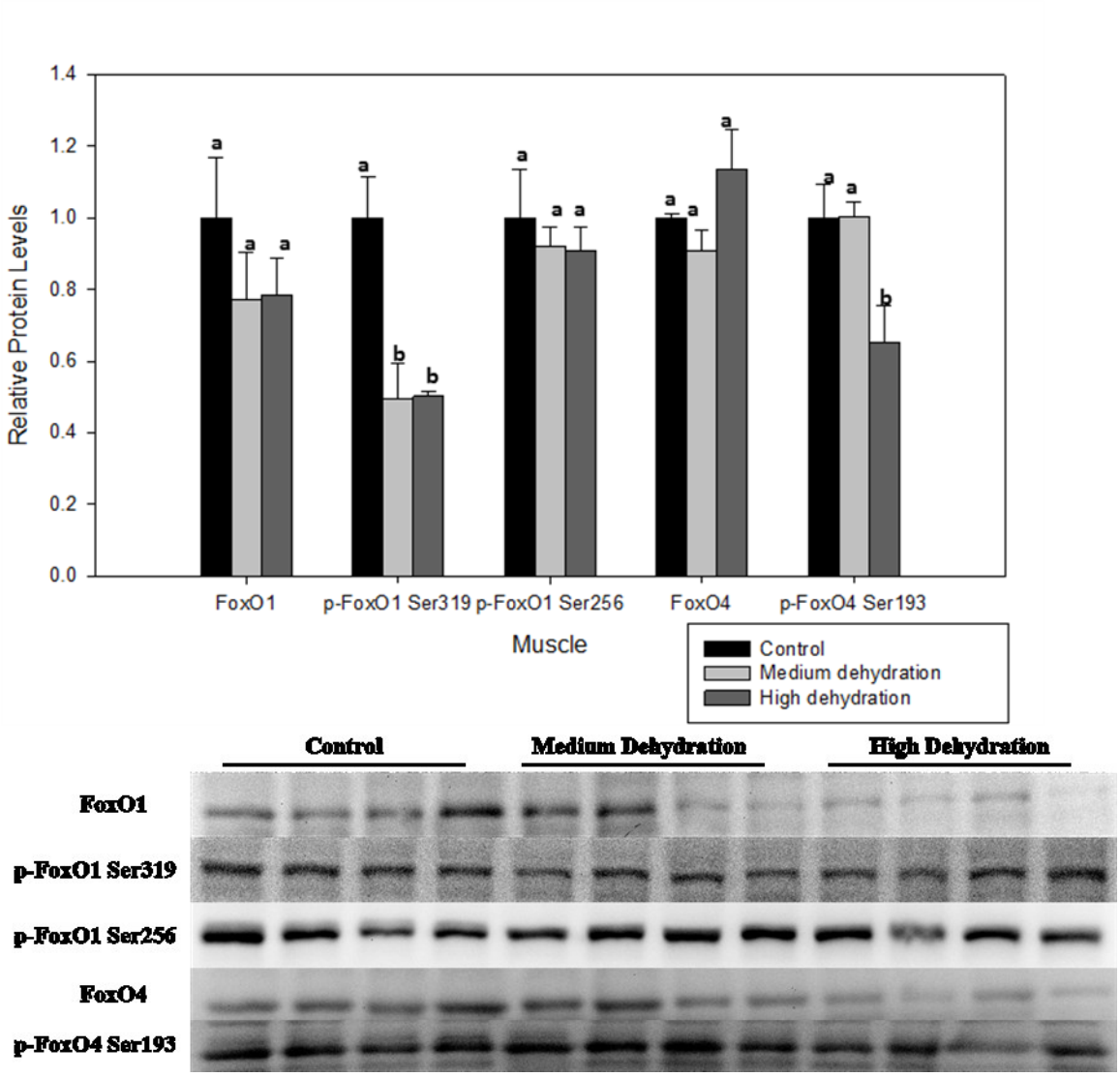

Figure 3.15. Western blot analysis demonstrating the effect of medium and high dehydration on FoxO1 and FoxO4 protein expression and phosphorylation at serine 319, 256 (FoxO1) and serine 193 (FoxO4) in *Xenopus laevis* skeletal muscle. Statistically significant differences were determined by one-way ANOVA and Tukey's post-hoc test, and denoted by different letters above each bar, where $p < 0.05$. Other information as in Figure 3.3.

Table 3.4. Cross-species referencing of coding sequences within mRNA and respective protein sequences for selected genes to determine sequence conservation in *Xenopus laevis*. Akt, TSC2, Raptor and 4EBP sequences from *Xenopus tropicalis*, *Danio rerio*, and *Mus musculus* were compared to *Xenopus laevis* using NCBI, Xenbase and Ensembl databases to assess nucleotide/amino acid conservation.

Gene – Species	Description of best NCBI nucleotide BLAST result	Nucleotide percent Identity (%)	Description of best NCBI protein BLAST result	Protein Percent Identity (%)	Conserved protein domains
Akt - Xenopus tropicalis	Xenopus laevis v-akt murine thymoma viral oncogene homolog 2 (akt2), mRNA (NM_001086622.1)	96	Xenopus laevis Akt1/Protein Kinase B (NP_001083878.1)	82	cd01241, Protein Kinase B-like pleckstrin homology, cd05571, Catalytic domain of the Protein Serine/Threonine Kinase, Protein Kinase B
Akt - Danio rerio	Xenopus laevis v-akt murine thymoma viral oncogene homolog 2 (akt2), mRNA (NM_001086622.1)	74	Xenopus laevis Akt/Protein Kinase B (NP_001085101.1)	81	
Akt - Mus musculus	Xenopus laevis v-akt murine thymoma viral oncogene homolog 1 (akt1), mRNA >gb|AF317656.1|(NM_001090409.1)	76	Xenopus laevis Akt1/Protein Kinase B (NP_001083878.1)	93	
TSC2 - Xenopus tropicalis	Xenopus laevis TSC2 mRNA Xenbase ID 1691717	92	Xenopus laevis TSC2 Protein Xenbase ID 1691717	95	Tuberin superfamily
TSC2 - Danio rerio	Xenopus laevis TSC2 mRNA Xenbase ID 1691717	65	Xenopus laevis TSC2 Protein Xenbase ID 1691717	54	Tuberin superfamily
TSC2 - Mus musculus	Xenopus laevis TSC2 mRNA Xenbase ID 1691717	68	Xenopus laevis TSC2 Protein Xenbase ID 1691717	69	Tuberin superfamily
Raptor - Xenopus	Xenopus laevis regulatory associated protein of MTOR, complex 1 (rptor), mRNA	92	regulatory associated protein of MTOR, complex	98	cd00200, WD40 domain, found in

tropicalis	(NM_001094708.1)		1 [Xenopus laevis] >gb|AAH84088.1| LOC495002 protein [Xenopus laevis] (NP_001088177.1)		a number of eukaryotic proteins that cover a wide variety of functions including adaptor/regulatory modules in signal transduction, pre-mRNA processing and cytoskeleton assembly
Raptor - Danio rerio	Xenopus laevis regulatory associated protein of MTOR, complex 1 (rptor), mRNA (NM_001094708.1)	76	regulatory associated protein of MTOR, complex 1 [Xenopus laevis] >gb|AAH84088.1| LOC495002 protein [Xenopus laevis] (NP_001088177.1)	88	
Raptor - Mus musculus	Xenopus laevis regulatory associated protein of MTOR, complex 1 (rptor), mRNA (NM_001094708.1)	78	regulatory associated protein of MTOR, complex 1 [Xenopus laevis] >gb|AAH84088.1| LOC495002 protein [Xenopus laevis] (NP_001088177.1)	91	
4EBP - Xenopus tropicalis	**Xenopus laevis** eukaryotic translation initiation factor 4E binding protein 2 (eif4ebp2), mRNA	96	eukaryotic translation initiation factor 4E binding protein 2 [Xenopus laevis] >gb|AAH68624.1| (NP_001084529.1)	96	eIF-4EBP Superfamily, pfam05456, Eukaryotic translation initiation factor 4E binding protein (EIF4EBP)
4EBP - Danio rerio	**Xenopus laevis** eukaryotic translation	74	eukaryotic translation initiation factor 4E binding	72	

	initiation factor 4E binding protein 2 (eif4ebp2), mRNA		protein 2 [Xenopus laevis] >gb|AAH68624.1| (NP_001084529.1)		
4EBP - Mus musculus	**Xenopus laevis** eukaryotic translation initiation factor 4E binding protein 2 (eif4ebp2), mRNA	77	eukaryotic translation initiation factor 4E binding protein 2 [Xenopus laevis] >gb|AAH68624.1| (NP_001084529.1)	75	

Figure 3.16. Amino acid sequence alignment analysis between *X. laevis*, *X. tropicalis, H. sapiens and R. norvegicus* for proteins TSC2, Akt and 4EBP done on EMBL-EBI's Clustal Omega program. Of interest are the phosphorylated sites threonine 1462 in TSC2, serine 473 in Akt, and threonine 37/46 in 4EBP (boxed in red). These residues, when phosphorylated, are detected by antibodies listed in Table 3.2. However, threonine 1462 in *Xenopus* TSC2 does not appear to be conserved when compared to the human TSC2 protein, which explains why it failed to cross-react with an anti-phospho-TSC2 (T1462) antibody designed for humans and mice.

3.4. DISCUSSION

3.4.1 Suppression of Akt activity in the dehydrating African clawed frog

The first part of this study was to establish the state of Akt itself during exposure to dehydration. Akt requires phosphorylation of both serine 473 and threonine 308 sites in order to be active. The results suggested that in both liver and skeletal muscle, Akt activity decreases in response to dehydration stress (Figures 3.3 and 3.4). A particularly strong decrease in Akt was seen in muscle where both total Akt protein and relative phosphorylation at both sites decreased by 40-65% under both medium and high dehydration. In current literature, it is known that mTORC2 phosphorylates Akt at serine 473 before PDK1 phosphorylates the threonine 308 residue (Dann *et al*., 2007). Hence, to understand the mechanism by which Akt phosphorylation was regulated, the study next examined the upstream regulators of Akt Thr 308 phosphorylation – PDK1 and PTEN. In liver, Akt phosphorylation at threonine 308 remained constant throughout dehydration as did total PDK1 levels and PDK1 phosphorylation state which regulates PDK1 kinase activity (Figure 3.5). An increase in PTEN phosphorylation inhibits the phosphatase activity of this enzyme which may explain why PDK1 phosphorylation and Akt phosphorylation (threonine 308) remained constant throughout dehydration exposure in liver. However, the reduction in Ser 473 phosphorylation of about 25% does indicate reduced Akt activity in liver. This decrease in Akt phosphorylation may be due to decreases in mTORC2 kinase activity and suggests that this complex warrants further study with respect to its behavior during dehydration. In skeletal muscle, reduced phosphorylation of Akt was noted at both serine 473 and threonine 308 (Figure 3.4). The decrease in muscle Thr 308 phosphorylation may be accounted for by decreases in PDK1

protein levels seen in late dehydration, and reduced PDK1 phosphorylation in medium dehydration (Figure 3.6). Unlike in liver, trends in muscle PTEN regulation during dehydration suggest that it may play a less important role in regulating Akt phosphorylation. Likewise, dehydration-induced regulation of mTORC2 may account for decreases in muscle Akt Ser 473 phosphorylation and requires further study. Ultimately, the results of this study are consistent with reduced Akt kinase activity in response to dehydration exposure in the liver and skeletal muscle of the African clawed frog.

3.4.2 Akt regulates protein translation via mTORC1 dissociation

One of the purposes of this study was to understand how the mTORC1 complex was regulated in a non-mammalian vertebrate model that underwent metabolic rate depression. As stated in the introduction, mTORC1 activity has been shown to be depressed in mammalian hibernators via the traditional Akt/TSC2/mTOR pathway (Wu and Storey, 2012; Figures 3.1 and 3.2). However, during hypometabolism in invertebrates, previous studies suggested that the Akt/TSC2/mTOR pathway had been uncoupled – indicating that there were other mechanisms at work that controlled the RPP of 4EBP to regulate protein translation (Storey and Storey, 2012). In the African clawed frog, the current results do indicate that Akt plays a pivotal role in the regulation of the mTORC1 complex. This regulation ultimately results in the suppression of protein translation as part of the overall hypometabolic state. However, the mechanism by which it occurs seems to differ from the traditional Akt/TSC2/mTOR/Raptor pathway seen in mammals.

3.4.3 Akt does not regulate mTORC1 via TSC2 in X. laevis: TSC2 is not conserved

The members of mTORC1 were differentially regulated in liver and muscle throughout dehydration at both the protein level and phosphorylation state. In liver, mTOR protein and phosphorylation state both increased in medium dehydration (Figure 3.7). Phosphorylation of mTOR (serine 2448) is a modification that actually promotes mTORC1 formation and subsequent facilitation of protein translation. Furthermore, although Raptor protein levels decreased in liver in response to dehydration (which could reduce mTORC1 formation), its phosphorylation state remained constant (Figure 3.7). It would have been expected that if Akt played a role in the dissociation of mTORC1 during dehydration, that a decrease in Raptor phosphorylation would occur. As mentioned earlier, both the pro-complex phosphorylation of mTOR at serine 2448 and Raptor at serine 863 are regulated by Akt-controlled TSC2. Unlike Akt and Raptor, TSC2 could not be detected in *X. laevis* tissue extracts using mammalian antibodies and a search for a TSC2 sequence within the *X. laevis* genome suggests why. A key TSC2 residue known to be phosphorylated by Akt (Thr 1462) is not conserved in *X. laevis* (Figure 3.16). This suggests that TSC2 in *X. laevis* regulation warrants further study and this could alter the signaling and regulation of protein synthesis. In skeletal muscle, mTOR total protein and relative phosphorylation levels decreased (Figure 3.8). Phosphorylation of Raptor in skeletal muscle also decreased. Although these results could indicate a similar mechanism to mTORC1 regulation as in mammals, the noted changes in TSC2 protein sequence clearly has potential to disrupt the traditional Akt/TSC2/mTOR/Raptor pathway seen in mammals.

3.4.4 mTORC1 formation is regulated by Akt-targeted PRAS40 and GβL

Although TSC2 is crucial for Akt regulation of mTORC2 in another model of hypometabolism, the hibernating thirteen-lined ground squirrel, it is not well conserved in the African clawed frog. Hence, it appears that the mechanism by which Akt regulates mTORC1 in the African clawed frog is via the phosphorylation of PRAS40. PRAS40 is inactivated when phosphorylated by Akt. When active, PRAS40 binds to the mTORC1 member Raptor and physically prevents the formation of the mTORC1 complex. The present results suggest that the decrease in Akt activity seen under dehydration exposure is responsible for activation (de-phosphorylation) of PRAS40 in both liver and skeletal muscle tissues (Figures 3.7 and 3.8). This ultimately signals PRAS40 to sequester Raptor away from mTOR and prevent mTORC1 formation. In the mammalian hibernator, PRAS40 has also been studied but did not appear to play an active role in the dissociation of mTORC1 (Wu and Storey, 2012). In both liver and skeletal muscle of *X. laevis*, total protein levels of GβL also decreased with increasing dehydration exposure (Figures 3.7 and 3.8). As a member of the mTORC1 complex, a decrease in GβL levels has also been associated with mTORC1 dissociation (Kim *et al*., 2003) and reduced GβL levels were also seen in the thirteen-lined ground squirrel during torpor, concurrent with reduced TORC1 (Wu and Storey, 2012). Hence, the reduction in GβL total protein along with Akt-mediated activation of PRAS40 seem to be the two mechanisms by which the African clawed frog depresses mTORC1 activity in response to dehydration.

3.4.5 Downstream effects of Akt-mediated mTORC1 dissociation in dehydration

To assess the effects of Akt-mediated decreases in mTORC1 kinase activity during dehydration, two downstream targets were studied, 4EBP and p70 phosphorylation (Figures 3.9, 3.10). When 4EBP is activated (by de-phosphorylation), it binds with eIF4E and prevents it from bringing mRNA transcripts to the ribosome for translation. Hence, reduced phosphorylation of 4EBP (as seen during dehydration) means that a greater proportion of eIF4E is bound and unable to participate in message delivery to the ribosome. Therefore, decreased levels of phosphorylated 4EBP signaled translational suppression. Since mTORC1 is suppressed in both liver and skeletal muscle, 4EBP phosphorylation accordingly decreased in both liver and muscle in response to dehydration (Figures 3.9, 3.10). Liver 4EBP and eIF4E levels remained constant throughout dehydration as did muscle eIF4E (although muscle 4EBP decreased), indicating that the translational machinery remains in place under stress conditions and thereby highlighting the importance of phosphorylation in protein translation suppression (Figures 3.9, 3.10). Another target of mTORC1 is the kinase p70, which also showed a reduced phosphorylation state in both liver and muscle during dehydration (Figures 3.9, 3.10). An Akt/mTORC1 mediated decrease in p70 phosphorylation would result in a decrease of phosphorylation in its most established target, the ribosomal protein s6. This could serve as another mechanism of halting protein translation under dehydration stress. However, the results show that ribosomal protein s6 phosphorylation increased strongly in both liver and skeletal tissue in response to dehydration stress (Figures 3.9, 3.10). A possible explanation for this result is that s6 is subject to phosphorylation by other kinases. Indeed, the MEK/ERK pathway has been shown to activate p90 kinase in

response to dehydration in *X. laevis* (Malik and Storey, 2009; Storey and Storey, 2012). Although both p70 and p90 protein kinases can phosphorylate ribosomal s6 protein, they are both regulated by different pathways. The role played by p70 in translational suppression in the dehydrating African clawed frog is therefore not as important as the inhibition of eIF4E via 4EBP. However, recent studies have shown that p70 kinase activation coupled with eIF4E inactivation may play a role in facilitating G1 cell cycle arrest (Yellen *et al*., 2013). Cell cycle arrest is further studied in Chapter 4. From the present results, Akt-targeted mTORC1 appears to be responsible for facilitating depression of protein translation and potentially facilitating cell cycle arrest during dehydration of both liver and muscle.

3.4.6 Akt-regulated cell cycle inhibitors p21/p27 (Cip/Kip)

As previously stated, Akt is known to phosphorylate the cell cycle inhibitors p21 and p27. By phosphorylating p21 at threonine 145 and p27 at serine 187, Akt inactivates these cell cycle inhibitors thereby facilitating for cell cycle progression. Both cell cycle inhibitors in liver and p27 in muscle, showed reduced phosphorylation during dehydration, potentially Akt-mediated (Figures 3.11 and 3.12). However, re-phosphorylation of muscle p21 occurred during the medium to high dehydration transition which suggests that Akt-mediated phosphorylation may not be the only factor involved in p21 control in muscle since total Akt and Akt phosphorylation state did not change between medium and high dehydration. These results suggest that decreasing Akt activity in response to dehydration may be facilitating cell cycle arrest by activating the

cell cycle inhibitors p21 and p27 particularly in liver, although p27 also appears to be active in dehydrated skeletal muscle.

3.4.7 GSK-3β, FoxO1 and FoxO4 are not tightly regulated by Akt in dehydration

Akt is also well-known to phosphorylate and activate GSK-3β kinase on serine 9, thereby exerting an effect on glucose/glycogen metabolism as well as the many other targets of GSK-3β action. From the results of this study, the Akt/GSK-3β pathway appears to be uncoupled in dehydrating frogs. Despite decreased Akt activity in liver and muscle, GSK-3β phosphorylation either increased (medium dehydration liver) or remained constant (Figure 3.13). Although GSK-3β was explored as a potential target for glucose metabolism during dehydration, GSK-3β may also play a role in the facilitation of cell cycle arrest by phosphorylating cyclin D (Yang *et al*., 2006a, b). The role of GSK-3β will be further explored in Chapter 4. However, Akt does not appear to play a role in regulating GSK-3β in dehydration.

Results of this study also showed that Akt localization to the nucleus was reduced during dehydration in both liver and muscle (Figures 3.3 and 3.4). From this result, it was hypothesized that removal of Akt from the nucleus would allow for de-phosphorylation and activation of FoxO transcription factors which would allow transcription of key pro-survival genes. Studies have shown that Akt is responsible for phosphorylating FoxO1 at serine 256 and 319, and FoxO4 at serine 193 (Obsil *et al*., 2003; Zhang *et al*., 2002). Although some key FoxO phosphorylation sites decreased in dehydration, muscle FoxO1 serine 256 phosphorylation remained constant throughout dehydration, and liver FoxO1 serine 256 and FoxO4 serine 193 phosphorylation actually increased in medium

dehydration (Figures 3.14, 3.15). This differential phosphorylation suggests that FoxO1 and FoxO4 may play key roles in the cellular responses to dehydration; indeed, Malik and Storey, 2011) linked changes in FOXO1 with upregulation of antioxidant enzymes, catalase and superoxide dismutase, during *X. laevis* dehydration. However, the present results suggest that Akt does not tightly regulate the activity of FoxO1 and FoxO4 in dehydration.

3.4.8 Conclusion

In response to dehydration stress, Akt activity is reduced in both liver and skeletal muscle of the African clawed frog. As a result, the mTORC1 pathway is dissociated and suppressed. However, dissociation of mTORC1 in *X. laevis* does not appear to follow the same pathway as seen in mammalian models, since TSC2 is poorly conserved or lacking. Instead, PRAS40 appears to play a pivotal role in deactivating mTORC1 by sequestering Raptor away from mTOR. Reduced GβL levels also contribute to mTORC1 dissociation in both tissues. As a result of mTORC1 deactivation, 4EBP is activated and binds to eIF4E to suppress protein translation initiation. Furthermore, mTORC1 dissociation leads to inactivation of p70 s6 kinase. Akt does not appear to tightly regulate FoxO transcription factors or the kinase GSK-3β in response to dehydration. However, differential phosphorylation of FoxO1 and FoxO4 suggests that they play important roles in dehydration. Differential phosphorylation of p70 s6 kinase and GSK-3β may suggest that they may play roles in cell cycle regulation, which is discussed in the following chapter.

CHAPTER 4

METABOLIC DEPRESSION IN THE ESTIVATING AFRICAN CLAWED FROG BY CELL CYCLE ARREST

4.1 INTRODUCTION

Various environmental stressors, such as cold, anoxia, and dehydration are dealt with by animals via entry into hypometabolic states. A major regulator of metabolic rate depression in these key animal models is posttranslational modification of proteins, such as by phosphorylation. As discussed in Chapter 3, complex cascade reactions of changes in phosphorylation state have the potential to control energy expensive processes such as gene transcription, glucose metabolism, protein translation, and cell cycle control. In the dehydrating *Xenopus laevis*, my results have suggested that phosphorylation plays a key role in suppressing protein translation and activating cell cycle inhibitors. Indeed, animals adapting to environmental stresses use cell cycle arrest as a crucial strategy for energy conservation (Storey, 2012). For example, a study of cell cycle regulators in the freeze tolerant wood frog showed elements of cell cycle suppression in response to freezing, anoxia and dehydration stress, with reversal during recovery of these stresses (Zhang and Storey, 2012). Likewise, studies of the hibernating thirteen-lined ground squirrel demonstrated that decreases in select cyclin proteins coupled with increases in cyclin dependent kinase (CDK) inhibitors facilitated cell cycle arrest during periods of torpor (Wu and Storey, 2012). Furthermore, in overwintering anoxia tolerant turtles, studies have shown that microRNA-facilitated reduction of cyclin D protein levels is pivotal to cell cycle arrest (Biggar and Storey, 2012). Similar to the importance of the kinase Akt, which facilitates energy conservation in response to environmental stressors by suppressing protein translation, cell cycle arrest appears to be another conserved strategy which promotes survival during hypometabolism in animals.

The present chapter focuses on characterizing the state of the cell cycle in liver and skeletal muscle of *X. laevis* under dehydration stress. To do this, a broad study of cyclins and CDKs was performed. In chapter 3, negative regulators of the cell cycle (the CDK inhibitors p21 and p27) were found to be activated under dehydration stress. The present chapter explores the role of positive cell cycle regulators, the protein phosphatases cdc25a and cdc25c. Lastly, this chapter analyzes the transcription factor E2F which plays a key role in cell cycle regulation. The cell cycle promoting E2F1 isoform and cell cycle inhibiting E2F4 isoform were analyzed along with the retinoblastoma protein (Rb) which is a crucial regulator of E2F activity. Studies demonstrate that E2F1 is responsible for cell cycle progression by promoting the gene expression of cyclins A, B and E, among other pro-cycling targets (Li *et al*., 2012; Russo *et al*., 2006; Ohtani *et al*., 1995; Heinglein *et al*., 1994; Botz *et al*., 1996).

4.1.1 The regulation of the transcription factor E2F and the retinoblastoma protein (Rb)

The E2F transcription factor family is comprised of eight members that regulate cell cycle progression. Transcription factors E2F1, E2F2, and E2F3a are cell cycle activators and are responsible for the expression of pro-cycling genes. The E2F family also includes E2F3b, E2F4, E2F5, E2F6, E2F7 and E2F8, which are cell cycle inhibitors. All inhibitory E2F proteins work to prevent the gene expression of activating E2F targets. However, the mechanisms by which the inhibitory E2Fs function differ between members. The E2F3b, E2F4, and E2F5 members inhibit gene expression by associating with E2F binding elements on E2F target promoters so that activating E2F transcription

factors cannot induce gene expression (Timmers *et al*., 2007). The E2F6 member acts by recruiting polycomb-group proteins, which ultimately result in bringing chromatin remodelling complexes to E2F target genes so that transcription is inhibited (Timmers *et al*., 2007). E2F7 and E2F8 are inhibitors of cycle progression, but the mechanism by which they work is yet to be understood (Timmers *et al*., 2007). In this chapter, the relative total and nuclear levels of E2F1 (activating) and E2F4 (inhibitory), as well as the relative DNA binding by these two E2F proteins was assessed in response to dehydration of African clawed frogs.

Unlike the FoxO transcription factors which were previously discussed in Chapter 3, E2F regulation due to phosphorylation is not well characterized. However, E2F1 regulation by the tumour repressor protein Rb (retinoblastoma protein), has been extensively studied. In cycling cells, Rb remains hyperphosphorylated, which prevents it from interacting with E2F1 (Nicholas *et al*., 1998; Tyagi *et al*., 2002; Burke *et al*., 2010; Brantley and Harbour, 2000). Phosphorylation of Rb is therefore required for cell cycle progression (Figure 4.1a). Phosphorylation of Rb by cyclin-CDK complexes crucially occurs on serine 780 (Tagliati *et al.*, 2006; Tyagi *et al*., 2002). However, other key phosphorylation sites include serine 608 and serine 807 (Tyagi *et al*., 2002; Burke *et al*., 2010; Brantley and Harbour, 2000). When Rb is hypophosphorylated (or dephosphorylated), it is in its active state. Hypophosphorylated Rb is able to bind to E2F1, thereby preventing E2F1 action in stimulating the expression of target genes required to facilitate cell cycle progression. Hence, rather than post-translationally targeting E2F1 directly, regulation of E2F1 is dependent on the phosphorylation state of Rb. Lastly, there are conflicting studies which disagree on the role played by acetylated

Rb in cycling or arrested cells, as the mechanism of Rb acetylation has yet to be fully understood. Recently, however, acetylation has been shown to play a key role in Rb regulation. Acetylation of Rb was required for proper nuclear localization (Pickard *et al*., 2010). This chapter assesses how Rb is regulated post-translationally (phosphorylation and acetylation) at both whole cell and nuclear levels.

4.1.2 The regulation of cyclins and cyclin dependent kinases (CDKs)

Since E2F action in stimulating gene transcription is heavily dependent on the state of Rb, it is crucial to understand the regulation of the protein kinases which phosphorylate Rb under dehydration stress. During the M-to-G1 stage transition, Rb is hypophosphorylated in order to facilitate cell cycle arrest (Figure 4.1b). Cell cycle progression is allowed to continue only when cellular machinery has successfully analyzed the cell for DNA damage. A sequential series of phosphorylations to Rb follows a successful DNA integrity check, and then the cell is ready to progress from G1 to the S phase. First, CDK4/Cyclin D and CDK6/Cyclin D complexes phosphorylate Rb. Then, CDK2/Cyclin E further phosphorylates Rb in order to produce a hyperphosphorylated state, where Rb can no longer prevent E2F1 from binding to DNA (Tagliati *et al*., 2006). Since it is well characterized that Rb remains phosphorylated throughout the S, G2 and M phases of the cell cycle, any significant drop in Rb phosphorylation state suggests that the cells have arrested at the G1 phase (Munger and Howley, 2002). Furthermore, one mechanism by which cell cycle arrest occurs is through the myostatin/GSK-3β/Cyclin D pathway, where GSK-3β targets Cyclin D for proteasomal degradation (Diehl *et al*.,

2013; Yang *et al*., 2007; Yang *et al*., 2006). As seen in Chapter 3, although GSK-3β does not appear to be under Akt control during dehydration stress, GSK-3β may play a role in inducing cell cycle arrest by signalling for rapid cyclin D degradation by proteasomes (Figure 3.13). Since CDKs (CDK1/CDC2, CDK2, CDK4, CDK6) and cyclin proteins (Cyclin A, B, D and E) play pivotal roles in Rb phosphorylation, these targets are also studied in the African clawed frog (both total and nuclear levels) to assess cell cycle regulation during dehydration stress.

Studies of cyclins are not only crucial because of their roles in cell cycle control by regulating CDK activities, but also because they are downstream targets of E2F1. As previously mentioned, the transcription factor E2F1 regulates the transcription of targets required for cell cycle progression. E2F1 has been shown to regulate cyclin proteins, which act to facilitate cell cycle progression by activating CDKs (Li *et al*., 2012; Russo *et al*., 2006; Ohtani *et al*., 1995; Heinglein *et al*., 1994; Botz *et al*., 1996). However, E2F1 also regulates other target genes, such as proliferating cell nuclear antigen (PCNA) (Thacker *et al*., 2003; Egelkrout *et al*., 2002). The PCNA protein has a key role in DNA replication by acting as a processivity factor for DNA polymerase; it facilitates DNA polymerase activity without the enzyme having to let go of the target DNA strand (Funk *et al*., 1997). Without such a crucial mechanism in place, the cell cannot proceed from the G1 to the S phase where DNA replication occurs. An analysis of PCNA and the cyclin family of proteins in this chapter may shed light on changes to E2F-induced gene transcription and the state of the cell cycle under dehydration stress.

4.1.3 The regulation of the cell cycle promoting cdc25 phosphatases

Results from Chapter 3 suggested that a decrease in Akt activity may be responsible for the activation of the cell cycle inhibitors p21 and p27, which bind and inhibit cyclin-CDK complexes, and ultimately cause cell cycle arrest in the G1 phase. In addition to negative inhibitors of the cell cycle, there are positive cell cycle regulators which target CDKs to promote cell cycle progression. Unlike phosphorylation of Rb which results in cell cycle progression, phosphorylation of CDKs at certain sites results in cell cycle arrest. The phosphatases cdc25a and cdc25c are known to play diverse roles. Among these roles, cdc25a removes inhibitory phosphate groups from CDKs to allow transition from the G1 to S phase, and cdc25c removes phosphate groups from CDKs to facilitate the G2 to M transition (Rother *et al*., 2007; Li *et al*., 2008). Since negative cyclin/CDK regulators were studied in Chapter 3, this chapter analyzes the differential expression, nuclear localization, and phosphorylation of positive cyclin/CDK regulators, cdc25a and cdc25c, under dehydration stress.

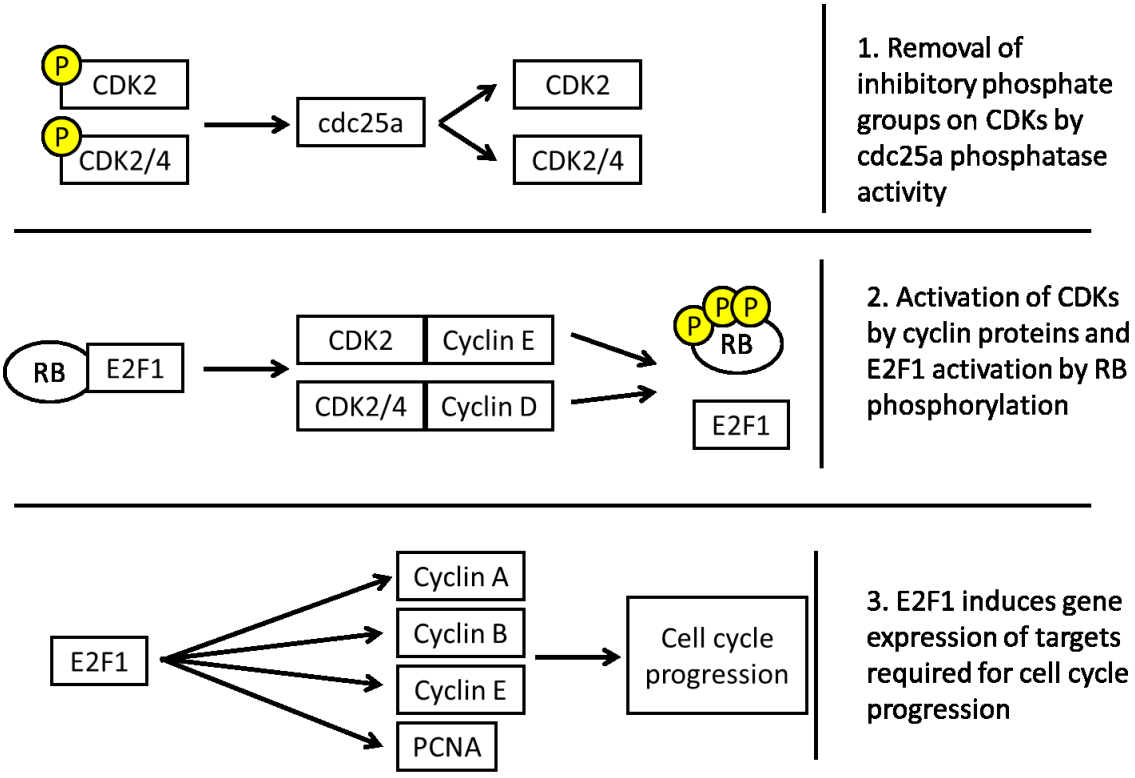

Figure 4.1a. Current understanding of the events during the G1 to S phase of the mammalian cell cycle in the literature. E2F1 is permitted to induce gene expression of targets required for cell cycle progression only when CDKs are capable of forming active complexes with their respective cyclin protein targets and then hyperphosphorylate and suppress Rb allowing E2F1 to be released.

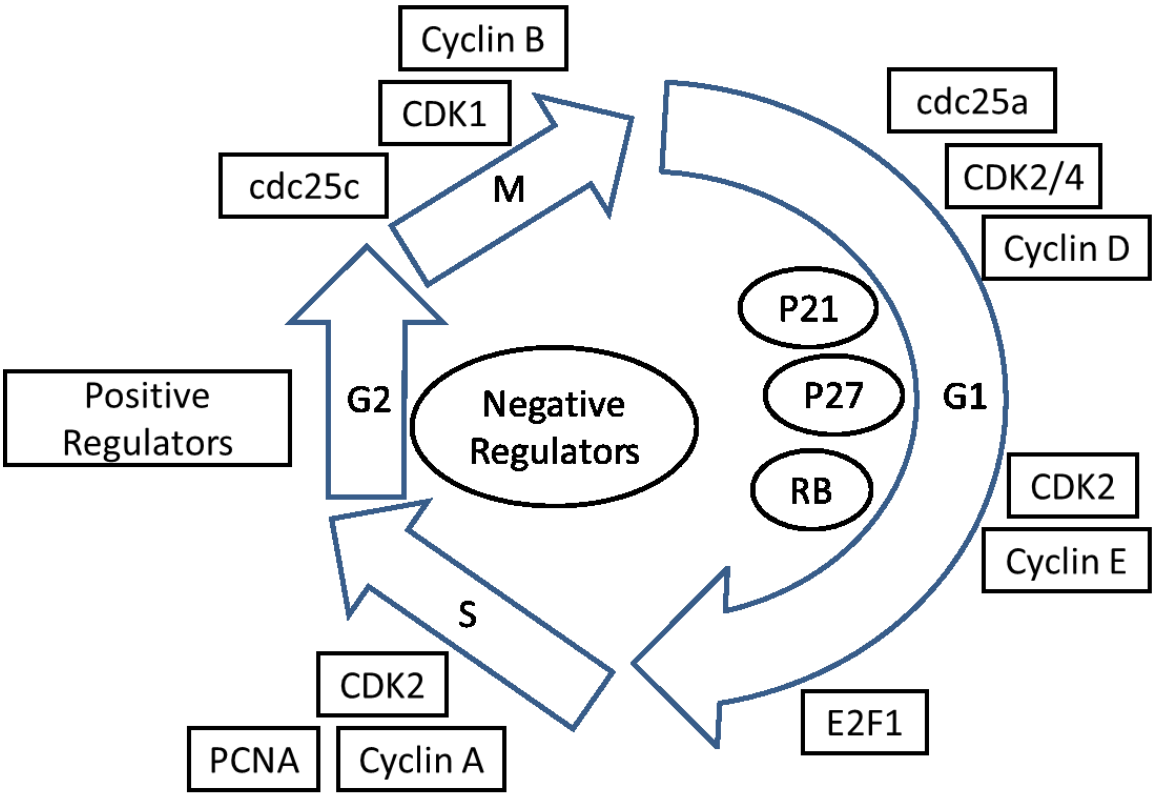

Figure 4.1b. Summary of the accepted pathway by which cell cycle progression occurs in mammalian models. Kinase activity by CDKs and phosphatase activity by cdc25s play key roles in allowing E2F1 to signal for expression of genes required for cell cycle progression.

4.2. MATERIALS AND METHODS

4.2.1 Animals and tissue collection

Adult African clawed frogs were treated, sacrificed, and dissected as in Chapter 2.

4.2.2 Soluble protein isolation and Western Blotting

Relative total protein and phosphorylated protein levels were determined using Western blotting as described in Chapter 2. Tables 4.1-4.4 summarize the antibodies and

conditions used for detecting protein and phospho-protein levels of Akt and its downstream targets.

3.2.3 Quantification of relative mRNA levels

Relative mRNA levels were determined using RNA extraction and PCR as described in Chapter 2. Primers used for *pcna* and *α-tubulin* were as follows: *pcna* (Forward 5'-GGTAATCCCTTACAGCCGCC-3'; Reverse 5'-AGCTGCTCCACATCAAGGTC-3') ; *α-tubulin* (Forward 5'-GGAAGATGCTGCCAATAACT-3'; Reverse

5'-GTCTGGAACTCGGTCAGATC-3'). The annealing temperature for *pcna* and *α-tubulin* were 58˚C and 54˚C, respectively.

Sequencing of PCR products was performed by BioBasic and sequence analysis was done on NCBI's nucleotide BLAST.

4.2.4 Statistics

Statistical analysis was performed as described in Chapter 2. Data in figures are presented relative to control data which were standardized to 1. Error bars represent standard error of the mean (SEM). Statistical analysis used one-way ANOVA and Tukey's post-hoc test with $p < 0.05$ accepted as significant.

Table 4.1. Summary of Rb/E2F-related antibodies and Western blot experimental conditions.

Primary Antibody	Size	Blocking Condition	Probing Conditions (dilution)	Secondary Antibody (dilution)	Source of Primary Antibody
Rabbit anti-E2F1	~ 43 kDa	2.5% w/v milk for 20 minutes	Overnight Incubation (1: 1000)	Anti-Rabbit IgG-HRP (1:8000)	SantaCruz Biotechnology sc-193
Rabbit anti-E2F4	~ 60 kDa	2.5% w/v milk for 20 minutes	Overnight Incubation (1: 1000)	Anti-Rabbit IgG-HRP (1:8000)	SantaCruz Biotechnology sc-6851
Rabbit anti-p130	~ 130 kDa	2.5% w/v milk for 20 minutes	Overnight Incubation (1: 1000)	Anti-Rabbit IgG-HRP (1:8000)	SantaCruz Biotechnology sc-317
Rabbit anti-p-Rb^{Ser780}	~ 110 kDa	2.0% w/v milk for 10 minutes	Overnight Incubation (1: 1000)	Anti-Rabbit IgG-HRP (1:8000)	Cell Signaling #9300
Rabbit anti-p-Rb^{Ser608}	~ 110 kDa	2.0% w/v milk for 10 minutes	Overnight Incubation (1: 1000)	Anti-Rabbit IgG-HRP (1:8000)	SantaCruz Biotechnology sc-19806
Rabbit anti-p-Rb^{Ser807}	~ 110 kDa	2.0% w/v milk for 10 minutes	Overnight Incubation (1: 1000)	Anti-Rabbit IgG-HRP (1:8000)	Cell Signaling #9308
Rabbit anti-Ac-$Rb^{Lys874/875}$	~ 110 kDa	2.5% w/v milk for 10 minutes	Overnight Incubation (1: 1000)	Anti-Rabbit IgG-HRP (1:8000)	Cell Signaling #2525

Table 4.2. Summary of antibodies and Western blot conditions for cell pro-cycling targets.

Primary Antibody	Size	Blocking Condition	Probing Conditions (dilution)	Secondary Antibody (dilution)	Source of Primary Antibody
Rabbit anti-Cyclin A	~ 55 kDa	2.5% w/v milk for 20 minutes	Overnight Incubation (1: 1000)	Anti-Rabbit IgG-HRP (1:8000)	Abcam Cat No. kit-ab6552
Rabbit anti-Cyclin B	~ 55 kDa	2.5% w/v milk for 20 minutes	Overnight Incubation (1: 1000)	Anti-Rabbit IgG-HRP (1:8000)	Abcam Cat No. kit-ab6552
Rabbit anti-Cyclin D	~ 36 kDa	2.5% w/v milk for 20 minutes	Overnight Incubation (1: 1000)	Anti-Rabbit IgG-HRP (1:8000)	SantaCruz Biotechnology sc-717

Rabbit anti-p-Cyclin D^{Thr286}	~ 36 kDa	5.0% w/v milk for 30 minutes	Overnight Incubation (1: 1000)	Anti-Rabbit IgG-HRP (1:8000)	Cell Signaling #2921
Rabbit anti-Cyclin E	~ 47 kDa	2.5% w/v milk for 20 minutes	Overnight Incubation (1: 1000)	Anti-Rabbit IgG-HRP (1:8000)	Abcam Cat No. kit-ab6552
Rabbit anti-PCNA	~ 17 kDa	2.5% w/v milk for 20 minutes	Overnight Incubation (1: 1000)	Anti-Rabbit IgG-HRP (1:8000)	SantaCruz Biotechnology sc-7907

Table 4.3.Summary of antibodies for CDKs and their Western blot conditions.

Primary Antibody	**Size**	**Blocking Condition**	**Probing Conditions (dilution)**	**2º Antibody (dilution)**	**Source of Primary Antibody**
Rabbit anti-CDK1/CDC-2	~ 34 kDa	2.0% w/v milk for 20 minutes	Overnight Incubation (1: 1000)	Anti-Rabbit IgG-HRP (1:8000)	GenScript Corp. A01295
Rabbit anti-CDK2	~ 34 kDa	2.5% w/v milk for 20 minutes	Overnight Incubation (1: 1000)	Anti-Rabbit IgG-HRP (1:8000)	SantaCruz Biotechnology sc-748
Rabbit anti-CDK4	~ 34 kDa	2.5% w/v milk for 20 minutes	Overnight Incubation (1: 1000)	Anti-Rabbit IgG-HRP (1:8000)	Abcam Cat No. ab6553
Rabbit anti-CDK6	~ 40 kDa	2.5% w/v milk for 20 minutes	Overnight Incubation (1: 1000)	Anti-Rabbit IgG-HRP (1:8000)	Abcam Cat No. ab6553

Table 4.4.Summary of antibodies for cdc25 phosphatases and their Western blot conditions.

Primary Antibody	**Size**	**Blocking Condition**	**Probing Conditions (dilution)**	**2º Antibody (dilution)**	**Source of Primary Antibody**
Rabbit anti-cdc25a	~ 65 kDa	2.5% w/v milk for 20 minutes	Overnight Incubation (1: 1000)	Anti-Rabbit IgG-HRP (1:8000)	SantaCruz Biotechnology sc-7157
Rabbit anti-cdc25a^{Ser76}	~ 65 kDa	2.5% w/v milk for 20 minutes	Overnight Incubation (1: 1000)	Anti-Rabbit IgG-HRP (1:8000)	SantaCruz Biotechnology sc-101655
Rabbit anti-cdc25c	~ 55 kDa	2.5% w/v milk for 20 minutes	Overnight Incubation (1: 1000)	Anti-Rabbit IgG-HRP (1:8000)	SantaCruz Biotechnology sc-5620

Rabbit anti-p-cdc25c^{Ser216}	~ 55 kDa	2.5% w/v milk for 20 minutes	Overnight Incubation (1: 1000)	Anti-Rabbit IgG-HRP (1:8000)	GenScript Corp. A00420

4.3 RESULTS

4.3.1 Regulation of protein expression, nuclear localization, and DNA-binding of E2F1 and E2F4 in response to dehydration in X. laevis liver and skeletal muscle.

Regulation of the transcription factors E2F1 and E2F4 during dehydration in the African clawed frog was assessed in liver and leg skeletal muscle. Relative changes in protein expression, nuclear localization, and DNA binding were assessed between control, medium and high dehydration (16.4 % and 31.2 % mean total water body loss, respectively). This was done by performing SDS-PAGE and immunoblotting on protein and nuclear extracts of liver and muscle utilizing appropriate antibodies. The anti-E2F1 and anti-E2F4 antibodies that recognize total E2F1 and E2F4 cross-reacted with frog proteins at approximately 43 and 60 kDa, respectively, the expected size of the vertebrate proteins (Figures 4.2, 4.3). *In vitro* DNA binding experiments were performed by using nuclear extracts in a modified ELISA which quantifies the interactions between native *X. laevis* proteins and oligonucleotide strands containing the E2F binding sequence (Figure 4.5). An electrophoretic mobility shift assay confirmed that the DNA probe used in the experiment successfully was recognized by frog proteins (Figure 4.4).

In liver, no statistically significant changes were found for E2F1 and E2F4 relative protein expression levels over medium and high dehydration, as compared with controls. However, muscle E2F1 content dropped to 41% of control levels under high

dehydration conditions (Figure 4.2). In addition, muscle E2F4 dropped to 75% and 82% of controls, in medium and high dehydration, respectively (Figure 4.2). As for nuclear localization, relative nuclear protein content of E2F1 decreased to 67% of controls in liver under high dehydration conditions, whereas oppositely E2F4 content increased by 1.7-fold over controls (Figure 4.3). In muscle, E2F1 nuclear localization also decreased to 70% and 61% of controls in medium and high dehydration respectively, but E2F4 nuclear content remained constant (Figure 4.3).

Changes in the presence of E2F in the nucleus in response to dehydration suggest that comparable changes in the DNA binding ability of E2F could occur and therefore lead to altered expression of genes regulated by E2F. However, prior to analyzing whether E2F transcription factor binding to DNA changes in response to dehydration, it is necessary to show that *Xenopus* E2F does in fact bind to the DNA probe used. To do this, an EMSA was performed to demonstrate that the DNA probe does form a complex with E2F in nuclear extracts of frogs. Figure 4.4 shows that complexes of protein and DNA were increasingly apparent when larger amounts of protein used (e.g. 40 vs 60 μg). An "antibody shift" negative control was also performed by adding an antibody specific to E2F1 in the reactions, which reduced the amount of DNA-protein complex present (either steric hindrance caused by the antibody inhibited interactions with DNA, or the complexes successfully formed and were significantly larger in molecular weight and migrated more slowly) (Figure 4.4). Two more negative controls were run (no DNA probe and no protein) which also did not result in DNA-protein complex formation (Figure 4.4). Hence, E2F binding to the DNA probe used was validated.

The *in vitro* TF-DNA binding assay was used to determine whether E2F binding to DNA was altered as a result of dehydration stress in liver and muscle tissues. In liver, E2F1 binding significantly decreased to 88% and 87% of control levels, respectively, in response to medium and high dehydration (Figure 4.5). However, liver E2F4 relative DNA binding did not change significantly during dehydration. In muscle, both E2F1 and E2F4 DNA binding decreased with dehydration exposure. Muscle E2F1 binding decreased to 68% and 75% of control levels, respectively, under medium and high dehydration and muscle E2F4 relative binding also decreased to 72% and 76% of control levels, respectively (Figure 4.5).

4.3.2 Regulation of the retinoblastoma protein (Rb) by post-translational modification and nuclear localization, and regulation of p130 (Rb2) protein expression in response to dehydration in X. laevis liver and skeletal muscle.

Regulation of the tumor suppressor retinoblastoma protein (Rb), and its family member p130 (Rb2) during dehydration of the African clawed frog was assessed in liver and skeletal muscle. Western blotting showed that the antibodies used to detect post-translationally modified Rb forms (phosphorylated serine 780, p-serine 608, p-serine 807, and acetylated lysine 874/875) all cross-reacted with frog Rb showing single bands at approximately 110 kDa (Figures 4.6, 4.7, 4.8, and 4.9). Likewise, Western blotting using a total anti-p130 antibody successfully cross-reacted with frog p130 to yield a single band at 130 kDa (Figures 4.6, 4.7, 4.8, and 4.9).

In liver, the detectable amounts of all three phosphorylated Rb sites decreased significantly and progressively with increasing dehydration. Ultimately, relative amounts of phospho-Rb serine 780 decreased to 34%, phospho-Rb serine 608 decreased to 62%, and phospho-Rb serine 807 decreased to 62% of control levels under high dehydration conditions (Figure 4.6). Acetylation of liver Rb also decreased to 72% and 67% of control levels, in medium and high dehydration, respectively (Figure 4.6). However, total liver p130 protein expression did not change significantly with dehydration exposure.

Muscle showed somewhat different responses. Neither acetylation nor phosphorylation of Rb at serine 780 changed over dehydration stress. However, relative levels of phospho-Rb serine 608 increased by 1.6-fold over control levels under high dehydration conditions whereas phospho-Rb serine 807 content decreased to 81% and 83% of control levels in medium and high dehydration, respectively (Figure 4.7). Total protein expression of p130 in muscle also decreased to 57% of control levels under high dehydration conditions (Figure 4.7).

Nuclear localization of phosphorylated Rb was found to change over dehydration stress. In liver phospho-Rb serine 780 levels decreased progressively to 53% and 34% of control levels under medium and high dehydration, respectively (Figure 4.8). Also, nuclear acetylated Rb was found to increase by 1.66 and 1.72-fold of control levels in medium and high dehydration. However, relative nuclear content of phospho-Rb serine 608 and serine 807, as well as total p130 remained constant throughout dehydration stress in liver.

In muscle nuclear fractions, relative amounts of phospho-Rb serine 608 and serine 807 remained constant throughout dehydration stress. However, nuclear localization

decreased to 81% of control for acetylated Rb under high dehydration, and phospho-Rb serine 780 content decreased to 50% of control values under medium dehydration (Figure 4.9). Nuclear localization of muscle p130 protein decreased significantly to 44% in medium dehydration, but rebounded to control levels high dehydrated frogs (Figure 4.9).

4.3.3 Regulation of the cell cycle regulating cyclin proteins (A, B, D, E) by differential protein expression and nuclear localization, and phosphorylation of cyclin D at threonine 286 in response to dehydration of X. laevis liver and skeletal muscle.

Regulation of the cyclin proteins (Cyclin A, B, D and E) during dehydration of the African clawed frog was assessed in liver and skeletal muscle. Western blotting showed that the antibodies used to detect cyclin A, cyclin B, cyclin D (total and phosphorylated at threonine 286), and cyclin E all cross-reacted with frog cyclins showing single bands at approximately 55, 55, 36 and 47 kDa, respectively, as expected for the vertebrate proteins (Figures 4.10, 4.11, 4.12, and 4.13). Western blotting was used to determine changes to total protein expression, and nuclear localization induced by dehydration stress.

In liver, total levels of cyclin A remained constant with respect to control levels. Cyclin B and E levels decreased under high dehydration to 66% and 46% of control levels, respectively (Figure 4.10). By contrast, cyclin D protein levels increased by 2.7-fold in medium dehydration, but returned to control levels under high dehydration conditions (Figure 4.10). Relative phosphorylation of cyclin D in liver decreased somewhat in medium dehydration to 79% of control levels, and remained low in high

dehydration (73% of control; Figure 4.10). In contrast to the results for liver, there were no statistically significant changes in these proteins in muscle under dehydration stress (Figure 4.11).

In liver, nuclear localization of cyclin proteins remained constant under dehydration stress, with the exception of cyclin D, and phosphorylated cyclin D. Nuclear cyclin D levels decreased to 89% and 71% in medium and high dehydration, respectively (Figure 4.12). The relative amount of phosphorylated cyclin D in nuclear extracts of liver also decreased similarly to 79% of control values under high dehydration (Figure 4.12). Similarly to total levels of muscle cyclin proteins, nuclear content of cyclin proteins did not change in muscle in response to dehydration stress (Figure 4.13).

4.3.4 Regulation of CDK1 (CDC2), CDK2, CDK4 and CDK6 by differential protein expression and nuclear localization, in response to dehydration of X. laevis liver and skeletal muscle.

Regulation of the cyclin dependent kinases (CDK1, CDK2, CDK4, and CDK6) during dehydration of the African clawed frog was assessed in liver and skeletal muscle. Western blotting showed that the antibodies used to detect CDK1/CDC2, CDK2, CDK4 and CDK6 all cross-reacted with the corresponding frog CDK proteins showing a single band at approximately 34, 34, 34 and 40 kDa, respectively (Figures 4.14, 4.15, 4.16, and 4.17). Western blotting was used to determine changes to total protein expression, and nuclear localization induced by dehydration stress.

For total protein expression, all CDK protein levels studied remained constant throughout dehydration stress in both liver and muscle with the exception of muscle CDK6 (Figures 4.14 and 4.15). Under medium and high dehydration, muscle CDK6 decreased to 69% and 62% of control values, respectively (Figure 4.15). However, regulation of CDKs was much more apparent in nuclear localization in both liver and muscle tissues. Under medium and high dehydration, liver CDK1 nuclear localization decreased to 49% and 53% of control values, respectively (Figure 4.16). Nuclear localization of liver CDK4 decreased to 58% of control in medium dehydration, but rebounded to 81% of control in high dehydration. There were no significant changes in nuclear localization for CDK2 and CDK6 in the liver. In muscle, nuclear localization changed under dehydration for CDK2, CDK4 and CDK6, but not CDK1. Muscle nuclear levels for CDK2 decreased to 72% of control in medium dehydration, and remained at that level (73% of control) in high dehydration (Figure 4.17). Muscle CDK4 localization increased in medium dehydration by 1.47-fold of control levels, but dropped to a 1.23-fold higher than controls under high dehydration (Figure 4.17). Nuclear localization of muscle CDK6 dropped to 80% and 81% in medium and high dehydration, as compared to controls (Figure 4.17).

4.3.5 Regulation of positive cell cycle regulators (cdc25a and cdc25c phosphatases) by differential protein expression, phosphorylation and nuclear localization, in response to dehydration of X. laevis liver and skeletal muscle.

Regulation of the positive cell cycle regulators cdc25a and cdc25c during dehydration of the African clawed frog was assessed in liver and skeletal muscle. Western blotting showed that the antibodies used to detect cdc25a (total and phosphorylated serine 76) and cdc25c (total and phosphorylated serine 216) all cross-reacted with frog cdc25a and cdc25c showing a single band at approximately 65 and 55 kDa, respectively (Figures 4.18, 4.19, and 4.20).

In liver, both total and phosphorylated cdc25a were found to decrease under high dehydration conditions. Total cdc25a decreased to 68%, and the phosphorylated form decreased to 76% of control levels (Figure 4.18). Phosphatase cdc25c protein and phospho-protein levels remained constant throughout dehydration stress in liver. In muscle tissue, total protein levels of cdc25a remained constant over dehydration, but relative phosphorylation levels increased to 1.64- and 1.49-fold over control values in medium and high dehydration, respectively (Figure 4.19). Although total cdc25c expression rose by 1.62-fold in high dehydration, total phosphorylated cdc25c was found to decrease to 74% and 76% in medium in high dehydration, with respect to control levels (Figure 4.19).

Similarly to total levels, nuclear levels of liver cdc25a also decreased significantly from control – to 52-80% in medium and high dehydration (Figure 4.20). In addition, phosphorylated liver cdc25a also significantly decreased to 79-80% in medium and high dehydration conditions (Figure 4.20). However, relative total and phosphorylated levels of cdc25c did not change in liver nuclear extracts (Figure 4.20). Nuclear localization muscle cdc25a protein was assessed and found to increase by 1.38-fold and 1.52-fold in medium and high dehydration, respectively (Figure 4.21). The relative levels of phospho-

cdc25a (serine 76) and total cdc25c protein levels in nuclear extracts did not change but phosphorylated cdc25c localization to the nucleus increased by 1.72-fold under high dehydration conditions (Figure 4.21).

4.3.6 Protein and transcript expression of PCNA, an E2F1 downstream target, in response to dehydration of X. laevis liver and skeletal muscle.

Regulation of the direct E2F1 downstream target protein, PCNA, during dehydration of the African clawed frog was assessed in liver and skeletal muscle. Western blotting showed that the antibodies used to detect PCNA cross-reacted with frog PCNA proteins, showing a single band at approximately 29 kDa in both tissues (Figure 4.21). In liver, total PCNA levels decreased to 64% of control values under high dehydration conditions. Oppositely, muscle PCNA levels increased by 1.67-fold and 1.55-fold over controls in medium and high dehydration, respectively (Figure 4.21). As for relative mRNA levels, liver *pcna* transcript levels decreased significantly to 27% and 12% in medium and high dehydration, respectively (Figure 4.21). There were no changes to relative *pcna* transcript levels in muscle in response to dehydration stress (Figure 4.21). The PCR product was sequenced by BioBasic and confirmed to be the *pcna* gene annotated on the annotated *X. laevis* genome using NCBI's nucleotide BLAST alignment program. The amplified transcript was 377 nucleotide bases long. The amplified partial transcript was translated to 123 amino acids which represents ~47% of the full length PCNA protein.

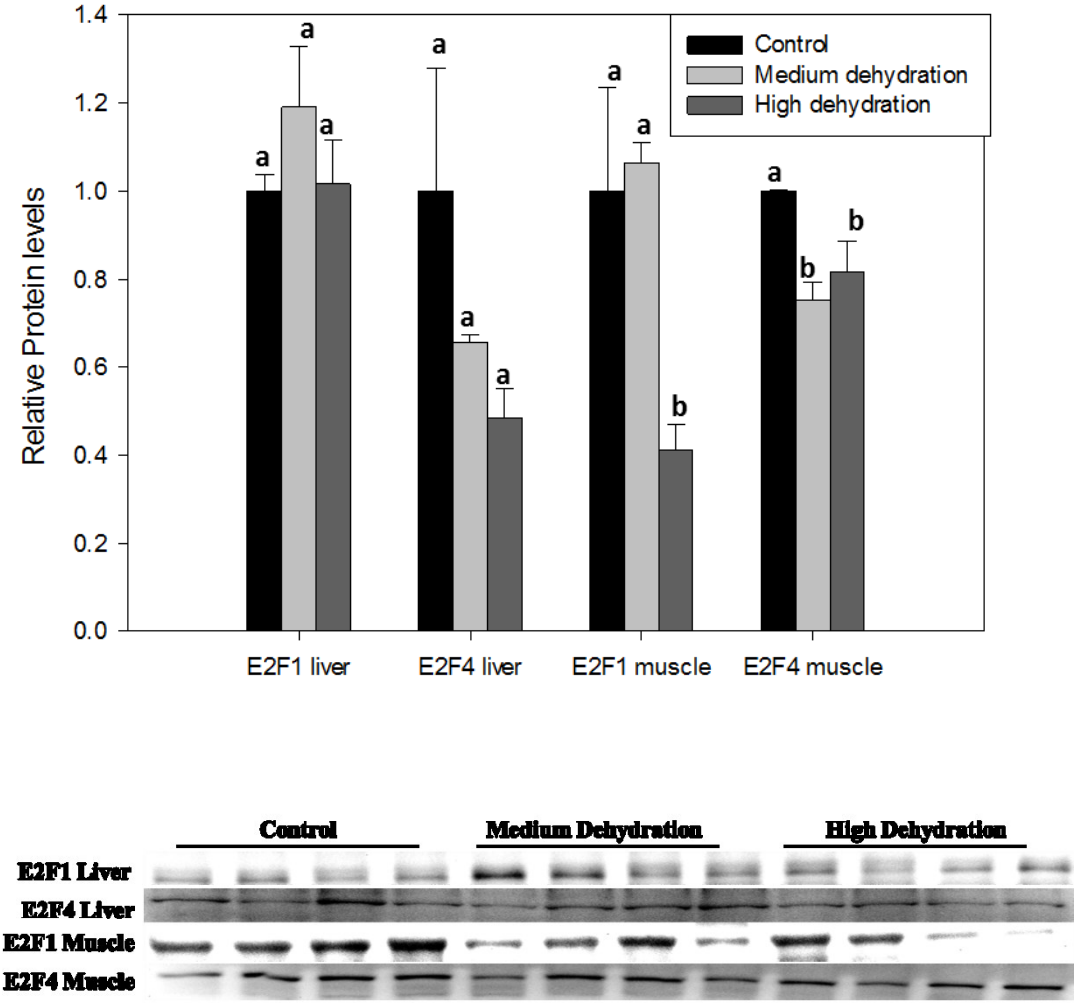

Figure 4.2. Western blot analysis demonstrating the effect of medium and high dehydration on the protein expression of E2F1 and E2F4 in *Xenopus laevis* liver and skeletal muscle. Histograms show mean values standardized to controls, where error bars represent the standard error of the mean derived from n = 4 independent biological replicates. Statistically significant differences were assessed by one-way ANOVA with Tukey's post-hoc test, and are denoted by different letters above each bar, where $p < 0.05$.

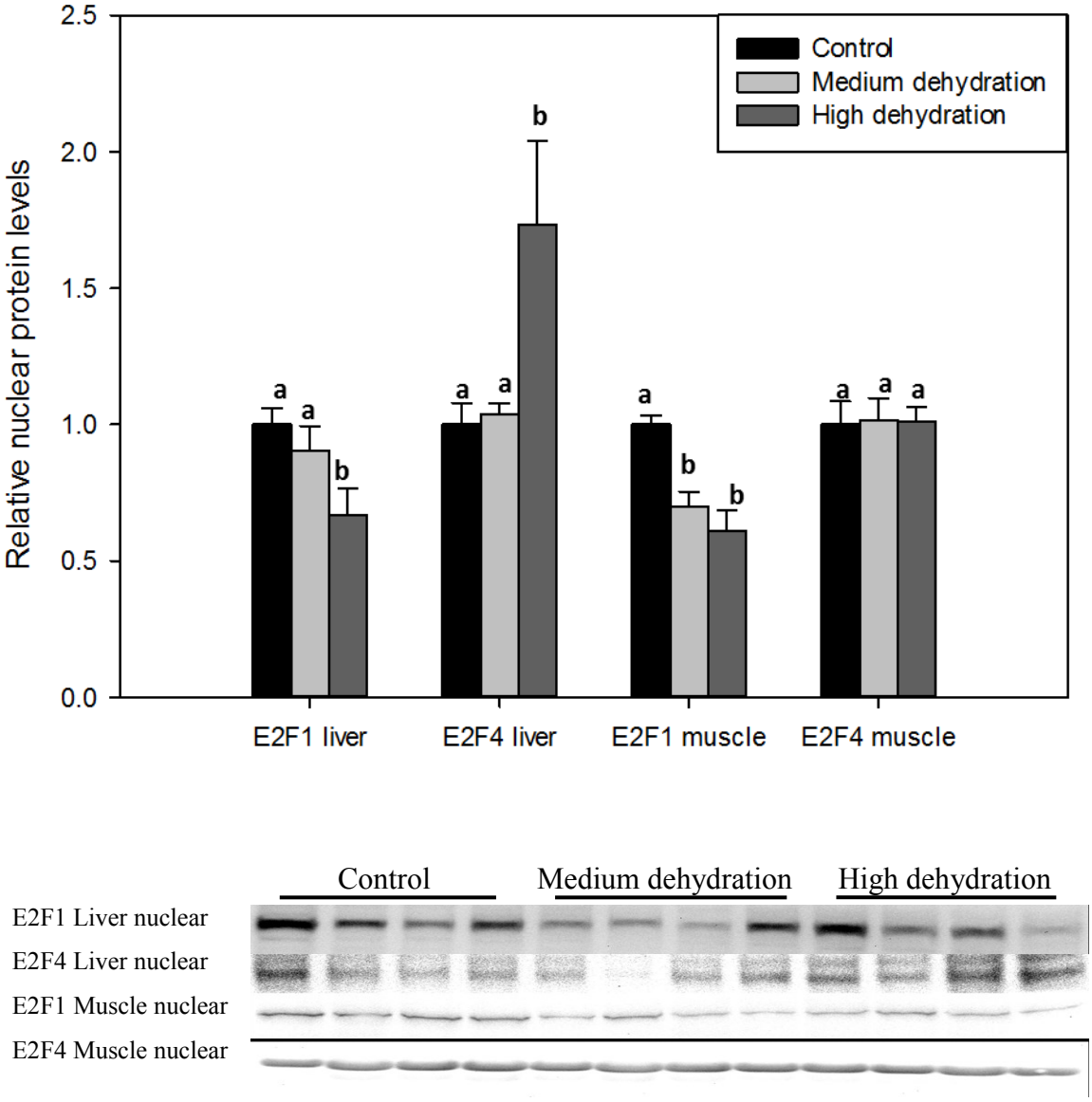

Figure 4.3. Western blot analysis demonstrating the effect of medium and high dehydration on the nuclear localization of E2F1 and E2F4 in *Xenopus laevis* liver and skeletal muscle. Statistically significant differences were assessed by one-way ANOVA with Tukey's post-hoc test, and are denoted by different letters above each bar, where $p < 0.05$. Other information as in Figure 4.2.

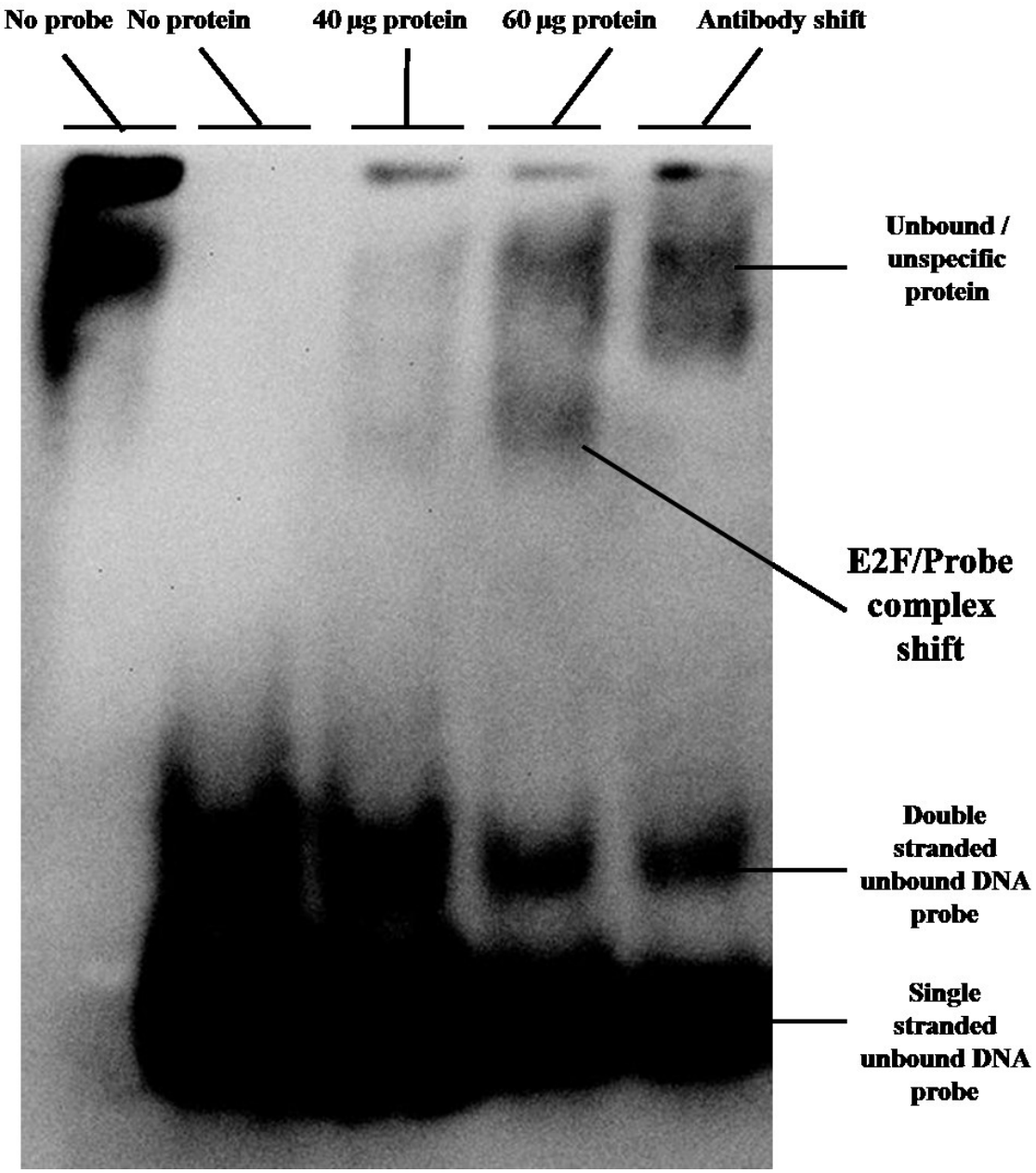

Figure 4.4. Electrophoretic mobility shift assay validating the binding of the DNA probe to protein. Negative controls (no DNA probe, no protein) were run and resulted in no visible protein/DNA shift. Reactions run with higher protein amounts resulted in larger shift bands. Antibody (anti-E2F1) shift reaction theoretically increases the size of the complex to validate that the DNA probe indeed targets *Xenopus laevis* E2F protein.

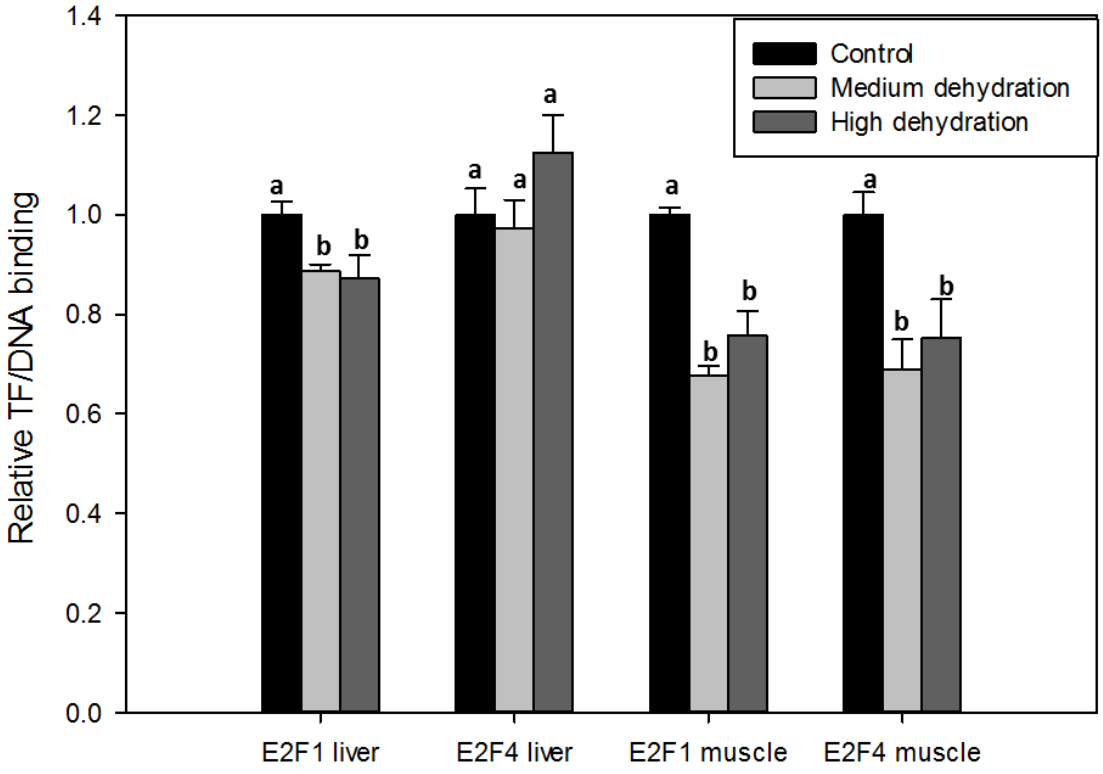

Figure 4.5. A modified TF/DNA ELISA was used to determine relative binding of E2F1 and E2F4 (from *Xenopus laevis* nuclear extracts) to the E2F binding domain. Analysis was performed to demonstrate the effects of medium and high dehydration on DNA binding in both liver and skeletal muscle. Statistically significant differences were assessed by one-way ANOVA with Tukey's post-hoc test, and are denoted by different letters above each bar, where $p < 0.05$. Other information as in Figure 4.2.

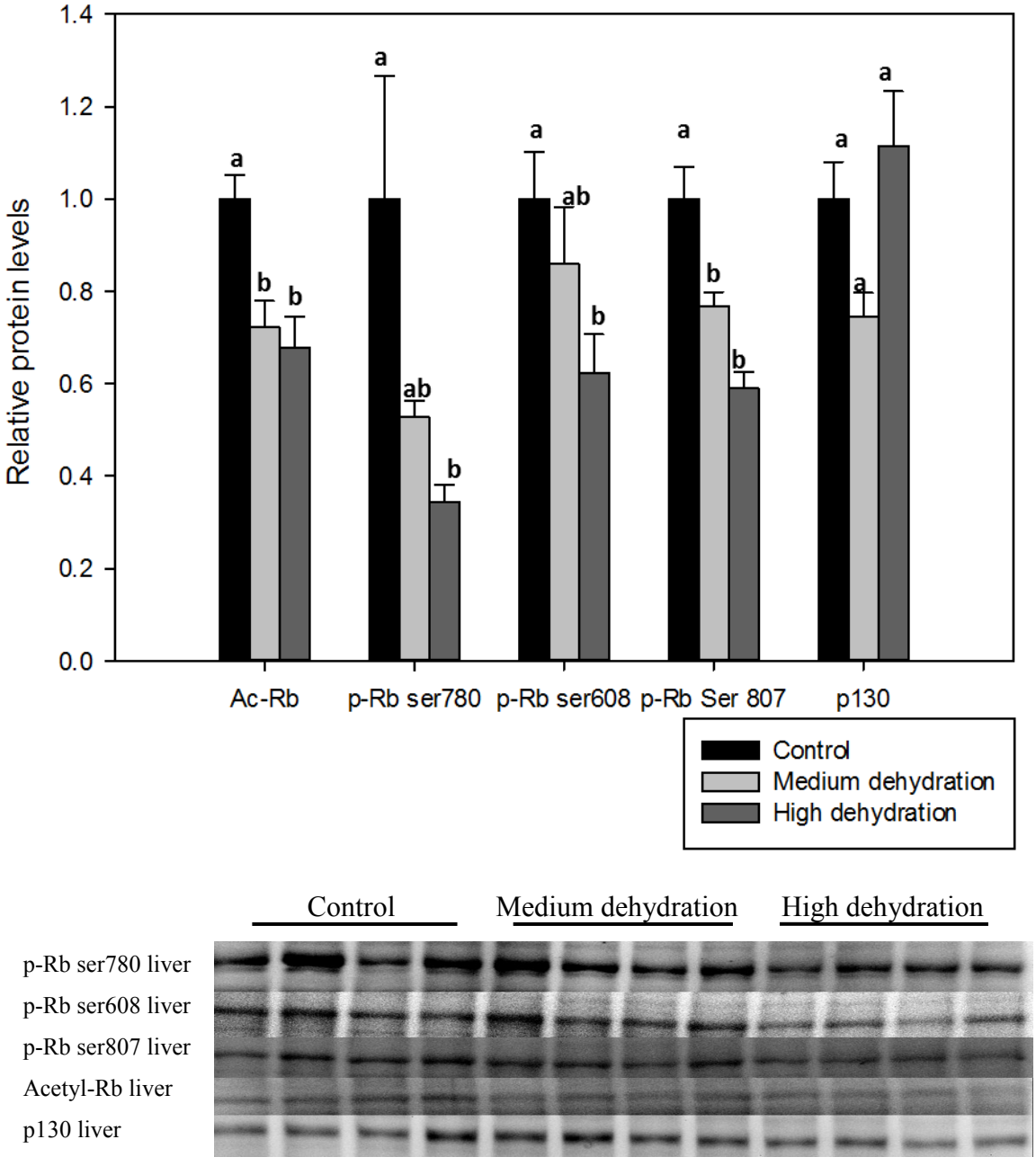

Figure 4.6. Western blot analysis demonstrating the effect of medium and high dehydration on posttranslational modifications of Rb and protein expression of p130 (Rb2) in *Xenopus laevis* liver. Other information as in Figure 4.2.

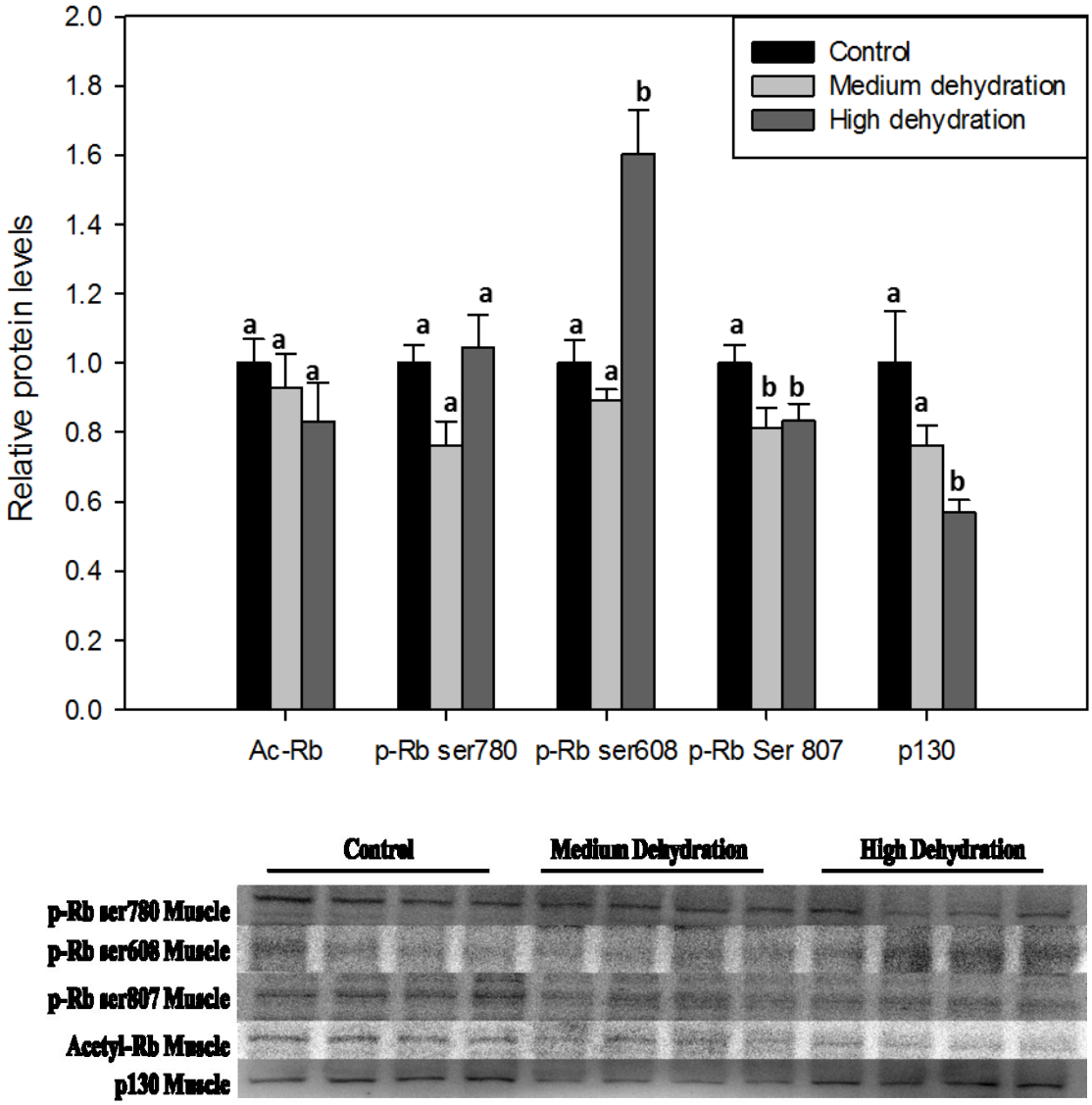

Figure 4.7. Western blot analysis demonstrating the effect of medium and high dehydration on posttranslational modifications of Rb and protein expression of p130 (Rb2) in *Xenopus laevis* skeletal muscle. Statistically significant differences were assessed by one-way ANOVA with Tukey's post-hoc test, and are denoted by different letters above each bar, where $p < 0.05$. Other information as in Figure 4.2.

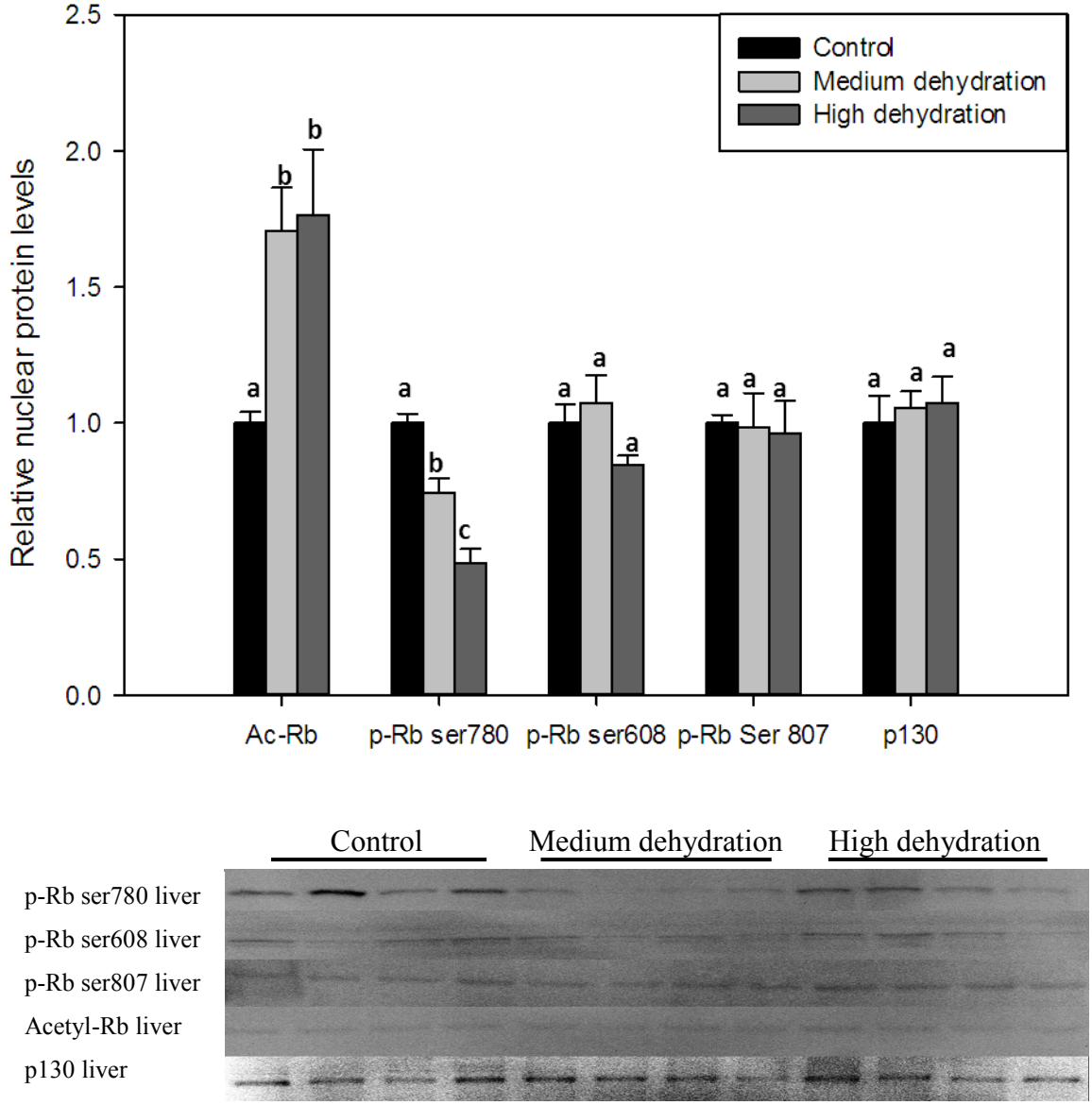

Figure 4.8. Western blot analysis demonstrating the effect of medium and high dehydration on the nuclear localization of posttranslationally modified Rb levels and p130 (Rb2) protein levels in *Xenopus laevis* liver. Statistically significant differences were assessed by one-way ANOVA with Tukey's post-hoc test, and are denoted by different letters above each bar, where $p < 0.05$. Other information as in Figure 4.2.

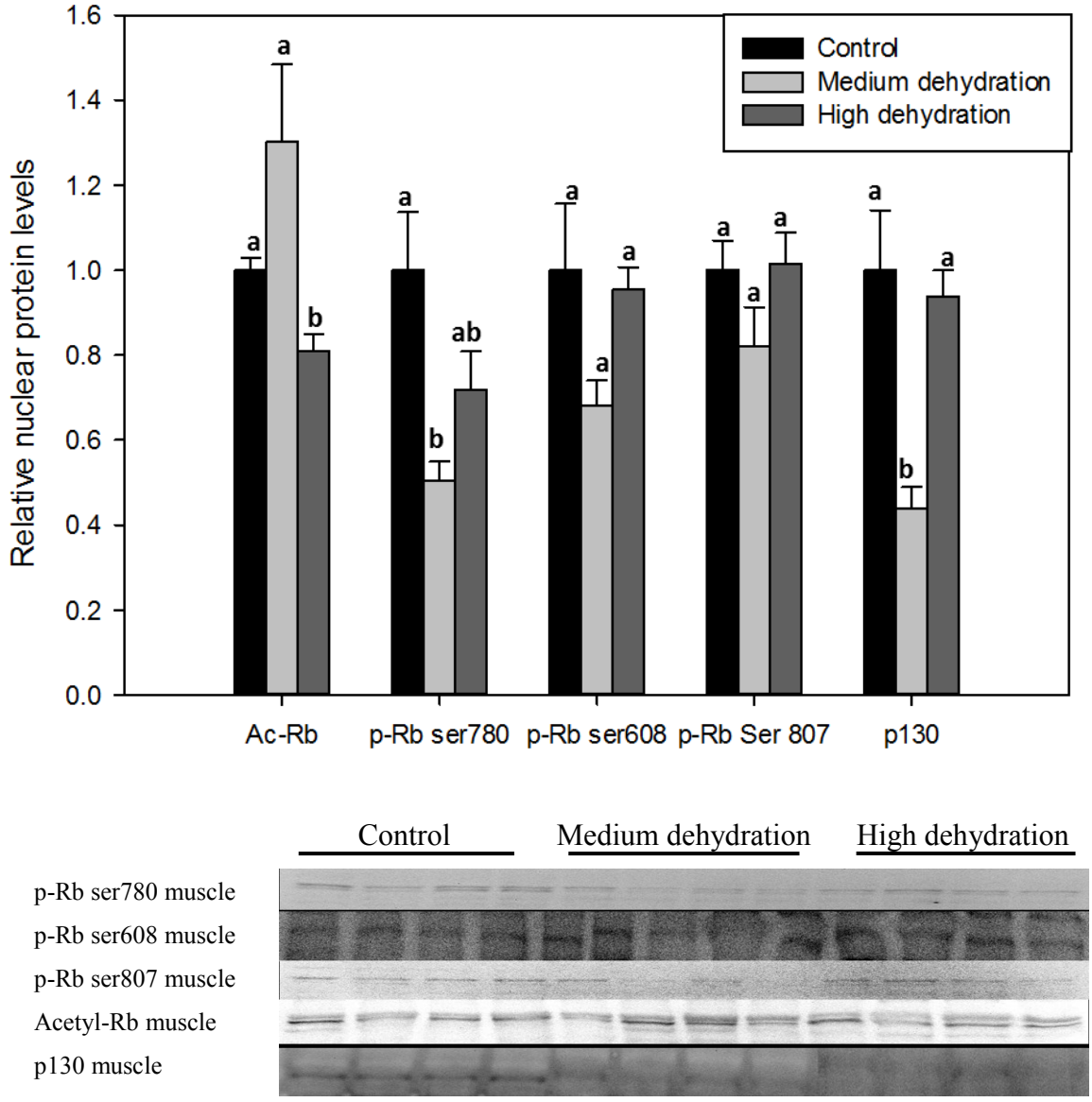

Figure 4.9. Western blot analysis demonstrating the effect of medium and high dehydration on the nuclear localization of post-translationally modified Rb levels and p130 (Rb2) protein levels in *Xenopus laevis* skeletal muscle. Statistically significant differences were assessed by one-way ANOVA with Tukey's post-hoc test, and are denoted by different letters above each bar, where $p < 0.05$. Other information as in Figure 4.2.

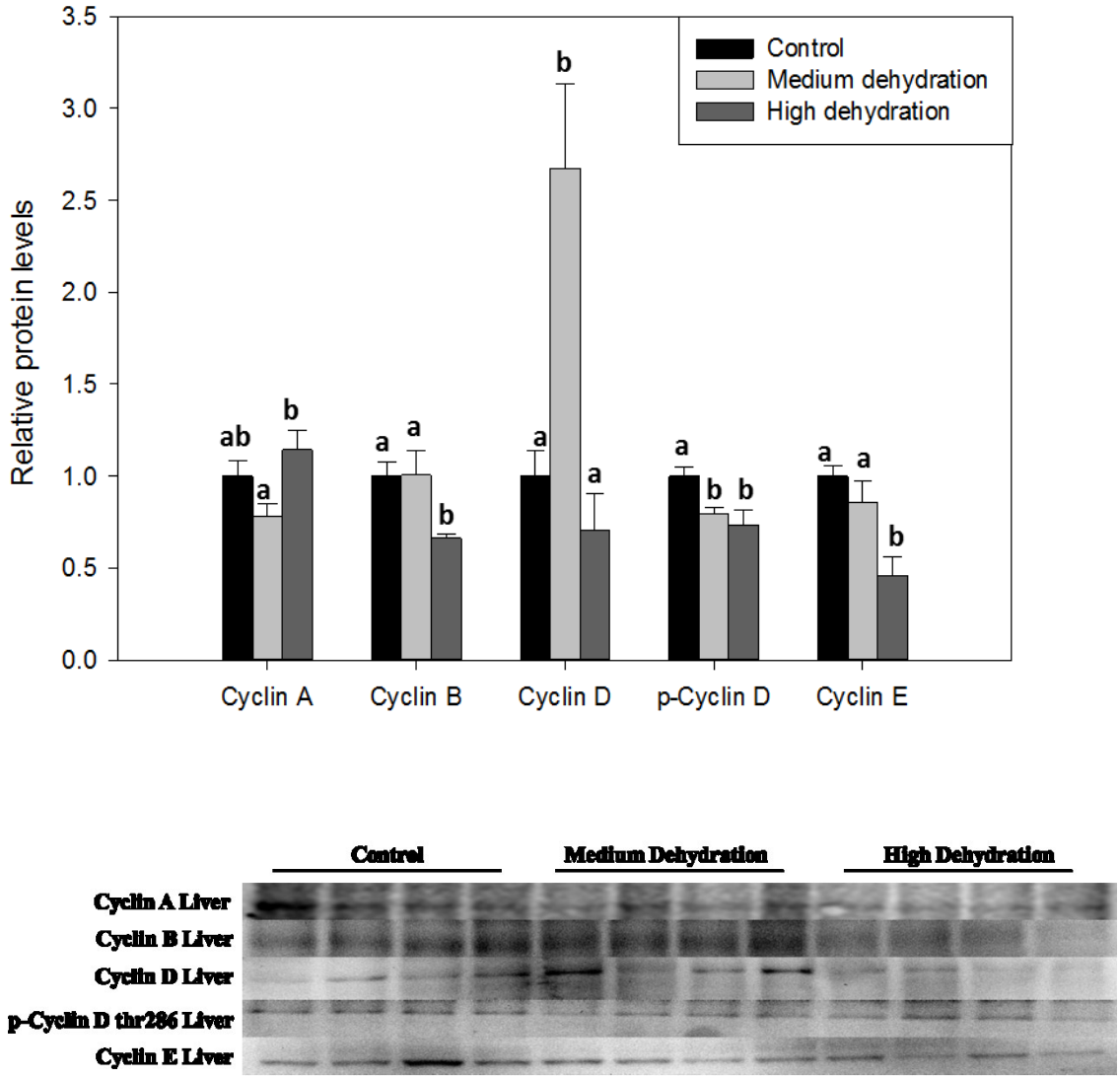

Figure 4.10. Western blot analysis demonstrating the effect of medium and high dehydration on the protein expression of Cyclins A, B, D and E as well as phospho-cyclin D (Thr 286) in *Xenopus laevis* liver. Statistically significant differences were assessed by one-way ANOVA with Tukey's post-hoc test, and are denoted by different letters above each bar, where $p < 0.05$. Other information as in Figure 4.2.

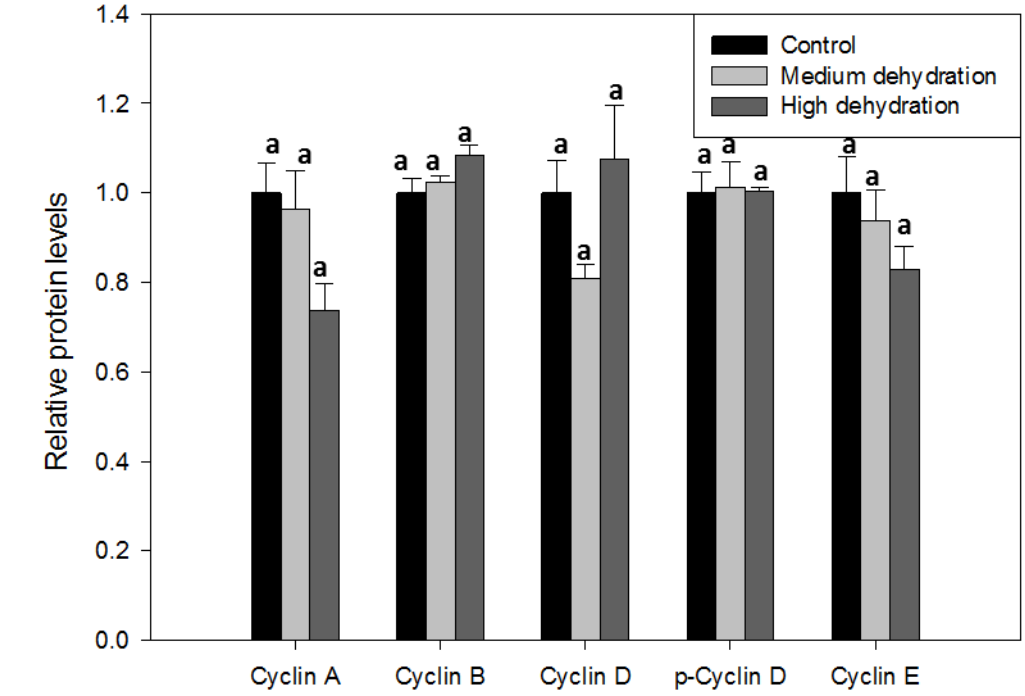

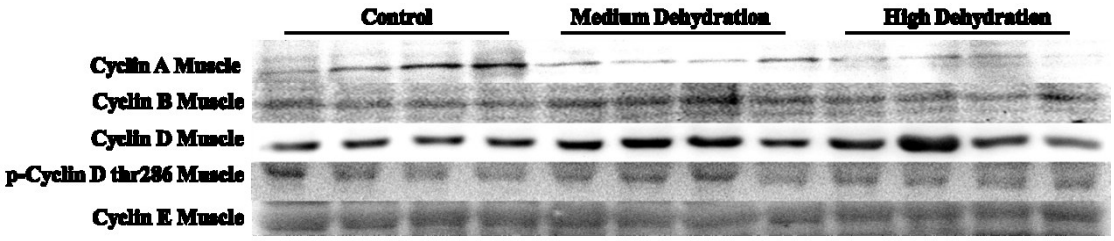

Figure 4.11. Western blot analysis demonstrating the effect of medium and high dehydration on the protein expression of Cyclins A, B, D and E as well as phospho-cyclin D (Thr 286) in *Xenopus laevis* skeletal muscle. Statistically significant differences were assessed by one-way ANOVA with Tukey's post-hoc test, and are denoted by different letters above each bar, where $p < 0.05$. Other information as in Figure 4.2.

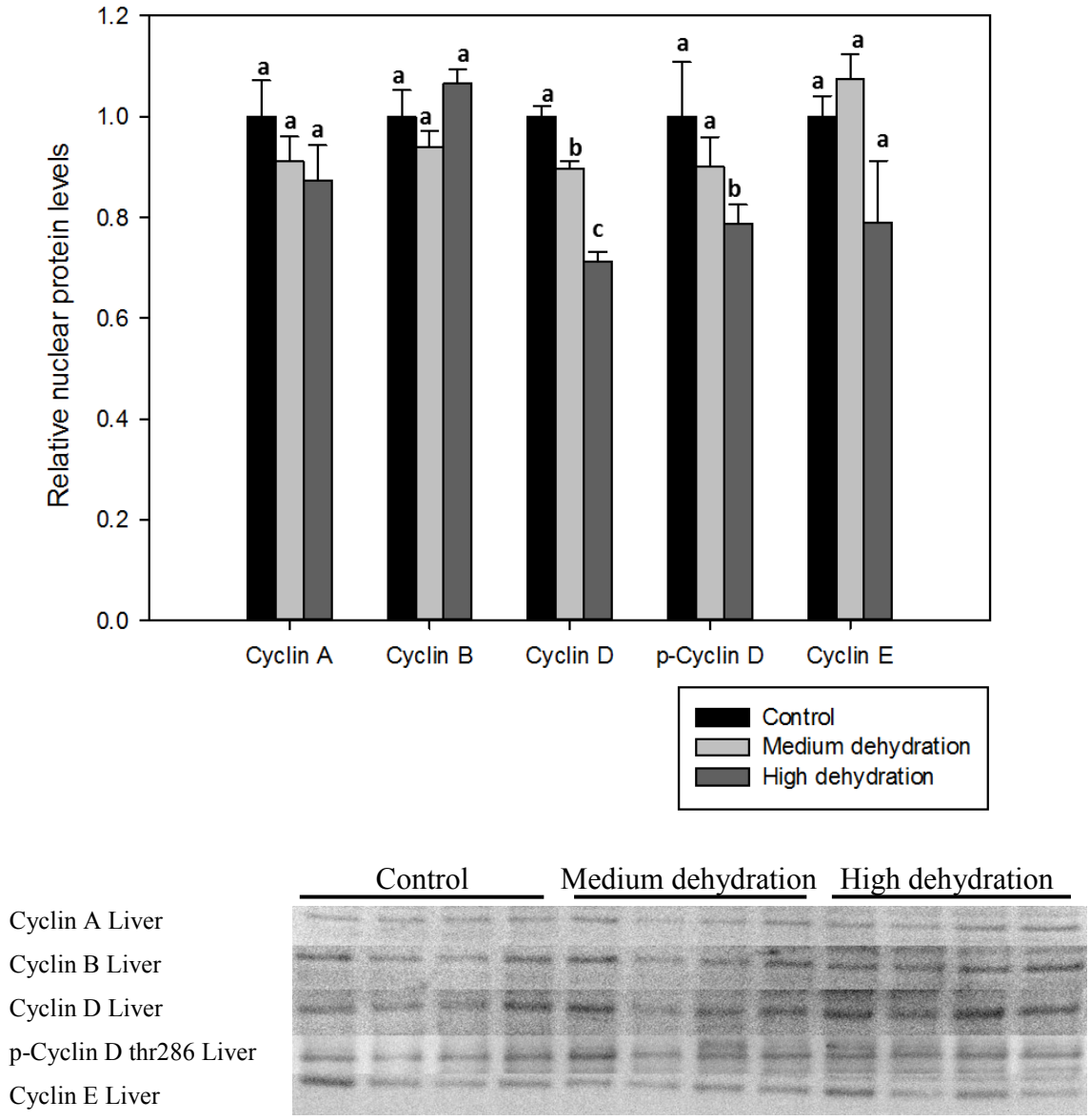

Figure 4.12. Western blot analysis demonstrating the effect of medium and high dehydration on the nuclear localization of cyclins A, B, D and E as well as phosphorylated cyclin D (Thr 286) in *Xenopus laevis* liver. Statistically significant differences were assessed by one-way ANOVA with Tukey's post-hoc test, and are denoted by different letters above each bar, where $p < 0.05$. Other information as in Figure 4.2.

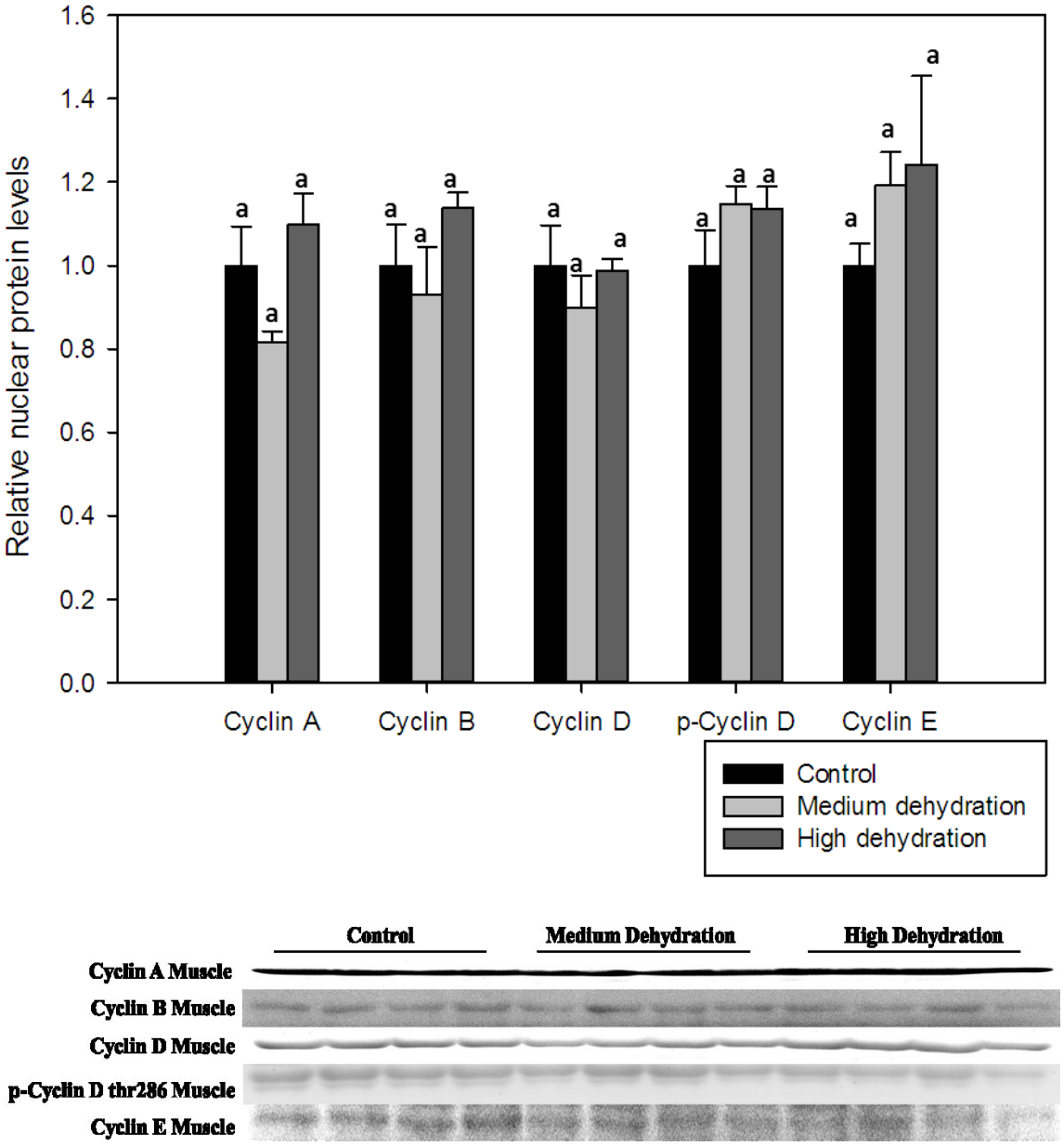

Figure 4.13. Western blot analysis demonstrating the effect of medium and high dehydration on the nuclear localization of cyclins A, B, D and E as well as phosphorylated cyclin D (Thr 286) in *Xenopus laevis* skeletal muscle. Other information as in Figure 4.2.

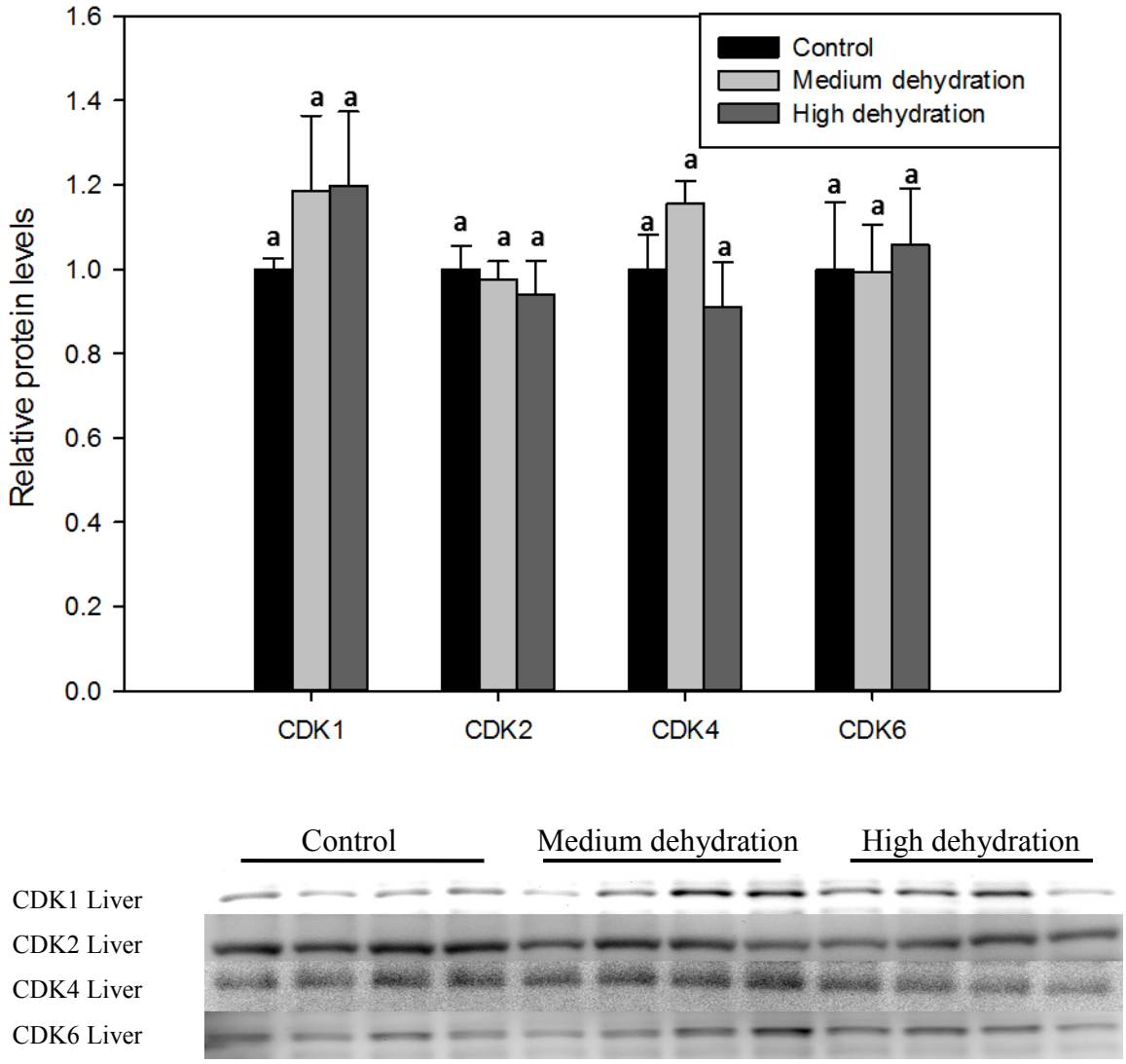

Figure 4.14. Western blot analysis demonstrating the effect of medium and high dehydration on the protein expression of CDK1/CDC2, CDK2, CDK4, and CDK6 in *Xenopus laevis* liver. Statistically significant differences were assessed by one-way ANOVA with Tukey's post-hoc test, and are denoted by different letters above each bar, where $p < 0.05$. Other information as in Figure 4.2.

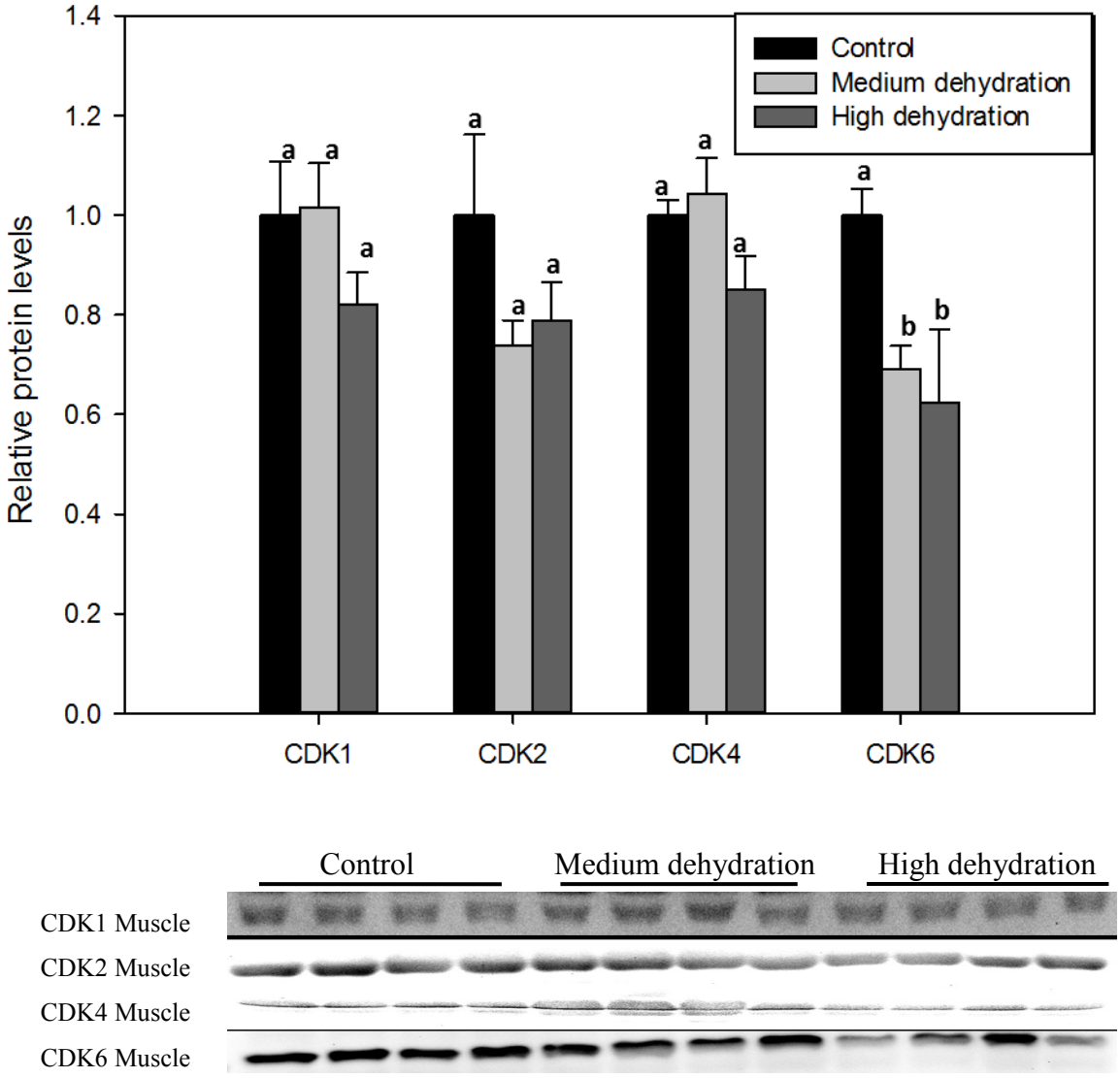

Figure 4.15. Western blot analysis demonstrating the effect of medium and high dehydration on the protein expression of CDK1/CDC2, CDK2, CDK4, and CDK6 in *Xenopus laevis* skeletal muscle. Other information as in Figure 4.2.

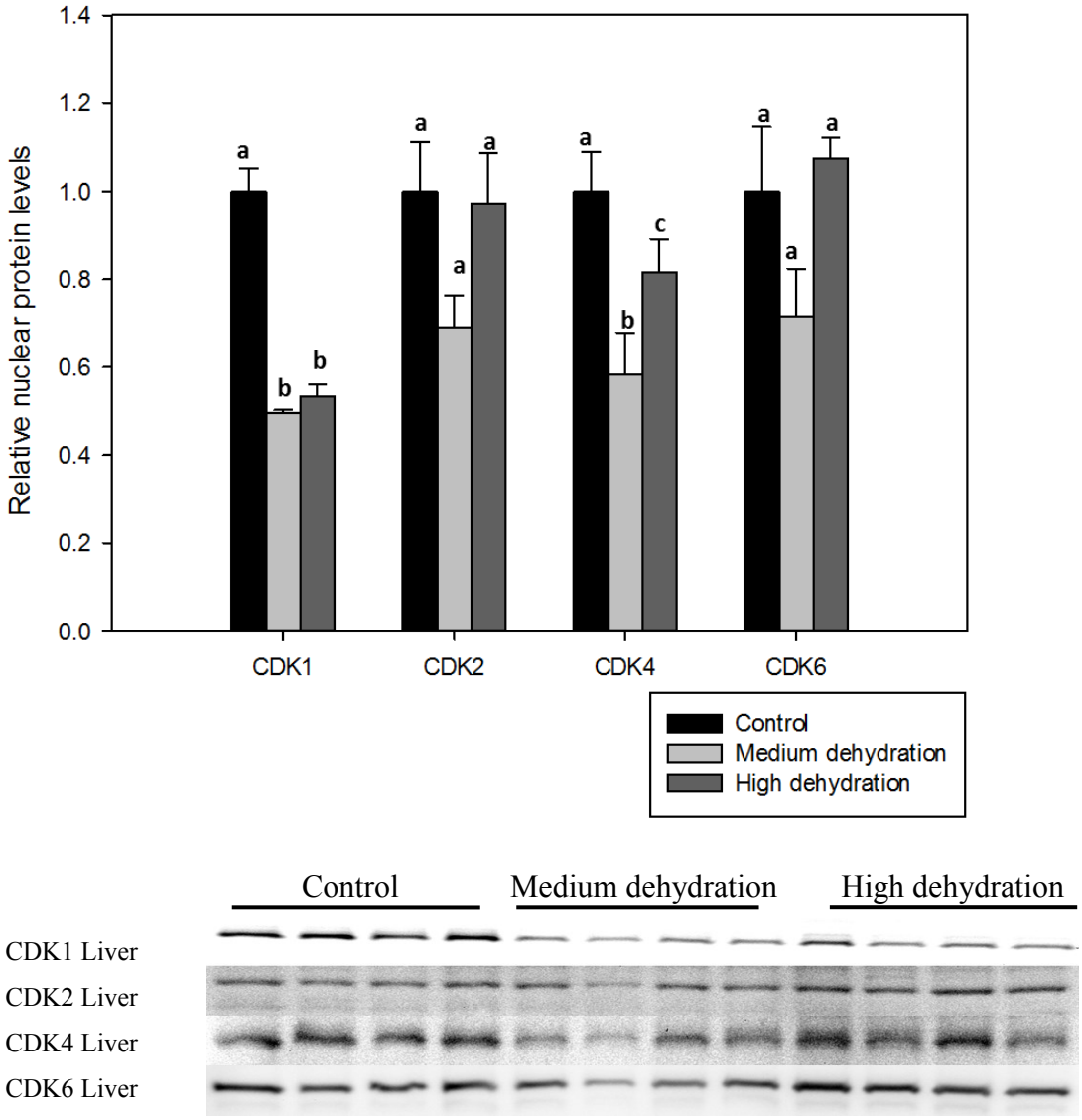

Figure 4.16. Western blot analysis demonstrating the effect of medium and high dehydration on the nuclear localization of CDK1/CDC2, CDK2, CDK4, and CDK6 in *Xenopus laevis* liver. Statistically significant differences were assessed by one-way ANOVA with Tukey's post-hoc test, and are denoted by different letters above each bar, where $p < 0.05$. Other information as in Figure 4.2.

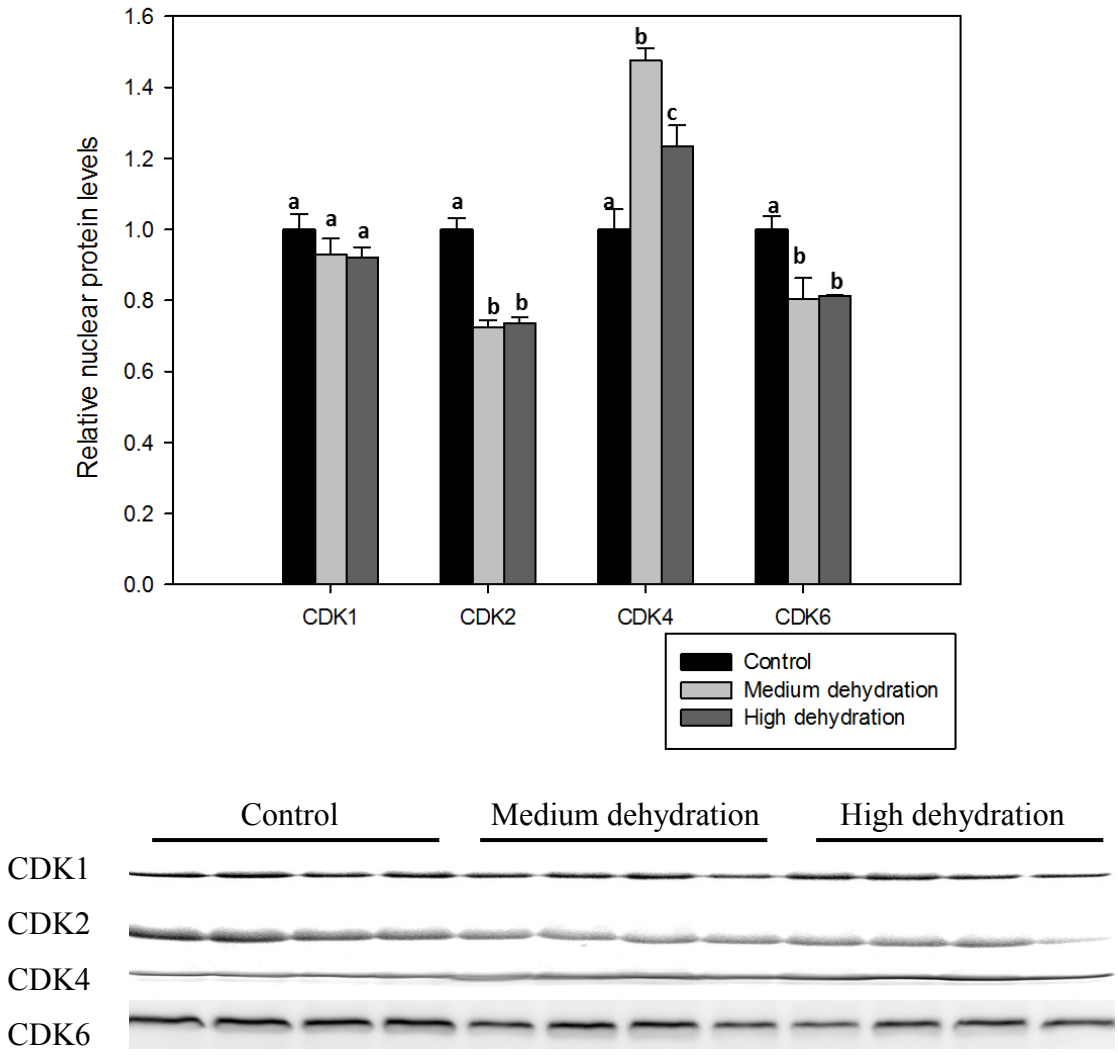

Figure 4.17. Western blot analysis demonstrating the effect of medium and high dehydration on the nuclear localization of CDK1/CDC2, CDK2, CDK4, and CDK6 in *Xenopus laevis* skeletal muscle. Statistically significant differences were assessed by one-way ANOVA with Tukey's post-hoc test, and are denoted by different letters above each bar, where $p < 0.05$. Other information as in Figure 4.2.

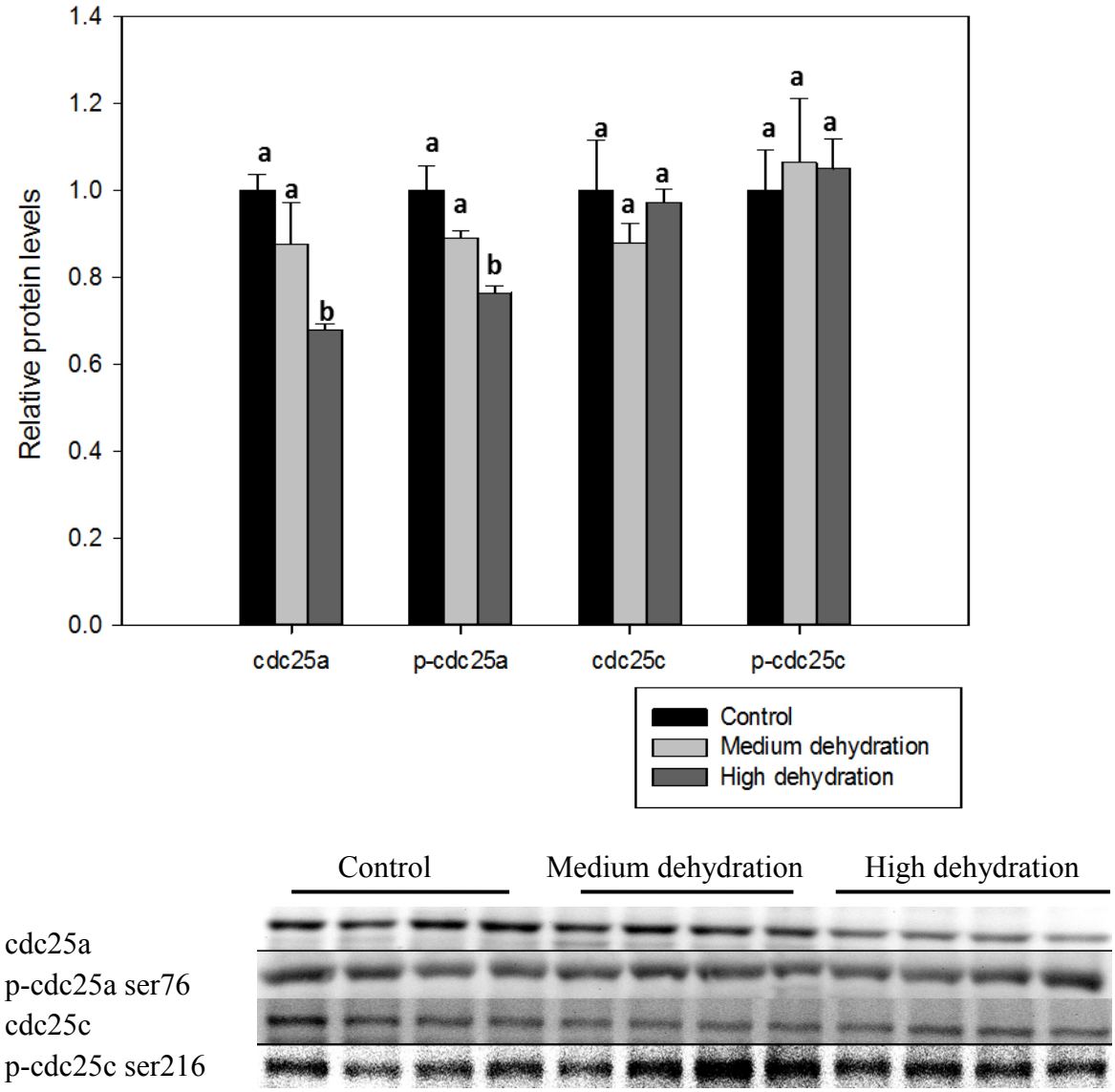

Figure 4.18. Western blot analysis demonstrating the effect of medium and high dehydration on the protein expression and phosphorylation of cdc25a (serine 76) and cdc25c (serine 216) in *Xenopus laevis* liver. Statistically significant differences were assessed by one-way ANOVA with Tukey's post-hoc test, and are denoted by different letters above each bar, where $p < 0.05$.Other information as in Figure 4.2.

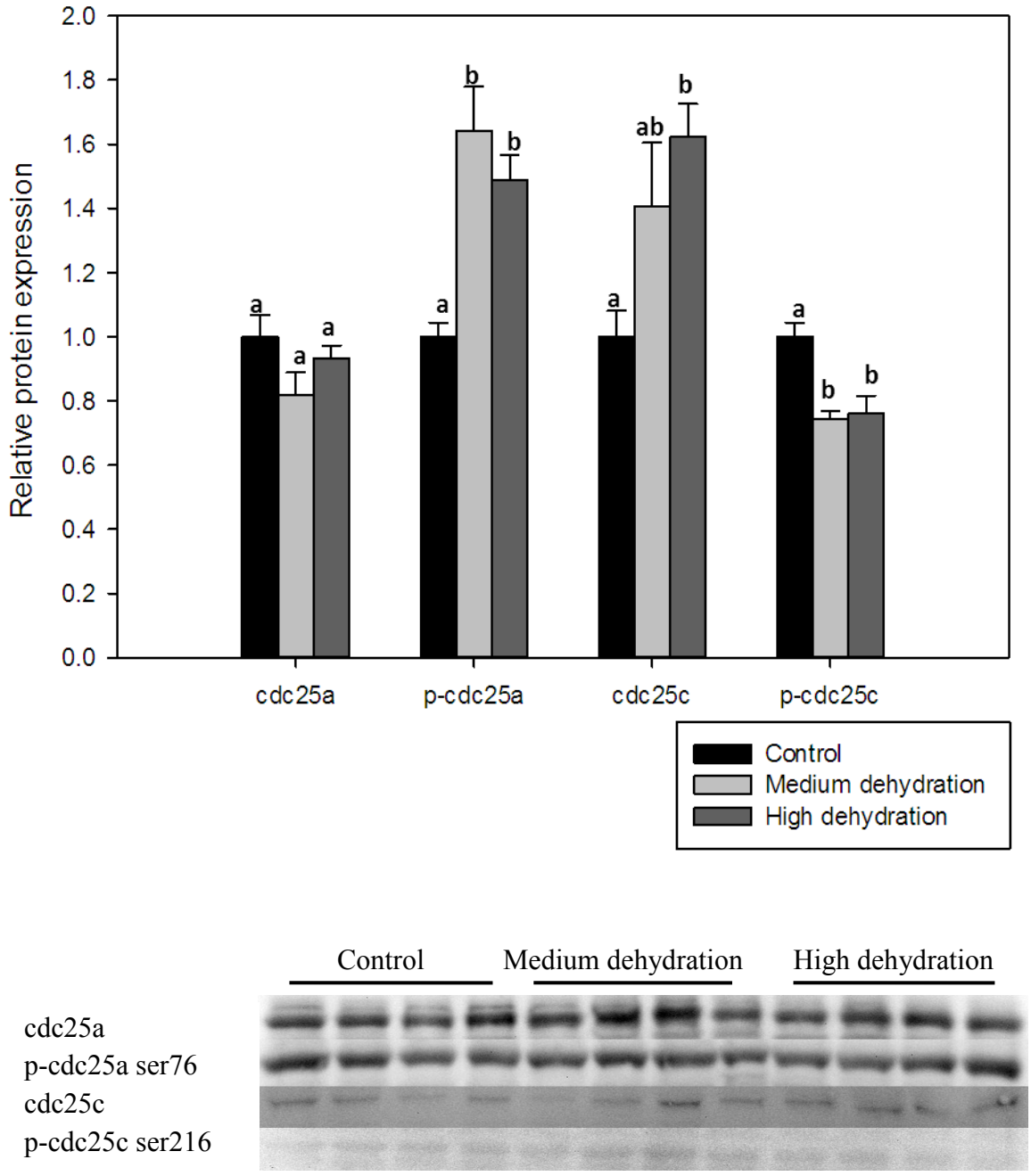

Figure 4.19. Western blot analysis demonstrating the effect of medium and high dehydration on the protein expression and phosphorylation of cdc25a (serine 76) and cdc25c (serine 216) in *Xenopus laevis* muscle. Other information as in Figure 4.2.

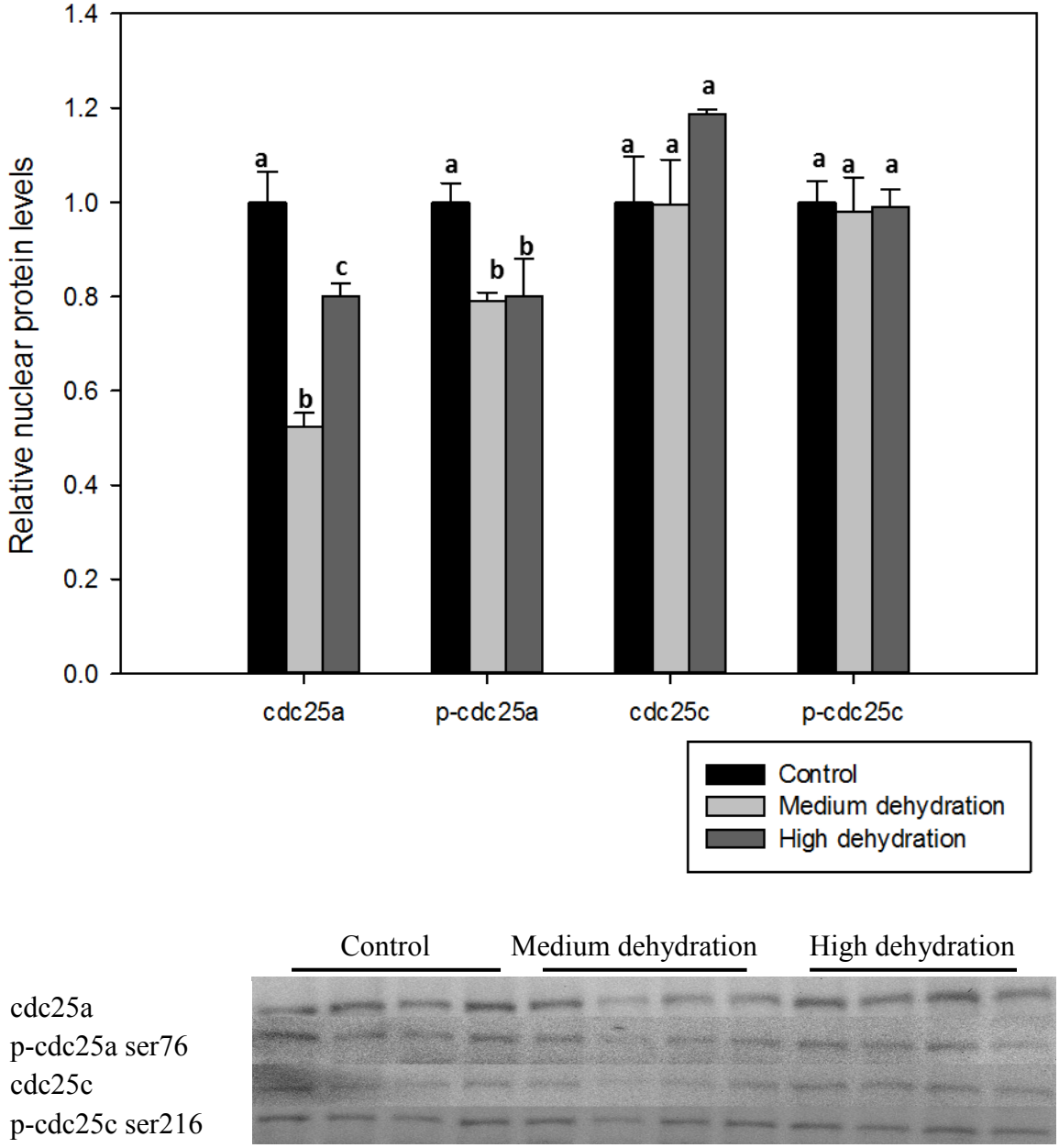

Figure 4.20. Western blot analysis demonstrating the effect of medium and high dehydration on the nuclear localization of total cdc25a, phospho-cdc25a (serine 76), total cdc25c and phospho-cdc25c (serine 216) in *Xenopus laevis* liver. Other information as in Figure 4.2.

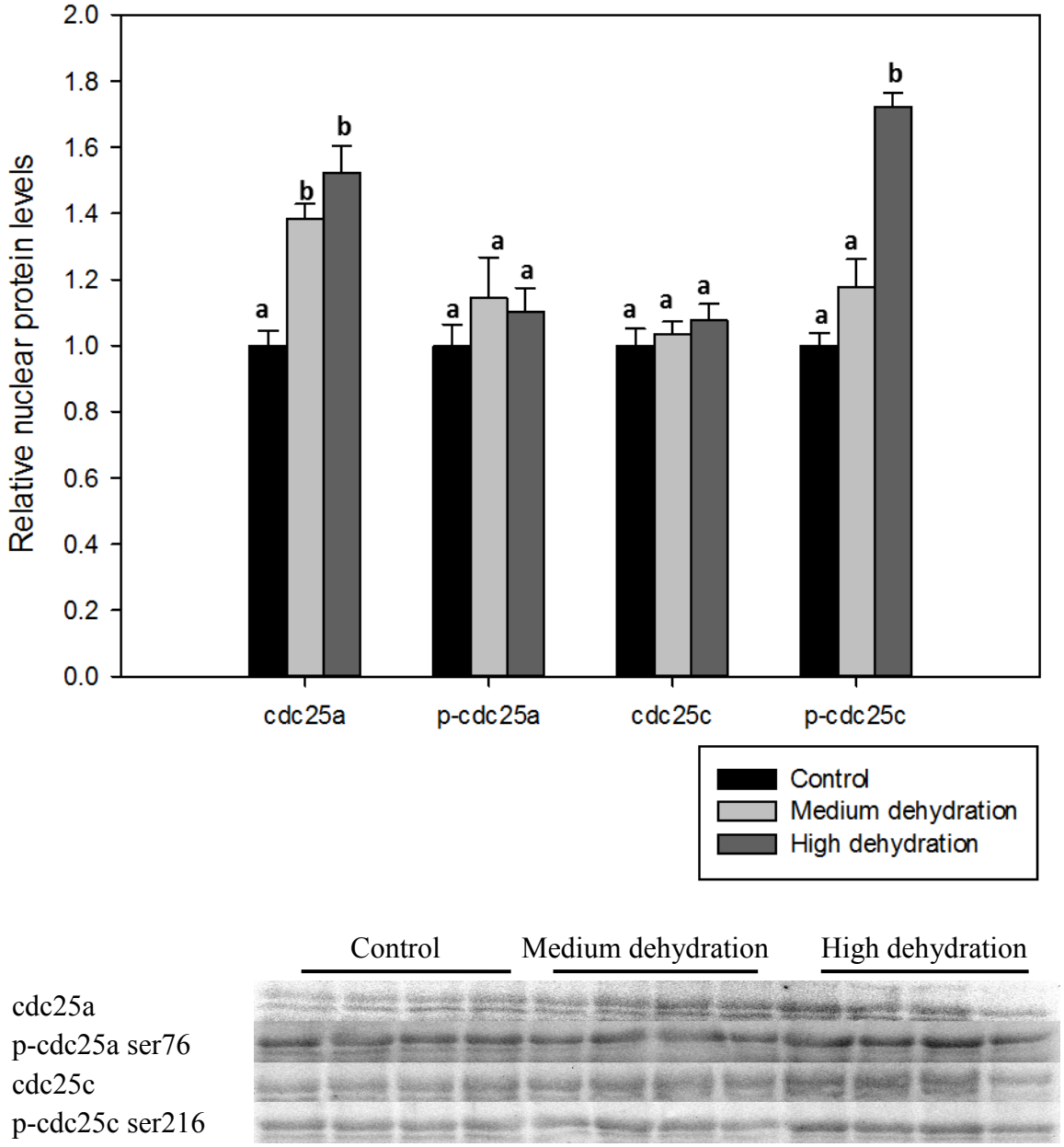

Figure 4.21. Western blot analysis demonstrating the effect of medium and high dehydration on the nuclear localization of total cdc25a, phospho-cdc25a (serine 76), total cdc25c and phospho-cdc25c (serine 216) in *Xenopus laevis* skeletal muscle. Other information as in Figure 4.2.

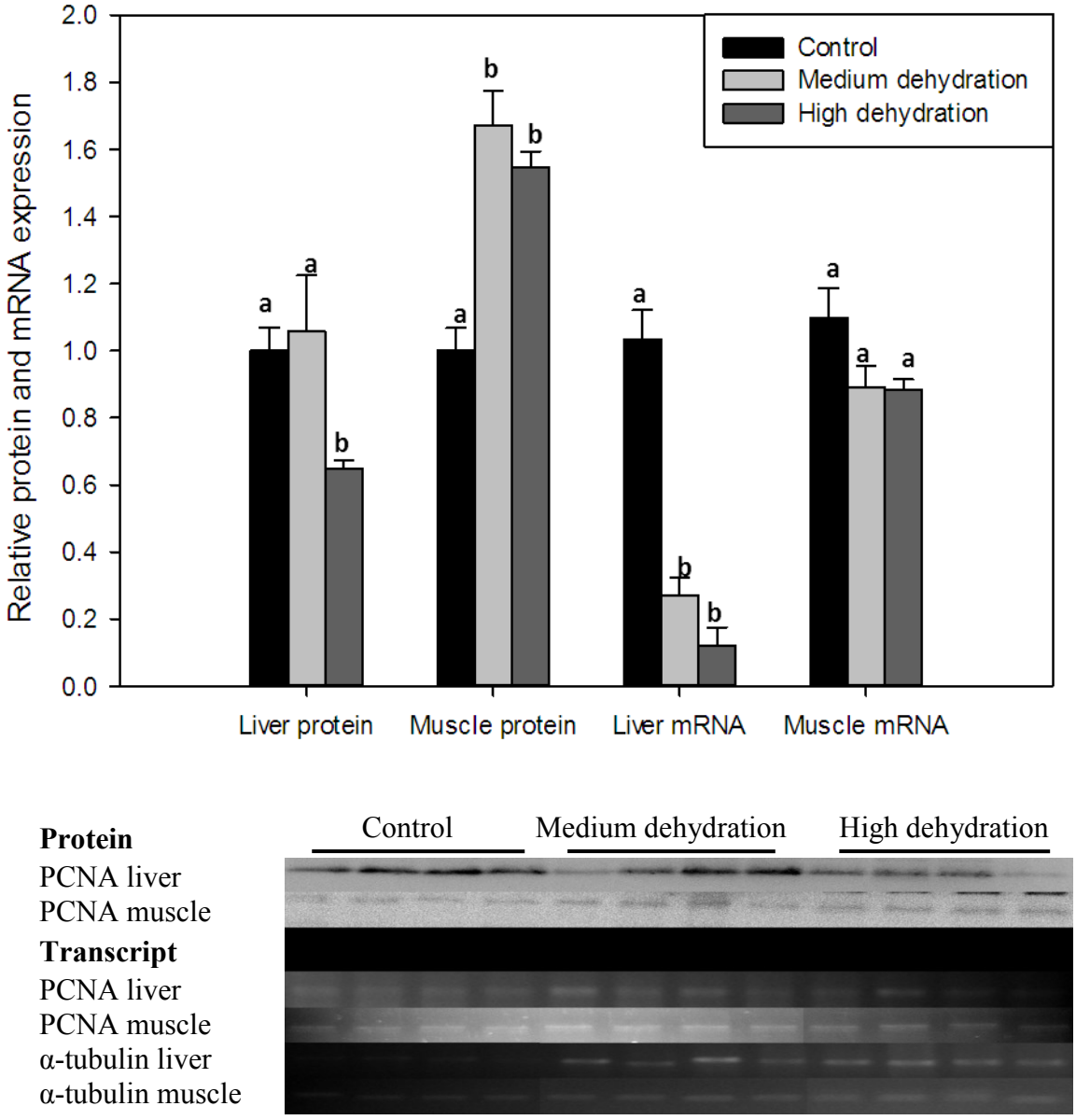

Figure 4.22. Western blot and PCR analysis demonstrating the effect of medium and high dehydration on relative PCNA protein levels and *pcna* mRNA transcript levels in *Xenopus laevis* liver and skeletal muscle. Band densities for *pcna* transcripts were normalized against bands for alpha-tubulin amplified from the same RNA samples. Other information as in Figure 4.2.

4.4 DISCUSSION

4.4.1 Dehydration-induced regulation of E2F mediates cell cycle arrest in liver, but not muscle

As previously stated in the introduction of this chapter, current literature suggests that E2F1 plays a key role in facilitating cell cycle progression. On the contrary, E2F4 induces cell cycle arrest by replacing E2F1 on target promoters and preventing the expression of genes required for cell cycle progression. The data in this chapter indicate that, during dehydration, E2F1 and E2F4 are strongly regulated in the liver, but not as extensively in skeletal muscle, to facilitate cell cycle arrest (Figures 4.2, 4.3, 4.4 and 4.5). In liver, total E2F1 and E2F4 protein expression remained constant (Figure 4.2). However, the study revealed that nuclear levels of E2F1 decreased significantly with respect to controls, whereas E2F4 increased under high dehydration (Figure 4.3). This suggests that E2F4 is inducing cell cycle arrest by replacing E2F1 in the nucleus, which prevents the expression of genes required for cell cycle progression, as also reported for other systems of cell cycle arrest (Wilson, 2007). In addition, protein-DNA binding experiments showed that E2F1 binding to its respective DNA binding motif decreased significantly in liver during dehydration, whereas E2F4 binding to the motif remained constant (Figures 4.4 and 4.5). These results may suggest that dehydration facilitates a decrease in E2F1 binding to genes so that the elevated nuclear E2F4 present could instead bind to DNA and inhibit gene expression. These results further demonstrate that dehydration-induced regulation to E2F1 and E2F4 is facilitating cell cycle arrest in *X. laevis* liver.

Although dehydration-induced E2F regulation in the skeletal muscle of *X. laevis* is also present, the necessary steps to facilitate G1 cell cycle arrest are not tightly controlled as in liver. Although muscle E2F1 levels decreased significantly in high dehydration, initially suggesting that dehydration also induces cell cycle arrest, the results also found that total protein expression of E2F4 decreased significantly – a result which favours cell cycle progression (Figure 4.2). Nuclear localization analysis for muscle showed decreases in E2F1, similar to what was seen as in liver, but unlike in liver, E2F4 localization did not change in response to dehydration (Figure 4.3). Although regulation of E2F1 was similar to what was found in liver and was characteristic of cell cycle arrest, E2F4 in muscle did not appear to play the expected role in inhibiting expression of genes required for cell cycle progression. It appeared that the mechanisms facilitating cell cycle arrest in dehydrating liver were not completely present in muscle. Further analysis of E2F1 and E2F4 DNA binding further supported this claim. Although E2F1 DNA binding in muscle decreased as expected with dehydration, E2F4 DNA binding also decreased (Figure 4.5). Hence, with respect to dehydration stress for *X. laevis* muscle, changes in E2F1 appear to facilitate cell cycle arrest, whereas E2F4 does not.

4.4.2 Post-translational modifications of Rb play a role in mediating cell cycle arrest in liver, but not muscle

As stated in the introduction of this chapter, post-translational modifications of Rb are a crucial mechanism by which E2F1, and consequentially the cell cycle, is regulated. The results for Rb analysis under dehydration stress continue to suggest that mechanisms

are present to induce cell cycle arrest in liver, but not muscle. In liver, relative phosphorylation levels of Rb at all phospho-sites analyzed decreased with dehydration exposure: p-serine 780, p-serine 608, and p-serine 807 (Figure 4.6). These results suggest that Rb is being signalled to bind to E2F1 to prevent expression of genes required for cell cycle progression. Furthermore, although acetylation of Rb was found to decrease with dehydration exposure in general, the amount of acetylated Rb in the nucleus increased (Figures 4.6 and 4.8). Some studies have suggested that acetylation of Rb facilitates Rb-E2F1 binding (Markham *et al*., 2006). Thus, taken together, acetylation and phosphorylation results suggest that Rb may be signalled to bind to E2F1 resulting in reduced expression of E2F1-regulated genes and promoting the export of the Rb-E2F1 complex out of the nucleus. This theory supports the decrease in nuclear E2F1 levels observed in high dehydration (Figure 4.3). Throughout dehydration exposure, total p130 (which facilitates cell cycle arrest) levels remained constant – which suggests that it may play a less crucial role in facilitating cell cycle arrest in *X. laevis* liver than does Rb. In skeletal muscle, there was no clear pattern of regulation for Rb acetylation and phosphorylation. Acetylation of Rb decreased in high dehydration compared to controls, which suggests that Rb is exported out of the nucleus. However, there was no evident pattern of increase or decrease of phosphorylation of Rb, which suggests that dehydration exposure does not significantly promote or suppress muscle Rb activity in muscle. Nuclear localization analysis of liver Rb further highlighted serine 780 as the key phosphorylated residue that activates Rb for E2F1 repression (Figure 4.8). Relative phosphorylation of serine 780 on nuclear Rb significantly decreased with dehydration in liver, but other residues (serines 608, 807) remained constant. Despite current knowledge

which states that hypophosphorylation is required for activation of Rb, studies have noted that serine 780 is a key target residue for cell cycle regulation (Tagliati *et al.*, 2006; Tyagi *et al*., 2002). As previously stated, increased acetylation coupled with a decrease in serine 780 phosphorylation of nuclear Rb suggests that Rb/E2F1 complexes are forming. Nuclear levels of p130 also stayed constant throughout dehydration exposure, which continues to suggest that this protein plays a less significant role (compared to E2F4) in facilitating cell cycle arrest. Nuclear analysis of dehydrating muscle failed to show any trends that would suggest cell cycle arrest. Hence, this study of Rb in the African clawed frog demonstrated evidence that dehydration exposure signals Rb to inhibit E2F1 in liver, but not skeletal muscle.

4.4.3 Regulation of cyclin A, B, D and E in mediating cell cycle arrest in liver, but not muscle

Up to this point, the data for E2F and Rb had suggested dehydration exposure triggered mechanisms to arrest the cell cycle in liver, but not muscle. Another point of study is the family of cyclin proteins. These proteins have pivotal roles in regulating the Rb-E2F complex by activating CDKs which phosphorylate Rb to allow the cell cycle to progress (Figure 4.1). Additionally, expression of cyclin family members is also regulated by the E2F1 transcription factor (Figure 4.1). In *X. laevis* liver, cyclin A protein expression remained constant with dehydration exposure, when compared to control levels. However, cyclin B and E significantly decreased in high dehydration (Figure 4.10). These decreases in liver cyclin proteins may be due to dehydration-induced E2F1 suppression. An interesting result was a significant increase in cyclin D protein levels in medium dehydration, before returning to control levels in high dehydration (Figure 4.10).

There is one theory that explains this phenomenon that involves cell cycle arrest. Cyclin proteins are each produced selectively since they are needed at a certain step in the cell cycle. Once they are produced, they interact with the appropriate CDK and this facilitates progression of the cell cycle to the next stage, before being rapidly signalled for degradation by proteasomes. In the active, proliferating liver, there would be a mixture of cells at different stages of the cell cycle – G1, S, G2 and M (Figure 4.1). In this active tissue, therefore, there would be a balance between cyclin A, B, D and E. However, if dehydration stress is indeed stimulating cells to halt between the G1 to S phase, there would be an accumulation of cells at the G1 phase. Thus, one could expect to see a significant increase in cyclin D in liver (the cyclin that is specifically produced in G1 phase), and significantly less cyclin A, B and E.

Nuclear localization of liver cyclin D protein decreased significantly with dehydration exposure (Figure 4.12). This result suggests that although there is an accumulation of cyclin D as cells are accumulating in the G1 phase, nuclear cyclin D is either degraded or exported out of the nucleus in order to facilitate cell cycle arrest. Since cyclin D and its respective CDK2/4 normally phosphorylates Rb in the nucleus to release and activate E2F1, a decrease in nuclear cyclin D content would be consistent with reduced phosphorylation of Rb as was indeed seen for the nuclear content of serine 780 phosphorylated Rb. Hence, nuclear cyclin D content also suggest that cell cycle arrest is occurring in the dehydrating liver. It is important to highlight the selective regulation of cyclin D and its role in halting the cell cycle since there were no changes to nuclear localization of cyclins A, B and E. However, the fact that total levels of cyclins B and E decreased with dehydration exposure further strengthens the argument that E2F1 was

suppressed from transcribing pro-cycling genes. One point of note is that liver cyclin A did not change in terms of either total protein expression or nuclear localization (Figures 4.10 and 4.12). Cyclin A may be prevented from increasing because it would promote cell cycle progression. However, cyclin A may also not be degraded as a preparatory mechanism for when the cell cycle resumes when the frog recovers from dehydration. In skeletal muscle, the results showed that there were no significant changes to total protein expression or nuclear localization of cyclins A, B, D and E throughout dehydration exposure (Figure 4.11 and 4.13). As for previous results presented in this chapter, this finding suggests that dehydration does not play a significant role in regulating the cell cycle machinery in skeletal muscle. In summary, then, it appears that the proliferative liver cells are halting at the G1 phase as evidenced by significant increases in cyclin D in the medium dehydration stage. However, the frog also has mechanisms to stop the cell cycle from progressing by preventing the localization of cyclin D into the nucleus. In skeletal muscle, there appears to be no significant regulation of the cyclin proteins in response to dehydration stress, which supports my hypothesis that cell cycle machinery is not tightly regulated in skeletal muscle as compared to liver.

4.4.4 Regulation of cyclin D in G1 arrest by GSK-3β in liver, but not muscle

In the summary in section 4.4.3, the results suggested that a significant increase in cyclin D in medium dehydration in liver was a result of an accumulation of liver cells in the G1 phase when cell cycling was brought to a halt by dehydration. By the time the frogs were highly dehydrated, these liver cells subsequently lowered their cyclin D levels

(Figure 4.10). Again, the results for liver cyclin D did suggest that the cells had accumulated in the G1 phase. Furthermore, results for Rb/E2F also suggested that the cell cycle had ceased to progress in liver during dehydration. Cyclin D nuclear localization also significantly decreased and this would also facilitate cell cycle arrest by inactivating the CDKs that might otherwise allow the cell cycle to progress by phosphorylating Rb (Figure 4.12). However, between medium and high dehydration states, liver cells decreased total cyclin D protein levels (Figure 4.10) and this would further suppress CDKs from phosphorylating Rb.

A mechanism that may be facilitating the reduction in total liver cyclin D between medium and high dehydration states is control via GSK-3β phosphorylation. Studies have thoroughly characterized the myostatin/GSK-3β/cyclin D pathway (Diehl *et al*., 2013; Yang *et al*., 2007; Yang *et al*., 2006). Myostatin is known to induce cell cycle arrest – and it does this by facilitating GSK-3β to phosphorylate cyclin D on threonine 286, which targets cyclin D for rapid proteasomal degradation. In Chapter 3, the data showed that GSK-3β was not apparently regulated by Akt (which was suppressed during dehydration exposure) (Figure 3.13). In liver, GSK-3β activity was found to be strongly suppressed (as evidenced by a strong increase in phosphorylation at serine 9) during medium dehydration, before returning to control levels in high dehydration (Figure 3.13). In this chapter, liver cyclin D protein levels followed the same pattern (Figure 4.10), suggesting a possible link between these two parameters. The results from Chapter 3 regarding GSK-3β also support the hypothesis that liver cells accumulated in the G1 phase – since an accumulation of cyclin D would not have been possible with active GSK-3β. Furthermore, the results from Chapter 3 which demonstrated that GSK-3β

activity returned to control levels (as evidenced by analysis of serine 9 phosphorylation) under high dehydration conditions (Figure 3.13) suggest that GSK-3β may play a role in restoring cyclin D expression to near control levels as also seen under high dehydration (Figure 4.10). In summary, I believe that liver cells are accumulating in the G1 phase of the cell cycle during medium dehydration. My claim is supported by the strong increase in cyclin D protein expression seen at this stage. Since GSK-3β is capable of targeting cyclin D for degradation, an increase in phospho-GSK-3β content (the inactive form) in liver in medium dehydration also supports the theory of liver cells accumulating at G1. Lastly, since GSK-3β phosphorylation is restored to relative control levels (ie. GSK-3β is reactivated) in high dehydration, this kinase may also play a role in the reduction in excess cyclin D protein levels seen at this stage (Figures 3.13 and 4.10). The results from this chapter have suggested that cell cycle machinery is regulated in response to dehydration in liver, but not in muscle. Results from Chapter 3 on GSK-3β suggest that not only does GSK-3β play a role in regulating the cell cycle by controlling cyclin D levels (as opposed to glucose metabolism as I had initially hypothesized), but also supports the idea that cell cycle control mechanisms are much more prevalent in liver than in muscle, since muscle GSK-3β phosphorylation at serine 9 did not change throughout dehydration exposure.

To further investigate the role of GSK-3β on the control of cyclin D levels, the relative phosphorylation of cyclin D levels at threonine 289 was analyzed in the dehydrating *X. laevis*. The results showed that liver cyclin D phosphorylated on threonine 289 decreased during dehydration (Figure 4.10). Furthermore, the relative amount of phosphorylated cyclin D in the nucleus also decreased significantly with dehydration

exposure (Figure 4.12). Although this first appeared as a disconnect between my argument concerning GSK-3β phosphorylation as a control mechanism for cyclin D protein levels, the results demonstrating reduced levels of phosphorylated cyclin D may actually suggest that the protein is indeed being degraded between medium and high dehydration exposure. Since GSK-3β is phosphorylating cyclin D between medium and high dehydration, phosphorylated cyclin D is also being targeted for rapid degradation by proteasomes – which explains the decrease in total liver cyclin D levels in high dehydration. For this theory to be feasible, it is important to note that previous studies have shown that phosphorylated cyclin D half-life is approximately 30 minutes (Diehl *et al*., 1997). Since the transition of medium to high dehydration was on the scale of hours rather than minutes, it was not possible to observe significant increases in phospho-cyclin D as proteolysis occurs shortly after phosphorylation. Ultimately, my results on cyclin D and GSK-3β have suggested that liver cells are arresting in the G1 stage during dehydration exposure, and that GSK-3β may play a role in regulating cyclin D levels during this process.

4.4.5 Dehydration-induced regulation of CDKs in liver and muscle

Another target of regulation is the family of cyclin dependent kinases (CDKs) that are responsible for facilitating cell cycle progression. They are dependent on cyclin availability, and facilitate E2F1-mediated gene transcription by hyperphosphorylating Rb and causing it to dissociate from E2F1 (Figure 4.1). In liver, total levels of CDK1/CDC-2, CDK2, CDK4 and CDK6 remained constant throughout dehydration exposure (Figure

4.14). This result suggests that CDK protein expression is not a target of the dehydration-induced regulation of the cell cycle in liver. Although total CDK protein expression in liver did not change, the results revealed that nuclear localization of CDK1 and CDK4 decreased significantly with dehydration exposure (Figure 4.16). Exportation of CDK4 out of the nucleus supports the hypothesis that G1-stage cell cycle arrest is occurring in liver of dehydrating frogs because it would facilitate the hypophosphorylation of Rb, which is required to prevent the expression of E2F1-dependent genes. However, CDK1 does not play a role in mediating cell cycle arrest in the G1 phase. The reason as to why CDK1 is exported out of the nucleus warrants further study. However, one hypothesis may be that CDK1 has unknown cytoplasmic targets that are involved in the survival of the frog during dehydration. Cell cycle machinery has appeared to be tightly regulated in the proliferating liver thus far. The results have shown that the dehydrating frog conserves total CDK levels in liver throughout dehydration as these will be necessary after recovery from dehydration, when the cell cycle resumes. Unlike in liver, protein expression of the CDK family was not well conserved in skeletal muscle, as evidenced by significant decreases to CDK6 with dehydration exposure (Figure 4.15). As for localization, the fact that CDK4 shows increased nuclear localization, while CDK2 and CDK6 nuclear levels drop (with CDK1 remaining constant) suggests that there is no specific conserved mechanism of regulation for the CDK family in dehydrating frog muscle. Together, my results suggest that nuclear exportation of CDK4 plays a key role in facilitating cell cycle arrest in the G1 phase in liver. In addition, trends in total protein expression and nuclear localization of CDKs continue to suggest that cell cycle regulation is poorly regulated in skeletal muscle.

4.4.6 Dehydration-induced regulation of cdc25a facilitates cell cycle arrest in liver, not muscle

The phosphatases cdc25a and cdc25c are known to play key roles in cell cycle progression. Their roles are to remove inhibitory phosphate groups from CDKs, which leads to the eventual release of Rb from E2F1, and cell cycle progression. In the liver, dehydration stress decreased the total amount of cdc25a as well as phosphorylated (serine 76) cdc25a content (Figure 4.18). This suggests that the liver is negatively regulating cdc25a over dehydration exposure. The phosphorylation of serine 76 on cdc25a leads to its degradation (Jin *et al*., 2008). Since both total levels and phosphorylated levels of cdc25a decreased under dehydration stress, these results may be suggesting that signalling pathways are stimulating cdc25a degradation during dehydration to ultimately promote CDK inhibition and cell cycle arrest. Nuclear localization results agree with this theory, and reveal that nuclear levels of liver cdc25a and phosphorylated cdc25a also decreased over dehydration exposure (Figure 4.20). A decrease in total and nuclear cdc25a availability will suppress the formation of CDK2/Cyclin E complexes, which will prevent liver cells from progressing past the G1 phase. The phosphatase cdc25c also acts to activate CDKs to promote cell cycle progression. Unlike cdc25a, cdc25c removes inhibitory phosphate groups from CDK1 (CDC2) to facilitate cell cycle progression from the G2 phase into mitosis. Phosphorylation of cdc25c on serine 216 prevents its phosphatase activity by sequestering it in the cytoplasm (Peng *et al*., 1998). In the liver of the African clawed frog, dehydration exposure did not change total or nuclear levels of cdc25c or its phosphorylation state (Figures 4.18 and 4.20). This suggests that the

dehydrating frog is selectively targeting cdc25a for degradation, which is crucial for cell cycle arrest in the G1 stage.

In skeletal muscle, regulation of cdc25a is not indicative of cell cycle arrest. Total levels muscle cdc25a remained constant throughout dehydration stress (Figure 4.19). Thus, unlike in liver, cdc25a does not appear to be playing a role in mediating any kind of cell cycle arrest in skeletal muscle in the G1 phase. Interestingly, phosphorylation of cdc25a significantly increases over dehydration exposure in whole muscle (Figure 4.19). Despite differential phosphorylation, the fact that total cdc25a levels remained constant over dehydration suggests that muscle cdc25a is not being targeted for degradation in dehydration. This phosphorylation of cdc25a may have resulted due to a stress response, but the frog is not expending energy to facilitate proteolysis. Increases to total muscle cdc25c and decreases to phospho-cdc25c further demonstrates that dehydration-mediated cell cycle arrest responses are not present in muscle. Nuclear localization of cdc25a and phosphorylated cdc25c both increase over dehydration exposure (Figure 4.21). This result suggests that cdc25a is acting to promote muscle cells to progress past the G1 phase, while cdc25c may be acting to block cells from entering mitosis from the G2 stage. However, in muscle, nuclear levels of the phosphorylated form of cdc25a and total levels of cdc25c remained constant throughout dehydration stress (Figure 4.21). These results are characteristic of cells which are progressing past the G1 stage, but are not permitted to enter mitosis. Ultimately, when data for cdc25 are taken together with the results of the rest of this chapter, the mechanisms promoting cell cycle arrest in liver of dehydrating frogs are much more prevalent than cell cycle arrest in skeletal muscle.

4.4.7 Downregulation of PCNA expression in liver suggest that E2F1 suppression is mediating cell cycle arrest in the G1 stage

One well-characterized downstream gene of E2F1 is PCNA. Before cells are allowed to progress from the G1 phase into the DNA synthesis phase, they must express PCNA for DNA synthesis to properly occur. In liver, the results suggested that PCNA was negatively regulated (Figure 4.22). Both protein and mRNA levels were significantly decreased in response to dehydration; this complements the data that suggests that E2F1-mediated gene expression is suppressed. This result, along with results for liver Rb/E2F analysis supports the hypothesis that dehydration is inducing cell cycle arrest in liver in the G1 phase. However, muscle PCNA protein levels increased in response to dehydration, while transcript levels remained constant (Figure 4.22). As a downstream target of E2F1, this result in muscle conflicts with the findings that E2F1 activity is suppressed during dehydration exposure. While the results in liver continue to suggest that G1 cell cycle arrest is occurring under dehydration stress, cell cycle machinery does not appear to be tightly regulated in skeletal muscle.

4.4.8 Conclusion

In response to dehydration stress, liver E2F1 activity is reduced so that expression of genes (like PCNA) that are required for cell cycle progression past the G1 stage is suppressed. E2F1 is suppressed by activation (or hypophosphorylation) of Rb which allows Rb to bind to E2F1 and halt its transcriptional activity. This decrease in phosphorylation of Rb is mediated by negatively regulating cyclin D, which is potentially

facilitated by GSK-3β (GSK-3β is studied in Chapter 3). Although total CDK levels remain constant, localization of CDK4 into the cytoplasm may facilitate E2F1 suppression in the dehydrating liver. Furthermore, suppression of CDK activity by decreases in cdc25a further facilitates liver G1 cell cycle arrest. Suppression of liver CDKs during dehydration exposure is also conducted by Akt-regulated p21 and p27, which were studied in Chapter 3. In skeletal muscle, data trends suggest that G1-stage cell cycle arrest is not occurring in response to dehydration. The mechanisms observed in the dehydrating frog liver are therefore organ-specific. The dehydrating African clawed frog has dehydration-induced molecular mechanisms to facilitate cell cycle arrest in the G1 phase in liver. These mechanisms which were evident in liver, were not found in skeletal muscle, which reflects the generally observed non-dividing senescent state of skeletal muscle in mature vertebrates.

CHAPTER 5

GENERAL DISCUSSION

The dehydrating African clawed frog, *Xenopus laevis*, is one of the animal models we are interested in understanding for its capabilities of tolerating environmental stresses. Our research group has become focused on the phenomenon of metabolic depression – a survival strategy that our animal models use to increase their chances of survival throughout tough environmental conditions. Among other species, our group studies anoxia-tolerant vertebrates, mammals which survive extended periods of cold, and amphibians which are tolerant to freezing and dehydration. In the lab, we are able to elucidate the molecular mechanisms by which these animals facilitate this phenomenon that allows them to survive stresses that would normally be fatal to other animals. Studies have led us to identify various energy-expensive cellular processes which are regulated under these stresses to facilitate metabolic depression.

From the enzyme to pathway level, glucose metabolism is regulated to promote survival of certain animals under stress (Lama *et al*., 2013; Wu *et al*., 2013). Animals undergoing anoxia and dehydration have been shown to shut down the majority of genes while selectively regulating transcriptional activity, which may play key roles in expressing key genes for survival – for example, antioxidant enzymes (Krivoruchko and Storey, 2013; Malik and Storey, 2011). Mammalian hibernators have been shown to shut down protein translation machinery as a means to facilitate metabolic depression (Wu and Storey, 2012). Well conserved kinase pathways (like Akt/Protein kinase B) have been studied in various models from hibernating bats and squirrels to wood frogs and land snails (Zhang *et al*., 2013; Abnous *et al*., 2008; Ramnanan *et al*., 2007; Eddy and Storey, 2003). After years of accumulating data on these molecular pathways, we are slowly painting a big picture of the molecular systems taking place in these animals.

What we have found is that these animals, despite thriving in different environments and enduring different stresses, all regulate their pathways – in one way or another – to facilitate metabolic rate depression. As research continues, we continue to gain an understanding of the mechanisms by which these animals metabolic processes. However, as our understanding of individual pathways and mechanisms among various animal models increases, we are also able to take on a comparative approach and ask the following questions to further our understanding: What do animals which undergo metabolic depression have in common on a molecular level? How are their regulations of pathways different? For example, protein translation is a process that is suppressed in both mammals and intertebrates during metabolic depression in order to conserve energy. However, the mechanism by which protein translation is regulated appears to be different between invertebrates aestivators and mammalian hibernators (Ramnanan *et al*., 2007; Wu and Storey, 2012; Storey, 2012). The protein kinase B (or Akt) is suppressed to facilitate depression of protein translation in the thirteen-lined ground squirrel during periods of torpor (Wu and Storey, 2012). However, in the invertebrate aestivator, whose protein translation processes are also depressed during periods of metabolic depression, Akt activity has been shown to be promoted (Ramnanan *et al*., 2007).

By studying key metabolic pathways in the estivating vertebrate African clawed frog, I was able to touch on both these focuses in our research. On one end, studying kinase processes that regulate energy expensive processes like protein translation and the cell cycle will help further our understanding in an aquatic vertebrate that withstands high levels of dehydration. Furthermore, since my present research is conducted in a lower vertebrate that undergoes metabolic depression, I will be able to compare the similarities

and differences that occur between invertebrate and higher vertebrate models of metabolic rate depression.

5.1 Akt/Protein Kinase B in the dehydrating African clawed frog

Previous studies have analyzed how Akt is regulated under response to different environmental stresses in various animal models. Study of Akt in estivating land snails suggested an increase in activity during periods of metabolic rate depression. This was correlated with increases in Akt phosphorylation sites that are characterized to regulate Akt activity (Ramnanan *et al*.,, 2007). In mammalian models, Akt suppression appeared to play a role in the suppression of protein translation. Results have suggested that suppression of Akt in the hibernating ground squirrel facilitated the shutting down of protein translation machinery via the Akt/TSC2/mTOR pathway (Wu and Storey, 2012). Knowing that it has differing roles in invertebrates and higher vertebrates, I wanted to know its role in a lower vertebrate. In this thesis, I explored the roles of Akt and its downstream targets to further understand its roles in facilitating a lower vertebrate's survival in periods of metabolic rate depression. I aimed to further understand what role this central kinase played in a dehydrating lower vertebrate specifically; in addition to furthering knowledge on the role Akt plays in facilitating metabolic rate depression in general.

Table 5.1. A summary of the results in Chapter 3 which suggest that Akt may play a role in suppressing protein translation and cell cycle in the dehydrating African clawed frog.

Target	Apparent effect under dehydration stress
Akt kinase ✓	Suppressed
GSK-3β kinase ✗	Not regulated by Akt under dehydration
Cell cycle inhibitors p21 and p27 ✓	De-phosphorylation
FoxO transcription factors ✗	Not regulated by Akt under dehydration
TSC1/TSC2	**TSC2 role to be determined**
mTOR	No change in phosphorylation state
Raptor	No change in phosphorylation state
PRAS40 ✓	PRAS40 is signalled to suppress mTORC1
P70 kinase (mTORC1 downstream target) ✓	Suppressed
4EBP (mTORC1 downstream target) ✓	Suppressed

According to my results, Akt in the estivating African clawed frog, *X. laevis*, is regulated similarly to higher vertebrates. Like in the hibernating squirrel, the dehydrating frog suppresses Akt activity when faced with an extreme environmental stress. However, my results have shown that there are disconnects in the frog's Akt pathway when compared to mammals. Regardless of these differences, Akt still played a pivotal role in inducing suppression of protein translation in the dehydrating frog. In the hibernating squirrel, it was observed that Akt suppression ultimately suppressed protein translation by acting in the traditional Akt/TSC2/mTOR pathway and resulted in suppression of mTOR phosphorylation during late torpor (Wu and Storey, 2012). In chapter 3, I have shown

that not only is this the case, but that TSC2 is not a well conserved protein in the *X. laevis* proteome (Table 3.4). However, I have discovered that PRAS40 is strongly regulated by Akt during dehydration, and acts to prevent formation of the active mTORC1 complex (Figures 3.7 and 3.8). The proline-rich Akt substrate of 40 kDa (PRAS40) was discovered in mammalian animal models long before it was studied in animals under environmental stresses, and was shown to play a key role in regulating mTORC1 complex formation and activation. However, results from Wu and Storey in 2012 demonstrated that PRAS40 was not regulated throughout the torpor-arousal cycle of the hibernating squirrel, and concluded that Akt facilitated suppression of protein translation by acting via the Akt/TSC2/mTOR pathway. In my lower vertebrate estivator, control of protein translation via the Akt/TSC2/mTOR pathway was not studied as there was poor conservation of the *Tsc2* gene in *X. laevis*. Regardless, the African clawed frog adapted by developing Akt-dependent regulation of PRAS40. My results in chapter 3 support this hypothesis as the phosphorylation state of mTOR on serine 2448 and Raptor (mTOR Complex 1 member) on serine 863 did not fully suggest mTORC1 deactivation. However, PRAS40 was shown to be activated by decreasing in phosphorylation on threonine 246, and mTORC1 substrate phosphorylation was found to decrease throughout dehydration exposure (Figures 3.7 – 3.10). Ultimately, these results do more than just show us the mechanism by which Akt works in the dehydrating frog. It first shows that the lower vertebrate estivator is similar to the higher mammalian vertebrate hibernator as it relies on Akt to facilitate metabolic rate depression by suppressing protein translation. Furthermore, although Akt in both these animals act to suppress protein translation, the squirrel does this by targeting TSC2 which results in a decrease in mTOR

phosphorylation (Wu and Storey, 2012). However, Akt in frog may not act by this pathway as the TSC2 residue target by Akt is not conserved (threonine 1462) in the *X. laevis* proteome. Since Akt cannot signal for modification of mTOR or Raptor itself, it activates an inhibitor of the mTORC1 complex during dehydration exposure to suppress mTORC1 kinase action. The results from Chapter 3 does not only show how the lower vertebrate estivator facilitates metabolic depression on a molecular level, but also offers a comparison of similarities and differences between the mechanisms used by invertebrates and higher vertebrates.

One target of note is GSK-3β, which has been previously shown in previous animal models to regulate glucose metabolism in metabolic rate depression. In the introduction of this thesis, I hypothesized that GSK-3β is regulated by Akt, it may play roles in glucose metabolism as a mechanism of energy conservation. However, my results did not demonstrate that GSK-3β was under Akt control in dehydration conditions. This was a surprise as this glucose-regulating enzyme was found to play roles in the freezing wood frog (Dieni *et al*., 2012). However, I soon discovered that GSK-3β may play a role in regulating levels of cyclin D. In Chapter 4, I discussed the potential roles that GSK-3β play be playing to regulate cyclin D levels as the cell cycle is arresting at the G1 phase. It involves GSK-3β targeting excess cyclin D for rapid degradation by proteasomes and further shows the variety of mechanisms in play between species to facilitate the common goal of achieving metabolic rate depression.

5.2 Cell cycle control in the dehydrating African clawed frog

Cell cycle arrest is a mechanism which various animal models employ to conserve energy and improve their chances of survival during periods of metabolic rate depression. In Chapter 3, Akt substrates p21 and p27 were studied, and were shown to be activated during dehydration stress. Akt phosphorylates p21 and p27 on threonine 145 and serine 187 to inhibit their action. In the dehydrating African clawed frog, p21 and p27 were found to be activated via Akt suppression (Figures 3.11 and 3.12). While activated, the roles of p21 and p27 are to inhibit cyclin/CDK complexes, which act to facilitate cell cycle progression (Figure 4.1). If active p21 and p27 are present during dehydration exposure, cyclin/CDK complexes would be inhibited, and as a result, the cell cycle would be arrested. Theoretically, inhibition of cyclin/CDK complexes via p21 and p27 activation is enough to suppress the cell cycle. However, the cell cycle is complex, and the mechanisms by which it is controlled during metabolic rate depression warrants further understanding. Chapter 3 revealed that Akt plays a role in arresting the cell cycle during dehydraion exposure as mode of facilitatin metabolic rate depression. The results in Chapter 4 of my thesis suggest that the African clawed frog does bear mechanisms to facilitate cell cycle arrest in addition to p21 and p27 regulation. However, unlike protein translation which was found to be suppressed in both liver and skeletal muscle, cell cycle arrest mechanisms were found to be organ-specific, well conserved in the proliferative liver, and poorly conserved in skeletal muscle.

Table 5.2. A summary of the results from Chapter 4 suggest that, in contrast to muscle, liver cell cycle is actively arrested in the frog in response to dehydration.

Target	Apparent effect under dehydration stress	Implication in dehydrating frog
E2F1, E2F4	E2F1 suppressed, E2F4 increase	G1-stage cell cycle arrest
Rb (retinoblastoma protein)	Rb is acetylated and de-phosphorylated in liver	G1-stage cell cycle arrest in liver
Cyclin proteins	General down-regulation, observed increase of cyclin D in medium dehydration in liver	G1-stage cell cycle arrest in liver
Cyclin-dependent kinases (CDK)	Negative regulation	Regulation of cyclins suppresses CDK activity
Positive cell cycle regulators cdc25a and cdc25c	Selective negative regulation of cdc25a in liver	G1-stage cell cycle arrest in liver
PCNA: Direct downstream target of E2F1	Suppression of PCNA protein and mRNA levels in liver	G1-stage cell cycle arrest in liver

Cell cycle arrest is regulated in the African clawed frog in various levels including post-translational modifications of key proteins, changes to gene expression by transcription factor regulation, localization of proteins (from transcription factors to kinases). Previous studies have shown that the mammalian hibernator regulates CDK inhibitors including p21, but also p15 (Wu and Storey, 2012 b). These CDK inhibitors prevent cyclin/CDK complexes from phosphorylating retinoblastoma protein (pRb), which is required for E2F1-mediated expression of genes required for cell cycle progression (Figure 4.1). In addition to CDKs, I also studied the levels and localization of the cyclin proteins – which are required for CDK action (Figure Reference). Positive regulators of the cell cyclin (phosphatase family cdc25) has been shown in Chapter 4 to

facilitate CDK action on pRb by removing inhibitory phosphate groups on certain CDK amino acid residues. Similarly to the freezing wood frog, the dehydrating African clawed frog also regulates cyclin protein and cdc25 phosphatase activity in order to facilitate cell cycle arrest. These studies which allow us to draw comparisons of mechanisms which facilitate cell cycle arrest between different animal models shed light on how two animal models which are attaining the same goal (metabolic rate depression whether by cell cycle arrest or suppression of protein translation), with the same machinery (pathways are conserved: cyclin/CDK, cdc25, p21/p27, E2F/Rb for cell cycle or Akt/mTOR for protein translation). When there are differences in attaining metabolic rate depression, it is not that the machinery/pathways are different, but the mechanism by which these pathways are regulated. In section 5.1, we observed that protein translation is regulated differently between mammals (via TSC2), invertebrates (Akt-independent manner) and lower vertebrates (dependence of PRAS40). In studying cell cycle regulation in the African clawed frog, I have shown that the mechanisms by which cell cycle arrest occurs are quite conserved to other animals previously studied (ie. The freezing frog and the hibernating squirrel).

Another focus in Chapter 4 was the study of the E2F/Rb complex. As explained in Chapter 4, E2F1 is a transcription factor that promotes cell cycle activity by expressing genes required for the progression past the G1 stage. It ties in with the cyclin, CDK, p21/p27 and cdc25a data which suggests that all of these components are being regulated to facilitate cell cycle arrest in the G1 stage. All four of those groups – cyclins, CDKs, CDK inhibitors, and CDK phosphatases all ultimately regulate pRb in order to control E2F1 activity. In addition to the outlying theme that Chapter 3 states – post-translational

modifications play a key role in facilitating metabolic rate depression over many species – the study of E2F/Rb states another – that transcriptional control is tightly regulated. Our group has demonstrated that transcriptional regulation is highly suppressed as a means of conserving energy – in addition to suppression of protein translation and cell cycle control. However, over the years we have identified certain transcriptional pathways which play key roles in aiding the animal through its bout with environmental stress. These roles played by key transcription factors range from producing antioxidant enzymes to providing crucial structural support to certain organs (Tessier and Storey, 2012; Malik and Storey, 2011; Krivoruchko and Storey, 2013; Krivoruchko and Storey, 2010). In Chapter 4, I have shown that cell cycle activating E2F members are negatively regulated (primarily by hypophosphorylated pRb) and inhibitory E2F members play a role in suppressing expression of genes required for cell cycle progression. This continues to demonstrate that gene transcription plays a key role in facilitating metabolic rate depression – whether the genes transcribed play roles in structural support, antioxidant support, or cell cycle regulation.

As previously stated, it is important to note that the regulation of pathways can be organ-specific. In section 5.1, it was discussed that protein translation suppression occurred in both liver and skeletal muscle tissues. However, cell cycle regulation in the African clawed frog appears to only be significant in the liver, and not the muscle. This is because the liver is a proliferative tissue. In active states, the liver is responsible for detoxification, among many other functions. By regularly encountering compounds which may cause cell damage, it is important for the liver to continually replace its cells. As a result, the liver is an important target for inducing cell cycle arrest when dropping

metabolic rates. On the contrary, muscle cells proliferate to a certain point, but eventually reach maturity and enter a state of senescence where cell division stops. Metabolic processes in muscle cells continue in order to provide energy and to grow (but not proliferate). This is why in Chapter 3, protein translation is well regulated in muscle, but the mechanisms for cell cycle arrest are not. In control conditions, the adult African clawed frog has halted cell proliferation in the muscle, and has limited muscle processes to growth. However, both protein translation and cell cycle of the liver are actively suppressed during periods of metabolic rate depression.

This thesis has shed light on the similarities and the differences of the strategies different animals use to attain a mutual goal – metabolic rate depression. My results have continue to demonstrate that in some processes, the pathways are regulated differently (although the same goal is attained), and in other cases, the pathways are regulated very similarly. In addition, it is important to note that these pathway regulations are also tissue specific. Since muscle cells have stopped dividing on their own, it would not make sense for the animal to actively spend energy to turn off further cell cycle switches – even cell cycle was already arrested. Between these different animal models that survive environmental stresses, there are differences that lie in the molecular mechanisms, but they are able to achieve a common goal when required by stressors.

5.3 Summary

The present study includes further understanding a number of focuses in the dehydrating African clawed frog. Firstly, the importance of post-translational

modifications and their roles in facilitating suppression of protein translation and the cell cycle. Phosphorylation (and acetylation in the case of pRb), regulated by different kinases (Akt, GSK-3β, mTOR, CDKs, etc.) play a crucial role in facilitating metabolic rate depression in animal models that encounter severe environmental stresses. Secondly, the suppression of translation by tight control of transcription factors offers another method of energy conservation. Third, although most of the machinery (kinase and transcription factor pathways, protein translation and cell cycle machinery) is conserved throughout different animal models that undergo bouts with extreme stress, the method by which these pathways are regulated can be different or similar. However, even if the mechanism of regulation differs between animals, the end goal is still achieved (facilitation of strategies to cope with stress). Ultimately, protein translation and the cell cycle appear to play key roles in the survival of the dehydrating African clawed frog.

5.4 Future directions

This thesis provided a study which provides insight into the roles of phosphorylation mediated by the central kinase Akt, and means of cell cycle regulation by both transcriptional control and post-translational modifications by E2F/Rb and cyclin/CDKs. I have shown that Akt regulates protein translation in both proliferative and non-proliferative tissues. On the contrary, cell cycle arrest is only actively regulated in proliferative liver tissue, but not in muscle. However, there is work to further strengthen these theories.

In Chapter 3, I claimed that unlike in invertebrates and higher vertebrates (mammals), protein translation was suppressed by PRAS40. When active, PRAS40 binds

to members of mTORC1 so that the full complex cannot assemble and act as an active kinase. To support this claim, I studied the downstream substrates of the mTORC1 complex. As I suggested that mTORC1 had dissociated (inactivated), the phosphorylation state of mTORC1 substrates had also decreased. However, in order to provide stronger conclusive evidence, a co-immunoprecipitation experiment should be performed. According to my work in Chapter 3, one can hypothesize that such an experiment would demonstrate that mTORC1 is as a whole complex under control conditions, and would be dissociated under stress conditions. Furthermore, a second co-immunoprecipitation experiment could be performed to observe if PRAS40 is physically interacting with mTORC1 subunits (ie. mTOR, Raptor).

In Chapter 4, my results suggested that pRb was activated to suppress E2F1 from facilitating cell cycle arrest. This was possible as a result of decreased CDK activity which resulted from localization of cyclin and CDKs out of the nucleus, cyclin degradation, regulation of inhibitory phosphorylation, and CDK inhibitors. Similarly for the work done in Chapter 3, there is more work that can be done to bolster the arguments made in the discussions of this thesis. Firstly, there are other targets that regulate the cell cycle which have yet to be studied. Although this study looked at both negative (p21 and p27) regulators of the cell cycle, in addition to positive regulators (cdc25a and cdc25c), there is p15/p16 which is also well characterized to regulating CDK activity. Furthermore, the upstream regulators of cdc25 (Chk1 and Chk2) have not been studied – but nevertheless have the potential to be crucially regulated as the African clawed frog encounters dehydration. I proposed that GSK-3β may be playing a role in regulating cyclin D protein levels during cell cycle arrest. However, the GSK-3β/Cyclin

D/proteasome pathway is regulated by myostatin. Myostatin is therefore a target which warrants further investigation in both liver and muscle. Although myostatin is well established as a regulator of muscle proliferation, it has recently been shown to also be expressed in liver tissue (Jiao *et al*., 2010). Similarly to the co-immunoprecipitation experiments that could be performed for Chapter 3, one can perform the same experiments to add to the research done in Chapter 4. In this thesis, phosphorylation state was used to assume the state of pRb – as to whether it was bound to E2F1 or not. However, just because a protein is phosphorylated, one cannot be completely sure that it is binding to E2F1. To be certain, a co-immunoprecipitation experiment should be performed to see if E2F/Rb complex formation is decreasing over dehydration exposure. This also applies for the cyclin/CDK complexes. Although the appropriate cyclin and CDK complexes are localized away from their usual location of action, and although there is an increase in active CDK inhibitors (p21 and p27), and a decrease in CDK activators (cdc25a), the association and dissociation of the cyclin/CDK complex itself is another mode of regulation that warrants study. This is possible with co-immunoprecipitation experiments. Lastly, chromatin immunoprecipitation experiments will deepen our understanding of the E2F transcription factors (both E2F1 and E2F4). By performing chromatin immunoprecipitation experiments on these DNA-interacting proteins, we can further understand which genes specifically are being inhibited during dehydration exposure.

REFERENCES

Acevedo, N., Ding, J., and Smith, G.D. Insulin signaling in mouse oocytes. 2007. Biology of reproduction. 77, 872-879.

Altomare, D.A., Khaled, A.R. 2012. Homeostasis and the importance for a balance between Akt/mTOR activity and intracellular signaling. Curr Med Chem. 19, 3748-3762.

Araujo, J., Breuer, P,. Dieringer, S., Krauss, S., Dorn, S., Zimmermann, K., Pfeifer, A., Klockgether, T., Wuellner, U., and Evert, B.O. 2011. Foxo4-dependent upregulation of superoxide dismutase-2 in response to oxidative stress is impaired in spinocerebellar ataxia type 3. Human Mol Genetics. 20(15) 2928-2941.

Biggar, K.K., Storey, K.B. 2012. Evidence for cell cycle suppression and microRNA regulation of cyclin D1 during anoxia exposure in turtles. Cell cycle. 11(9), 1705-1713.

Botz, J., Zerfass-thome, K., Spitkovsky, D., Delius, H., Vogt, B., Eilers, M., Hatzigeorgiou, A., and Jansen-durr, P. 1996. Cell cycle regulation of the murine cyclin E gene depends on an E2F binding site in the promoter. Mol and Cell Biol. 16(7), 3401-3409.

Brantley, M.A. and Harbour, J.W. 2000. Inactivation of retinoblastoma protein in uveal melanoma by phosphorylation of sites in the COOH-Terminal region. Cancer Res. 60, 4320-4323.

Burke, J.R., Deshong, A.J., Pelton, J.G., and Rubin, S.M. 2010. Phosphorylation-induced conformational changes in the retinoblastoma protein inhibit E2F transactivation domain binding. J Biol Chem. 285, 16286-16293.

Caccamo, A., Maldonado, M.A., Majumder, S., Medina, D.X., Holbein, W., Magri, A., and Oddo, S. 2011. Naturally secreted amyloid-B increases mammalian target of rapamycin (mTOR) activity via a PRAS40-mediated mechanism. J Biol Chem. 286(11), 8924-8932.

Cai, G., Wang, J., Xin, X., Ke, Z., and Luo, J. 2007. Phosphorylation of glycogen synthase kinase-3 B at serine 9 confers cisplatin resistance in overian cancer cells. Int J of Oncology. 31, 657-662.

Carvalho, J. E., Navas, C. A. and Pereira, I. C. (2010). Energy and water in aestivating amphibians. Prog. Mol. Subcell. Biol. 49, 141-169.

Cowan, K.J., Storey, K.B. 2003. Mitogen-activated protein kinases: new signaling pathways functioning in cellular responses to environmental stress. J Exp Biol. 206(7), 1107-1115.

Cross, D.A.E., Alessi, D.R., Cohen, P., Andjelkovich, M., and Hemmings, B.A. 1995. Inhibition of glycogen synthase kinase-3 by insulin mediated by protein kinase B. Nature. 378, 785-789.

Dann, S.G., Selvaraj, A., Thomas, G. 2007. mTOR complex1-s6k1 signaling: at the crossroads of obesity, diabetes and cancer. Trends Mol Med. 13(6), 252-9.

Diehl, J.A., Zindy, F., and Sherr, C.J. 1997. Inhibition of cyclin D1 phosphorylation on threonine-286 prevents its rapid degradation via the ubiquitin proteasome pathway. Genes Dev. 11, 957-972.

Egelkrout, E.M., Mariconti, L., Settlage, S.B., Cella, R., Robertson, D., and Hanley-Bowdoin, L. 2002. Two E2F elements regulate the proliferating cell nuclear antigen promoter differently during leaf development. Plant Cell. 14, 3225-3236.

Foster, K.G., Acosta-Jaquez H.A., Romeo, Y., Ekim, B., Soliman, G.A., Carriere, A., Roux, P.P, Ballif, B.A., and Fingar, D.C. 2009. Regulation of mTOR complex 1 by raptor ser863 and multisite phosphorylation. J Biol Chem. 285(1) 80-94.

Funk, J.O., Waga, S., Harry, J.B., Espling, E., Stillman, B., and Galloway, D.A. 1997. Inhibition of CDK activity and PCNA-dependent DNA replication by p21 is blocked by interaction with the HPV-16 E7 oncoprotein. Genes Dev. 11, 2090-2100.

Gao, N., Flynn, D.C., Zhang, Z., Zhong, X., Walker, V., Liu, K.J., Shi, X., and Jiang, B. 2004. G1 cell cycle progression and the expression of G1 cyclins are regulated by PI3K/Akt/mTOR/p70S6K1 signaling in human ovarian cancer cells. Am J Physiol Cell Physiol. 287, 281-291.

Glida, J.E., and Gomes, A.V. 2013. Stain-free total protein staining is a superior loading control to B-actin for Western blots. Anal. Biochem. 440: 186-88.

Greenway, S.C., and Storey, K.B. 2000a. Mitogen-activated protein kinases and anoxia tolerance in turtles. J Exp Zool. 287(7): 477-484.

Greenway, S.C., Storey, K.B. 2000b. Activation of mitogen-activated protein kinases during natural freezing and thawing in the wood frog. Mol Cell Biochem. 209(1-2): 29-37.

Grundy, J.E., Storey, K.B. 1994. Urea and salt effects on enzymes from estivating and non-estivating amphibians. Mol Cell Biochem. 131(1), 9-17.

Haar, E.V., Lee, S. Bandhakavi, S., Griffin, T.J., and Kim, D. 2007. Insulin signalling to mTOR mediated by the Akt/PKB substrate PRAS40. Nat Cell Biol. 9(3), 316-323.

Halaban, R. 2005. Rb/E2F: A two-edged sword in the melanocytic system. Cancer and Metastasis Reviews. 24, 339-356.

Henglein, B., Chenivesse, X., Wang, J., Eick, D., and Berchot, C. 1994. Structure and cell cycle regulated transcription of the human cyclin A gene. Proc Natl Acad Sci Usa. 91, 5490-5494.

Hermes-Lima, M., Storey, K.B. 1993a. Antioxidant defenses in the tolerance of freezing and anoxia by garter snakes. Am J Physiol. 265(3), 646-652.

Hermes-Lima, M., Storey, K.B. 1993b. In vitro oxidative inactivation of glutathione S-transferase from a freeze tolerant reptile. Mol Cell Biochem. 124(2), 149-158.

Hillman S. 1978. The roles of oxygen delivery and electrolyte levels in the dehydrational death of Xenopus laevis. J Comp Physiol. 128: 169-175.

Hillman S. 1980. Physiological correlates of differential dehydration tolerance in anuran amphibians. Copeia 1980: 125-129.

Hillman S. 1987. Dehydrational effects on cardiovascular and metabolic capacities in anuran amphibians. Physiol Zool. 60:608-613.

Hofler, A., Nichols, T., Grant, S., Lingardo, L., Esposito, E.A., Gridley, S., Murphy, S.T., Kath, J.C., Cronin, C.N., Kraus, M., Alton, G., Xie, Z., Sutton, S., Gehring, M., Ermolieff, J. 2011. Study of the PDK1/Akt signaling pathway using selective PDK1 inhibitors, HCS, and enhanced biochemical assays. Anal Biochem. 414, 179-186.

Huang, S., Chen, C.S., Ingber, D.E. 1998. Control of cyclin D1, p27, and cell cycle progression in human capillary endothelial cells by cell shape and cytoskeletal tension. Mol Biol of the Cell. 9, 3179-3193.

Inoki, K., Li, Y., Xu, T., Guan, K. 2003. Rheb GTPase is a direct target of TSC2 GAP activity and regulates mTOR signaling. Genes Dev. 17, 1829-1834.

Jiao, T., Yuan, T., Zhou, Y., Xie, W., Zhao, Y., Zhao, J., Ouyang, H., and Pang, D. 2011. Analysis of myostatin and its related factors in various porcine tissues. J Animal Sci. 89, 3099-3106.

Jin, J., Ang, X.L., Ye, X., Livingstone, M., and Harper, J.W. 2008. Differential roles for checkpoint kinases in DNA damage-dependent degradation of the cdc25a protein phosphatase. J Biol Chem. 283, 19322-19328.

Joanisse, D., Storey, K. 1996. Oxidative stress and antioxidants in overwintering larvae of cold-hardy goldenrod gall insects. J Exp Biol. 199(7), 1483-1491.

Kim, D., Sarbassov, D.D., Ali, S.M., Latek, R.R., Guntur, K.V.P., Erdjument-bromage, H., Tempst, P., and Sabatini, D.M. 2003. GBL, a positive regulator of the rapamycin-sensitive pathway required for the nutrient sensitive interaction between raptor and mTOR. Molecular Cell. 11, 895-904.

Krivoruchko, A., and Storey, K.B. 2013. Anoxia-responsive regulation of the FoxO transcription factors in freshwater turtles, Trachemys scripta elegans. Biochimica et Biophysica Acta. In press.

Kubrak, O.I., Lushchak, O.V., Lushchak, J.V., Torous, I.M., Storey, J.M., Storey, K.B., Lushchak, V.I. 2010. Chromium effects on free radical processes in goldfish tissues: comparison of Cr(III) and Cr(VI) exposures on oxidative stress markers, glutathione status and antioxidant enzymes. Comp Biochem PHysiol C Toxicol Pharmacol. 152(3), 360-370.

Lama, Judeh, L., Bell, R.A.V., and Storey, K.B. 2013. Hexokinase regulation in the hepatopancreas and foot muscle of the anoxia-tolerant marine mollusc, Littorina littorea. Comp Bioc and Physiol B. In press.

Larade, K., Storey, K.B. 2006. Analysis of signal transduction pathways during anoxia exposure in a marine snail: a role for p38 MAP kinase and downstream signaling cascades. Comp Biochem Physiol B Biochim Mol Biol. 143(1), 85-91.

Li, M., Yin, S., Yuan, J., Wei, L., Ai, J., Hou, Y., Chen, D., and Sun, Q. 2008. Cdc25A promotes G2/M transition in oocytes. Cell cycle. 7(9), 1301-1302.

Li, Y., Zhang, D., Ren, Q., Ye, F., Zhao, X., Daniels, G., Wu, X., Dynlacht, B., and Lee, P. 2012. Regulation of a novel androgen receptor target gene, the cyclin B1 gene, through androgen-dependent E2F family member switching. Mol Cell Biol. 32(13), 2454-2466.

Lopez-Bonet, E., Vazquez-Martin, A., Perez-Martinez, M.C., Oliveras, Ferraros, C., Perez-Bueno, F., Bernado, L., and Menendez, J.A. 2009. Serine 2481-autophosphorylation of mammalian target of rapamycin (mTOR) couples with chromosome condensation and segregation during mitosis: Confocal microscopy characterization and immunohistochemical validation of PP-mTOR serine 2481

as a novel high-contrast mitosis marker in breast cancer core biopsies. Int J of Oncol. 36, 107-115.

Macdonald, J.A., Storey, K.B. 2005a. Temperature and phosphate effects on allosteric phenomena of phosphofructokinase from a hibernating ground squirrel. FEBS J. 272(1), 120-128.

Macdonald, J.A., Storey, K.B. 2005b. Mitogen-activated protein kinases and selected downstream targets display organ-specific responses in the hibernating ground squirrel. Int J Biochem Cell Biol. 37(3), 679-691.

Malik, A. I., Storey, K.B. 2009. Activation of antioxidant defense during dehydration stress in the African clawed frog. Gene. 442(1-2), 99-107.

Malik, A. I., Storey, K.B. 2009. Activation of extracellular signal-regulated kinases during dehydration in the African clawed frog, Xenopus laevis. J Exp Biol. 212(16), 2595-2603.

Malik, A. I., Storey, K.B. 2011. Transcriptional regulation of antioxidant enzymes by FoxO1 under dehydration stress. Gene. 485(2), 114-119.

Mamady, H., Storey, K.B. 2006. Up-regulation of the endoplasmic reticulum molecular chaperone GRP78 during hibernation in thirteen-lined ground squirrels. Mol Cell Biochem. 292(1-2), 89-98.

McMullen DC, Hallenbeck JM. 2010. Regulation of Akt during torpor in the hibernating ground squirrel, Ictidomys tridecemlineatus. J Comp Physiol B. 180: 927-934.

Munger, K., and Howler, P.M. 2002. Human papillomavirus immortalization and transformation functions. Virus research. 89, 213-229.

Obsil, T., Ghirlando, R., Anderson, D.E., Hickman, A.B., Dyda, F. 2003. Two 14-3-3 binding motifs are required for stable association of forkhead transacription factor FOXO4 with 14-3-3 proteins and inhibition of DNA binding. Biochemistry. 42, 15264-15272.

Ohtani, K., DeGregori, J., and Nevins, J.R. 1995. Regulation of the cyclin E gene by transcription factor E2F1. Proc Natl Acad Sci Usa. 92, 12145-12150.

Peck, B., Ferber, E.C., Schulze, A. 2013. Antagonism between Foxo and Myc regulates cellular powerhouse. Frontiers in oncology. 3, 96.

Peng, C., Graves, P.R., Ogg, S., Thoma, R.S., Byrnes, M.J., Wu, Z., Stephenson, M.T., and Piwnica-worms, H. 1998. C-tak1 protein kinase phosphorylates human

cdc25c on serine 216 and promotes 14-3-3 protein binding. Cell Grow and Diff. 9, 197-208.

Pickard, A., Wong, P., and McCance, D.J. 2010. Acetylation of Rb by PCAF is required for nuclear localization and keratinocyte differentiation. Journal of Cell Science. 123, 3718-3726.

Ramnanan, C.J., Groom A.G., and Storey, K.B. 2007. Akt and its downstream targets play key roles in mediating dormancy in land snails. Comp Bioc and Physiol B. 148, 245-255.

Ross, A.H., and Gericke, A. 2009. Phosphorylation keeps PTEN phosphatase closed for business. Proc Nat Acad Sci Usa. 106(5), 1297-1298.

Rother, K., Kirschener, R., Sanger, K., Bohlig, L., Mossner, J., and Engeland, K. 2007. p53 downregulates expression of the G1/S cell cycle phosphatase cdc25a. Oncogene. 26, 1949-1953.

Russo, A.J., Magro, P.G., Hu, Z., Li, W., Peters, R., Mandola, J., Banerjee, D., and Bertino, J.R. 2006. E2F-1 overexpression in U2OS cells increases cyclin B2 levels and cdc2 kinase activity and sensitizes cells to antimitotic agents. Cancer Res. 66(14), 7253-7260.

Sarbassov, D.D., Guertin, D.A., Ali, S.M., Sabatini, D.M. 2005. Phosphorylation and regulation of Akt/PKB by the Rictor-mTOR complex. Science. 307, 1098-1101.

Secor S.M., Lignot J.H. 2010. Morphological plasticity of vertebrate aestivation. Prog Mol Subcell Biol. 49:183-208. doi: 10.1007/978-3-642-02421-4_9. Review.

Stambolic, V., Suzuki, A., Lois de la Pompa, J., Brothers, G.M., Mirtsos, C., Sasaki, T., Ruland, J., Penninger, J.M., Siderovski, D.P., and Mak, T.W. 1998. Negative regulation of Pkb/Akt-dependent cell survival by the tumor suppressor PTEN. Cell. 95, 29-39.

Storey KB, Storey JM. 2004. Metabolic rate depression in animals: transcriptional and translational controls. Biol Rev Camb Philos Soc. 79: 207-233.

Storey KB, Storey JM. 2007. Putting life on 'pause'--molecular regulation of hypometabolism. J Exp Biol. 210: 1700-1714.

Storey, K.B. and Storey, J.M. 2010. Metabolic regulation and gene expression during aestivation. In: Aestivation: Molecular and Physiological Aspects (Navas, C.A. and Carvalho, J.E., eds), Progress in Molecular and Subcellular Biology, Springer, Heidelberg, Vol. 49, pp. 25-45. doi: 10.1007/978-3-642-02421-4_2

Storey, K.B., Storey, J.M. 2010. Metabolic regulation and gene expression during aestivation. Prog Mol Subcell Biol. 49: 25-45.

Storey, K.B., Storey, J.M. 2012. Aestivation: signaling and hypometabolism. J Exp Biol. 215(9), 1425-1433.

Tagliati, F., Chiara, M., Zatelli, C., Bottoni, A., Piccin, D., Luchin, A., Culler, M.D., and Uberti, E.C. 2006. Role of complex cyclin D1/Cdk4 in somatostatin subtype 2 receptor-mediated inhibition of cell proliferation on a medullary thyroid carcinoma cell line in vitro. Endocrinology. 147(7), 3530-3538.

Thacker, S.A., Bonnette, P.C., and Duronio, R.J. 2003. The contribution of E2F-regulated transcription to drosophila PCNA gene function. Curr Biol. 13, 53-58.

Thomas, N.S.B., Pizzey, A.R., Tiwari, S., Williams C.D., and Yang, J. 1998. p130, p107, and pRb are differentially regulated in proliferating cells and during cell cycle arrest by a-interferon. J Biol Chem. 273, 23659-23667.

Timmers, C., Sharma, N., Opavsky, R., Maiti, B., Wu, L., Wu, J., Orringer, D., Trikha, P., Saavedra, H.I., and Leone, G. 2007. E2F1, E2F2, and E2F3 control E2F target expression and cellular proliferation via a p53-dependent negative feedback loop. Mol and Cell Biol. 27(1), 65-78.

Tommasi, S., and Pfeifer, G.P. 1995. In vivo structure of the human cdc2 promoter: release of a p130-E2F4 complex from sequences immediately upstream of the transcription initiation site coincides with induction of cdc2 expression. Mol and Cell Biol. 15(12), 6901-6913.

Tomoo, K., Matsushita, Y., Fujisaki, H., Abiko, F., Shen, X., Taniguchi, T., Miyagawa, H., Kitamura, K., Miura, K., Ishida, T. 2005. Structural basis for mRNA cap-binding regulation of eukaryotic initiation factor 4E by 4E-binding protein, studied by spectroscopic, X-ray crystal structural, and molecular dynamics simulation methods. Biochemica et biophysica acta. 1753, 191-208.

Trendelenburg, A.U., Meyer, A., Rohner, D., Boyle, J., Hatakeyama, S., and Glass, D.J. 2009. Myostatin reduces Akt/Torc1/p70s6k signaling, inhibiting myoblast differentiation and myotube size. Am J Physiol Cell Physiol. 296, 1258-1270.

Tripathy, S., Jump, D.B. 2013. Elovl5 regulates the mTORC2-Akt-FoxO1 pathway by controlling hepatic cis-vaccenic acid synthesis in diet-induced obese mice. J Lipid Res. 54, 71-84.

Tyagi, A., Agarwal, C., and Agarwal, R. 2002. Inhibition of retinoblastoma protein (Rb) phosphorylation at serine sites and an increase in Rb-E2F complex formation by

silibinin in androgen-dependent human prostate carcinoma LNCaP cells: Role in prostate cancer prevention 1. Mol Cancer Ther. 1, 525-532.

Vadlakonda, L., Dash, A., Pasupuleti, M., Kumar, K.A., and Reddanna, P. 2013. The paradox of Akt-mTOR interactions. Frontiers in Oncology. 3, 165.

Vazquez-Martin, A., Oliveras-Ferraros, C., Bernado, L., Lopez-Bonet, E., Menendez, J.A. 2009. Biochem and Biophys Res Comm. 380, 638-643.

Willmore, W.G., Storey, K.B. 1997a. Glutathione systems and anoxia tolerance in turtles. Am J Physiol. 273(1), 219-225.

Willmore, W.G., Storey, K.B. 1997b. Antioxidant systems and anoxia tolerance in a freshwater turtle Trachemys scrapta elegans. Mol Cell Biochem. 170(1-2), 177-185.

Wilson, A.C. 2007. Setting the stage for S phase. Molecular Cell. 27, 176-177.

Wu, C., and Storey, K.B. 2012. Regulation of the mTOR signaling network in hibernating thirteen-lined ground squirrels. J of Exp Biol. 215, 1720-1727.

Wu, C., Biggar, K.K., and Storey, K.B. 2013. Biochemical adaptations of mammalian hibernation: exploring squirrels as a perspective model for naturally induced reversible insulin resistance. Braz J of Med and Biol Res. 46, 1-13.

Xu, N., Lao, Y., Zhang, Y., and Gillespie, D. 2012. Akt: A double-edged sword in cell proliferation and genome stability. J Oncology. Epub doi: 10.1155/2012/951724.

Yang, K., Guo, Y., Stacey, W.C., Harwalkar, J., Fretthold, J., Hitomi, M., and Stacey, D.W. 2006. Glycogen synthase kinase 3 has a limited role in cell cycle regulation of cyclin D1 levels. BMC cell biology. 7, 33.

Yang, W., Zhang, Y., Li, Y., Wu, Z., and Zhu, D. Myostatin induces cyclin D1 degradation to cause cell cycle arrest through a phosphatidylinositol 3-kinase/Akt/GSK-3B pathway and is antagonized by insulin-like growth factor 1. Journal of Biol Chem. 282(6), 3799-3808.

Yellen, P., Chatterjee, A., Preda, A., Foster, D.A. 2013. Inhibition of S6 kinase suppresses the apoptotic effect of eIF4E ablation by inducing TGF-B-dependent G1 cell cycle arrest. Cancer Letters. 333, 239-243.

Zhang, J., Storey, K.B. 2012. Cell cycle regulation in the freeze tolerant wood frog, Rana sylvatica. Cell cycle. 11(9), 1727-1742.

Zhang, J., Storey, K.B. 2013. Akt signaling and freezing survival in the wood frog, Rana sylvatica. Biochim Biophys Acta. 1830(10), 4828-4837.

Zhang, J., Tessier, S.N., and Storey, K.B. 2011. PI3K-Akt regulation as a molecular mechanism of the stress response during aerobic dormancy. Hypometabolism: Strategies of survival in vertebrates and invertebrates.

Zhang, X., Gan, L., Pan, H., Guo, S., He, X., Olson, S.T., Mesecar, A., Adam, S., Unterman, T.G. 2002. Phosphorylation of serine 256 suppresses transactivation by FKHR by multiple mechanisms. 277(47), 45276-45284.

Zhou, X., Tan, M., Stone-Hawthorne, V., Klos, K.S., Lan, K., Yang, Y., Yang, W., Smith, T.L., Shi, D., and Yu, D. 2004. Activation of the Akt/Mammalian target of rapamycin/4E-BP1 pathway by ErbB2 overexpression predicts tumor progression in breast cancers. Clin Cancer Res. 10, 6779-6788.

APPENDICES

Publications in preparation with data from this thesis:

Luu, B.E., Storey, K.B. Cell cycle arrest in response to dehydration in the estivating African clawed frog.

Luu, B.E., Storey, KB. Akt suppresses protein translation in the African clawed frog by activating PRAS40 which suppresses the mTORC1 complex in response to dehydration stress.

Communications at Scientific Meetings attended during this thesis:

Luu, B.E.* and Storey, K.B. Akt extinguishes energy expensive activities in the estivating African clawed frog. 1st International Conference on Oxidative Stress in Aquatic Ecosystems. Los Cabos, Mexico, (2012).

Luu, B.E.* and Storey, K.B. Akt extinguishes energy expensive activities in the estivating African clawed frog. Canada-China Systems Biology Conference (2012).

Luu, B.E.* and Storey, K.B. Role of myogenic regulatory factors in resistance to muscle disuse atrophy in anoxia tolerant turtles. Concordia University's 15th Chemistry and Biochemistry Conference (2011).

Luu, B.E.* and Storey, K.B. Role of myogenic regulatory factors in resistance to muscle disuse
atrophy in anoxia tolerant turtles. Canadian Society of Zoologists' Annual National Conference (2011).

Tessier, S.N.*, Luu, B.E. and Storey, K.B. Adaptations of cardiac muscle function during mammalian hibernation. Canadian Society of Zoologists' Annual National Conference (2011).

Luu, B.E.*, Tessier, S.N., and Storey, K.B.The role of the troponin-tropomyosin complex and dystrophin-related glycoproteins in the hibernating thirteen-lined ground squirrel.26th Annual meeting, Federação de Sociedades de Biologia Experimental (FeSBE), Rio de Janeiro, Brazil, (2011).

Scientific Meetings organized during this thesis:

Co-Chair, Ottawa-Carleton Institute of Biology 2013 symposium

Examples of full lanes in Western Blots

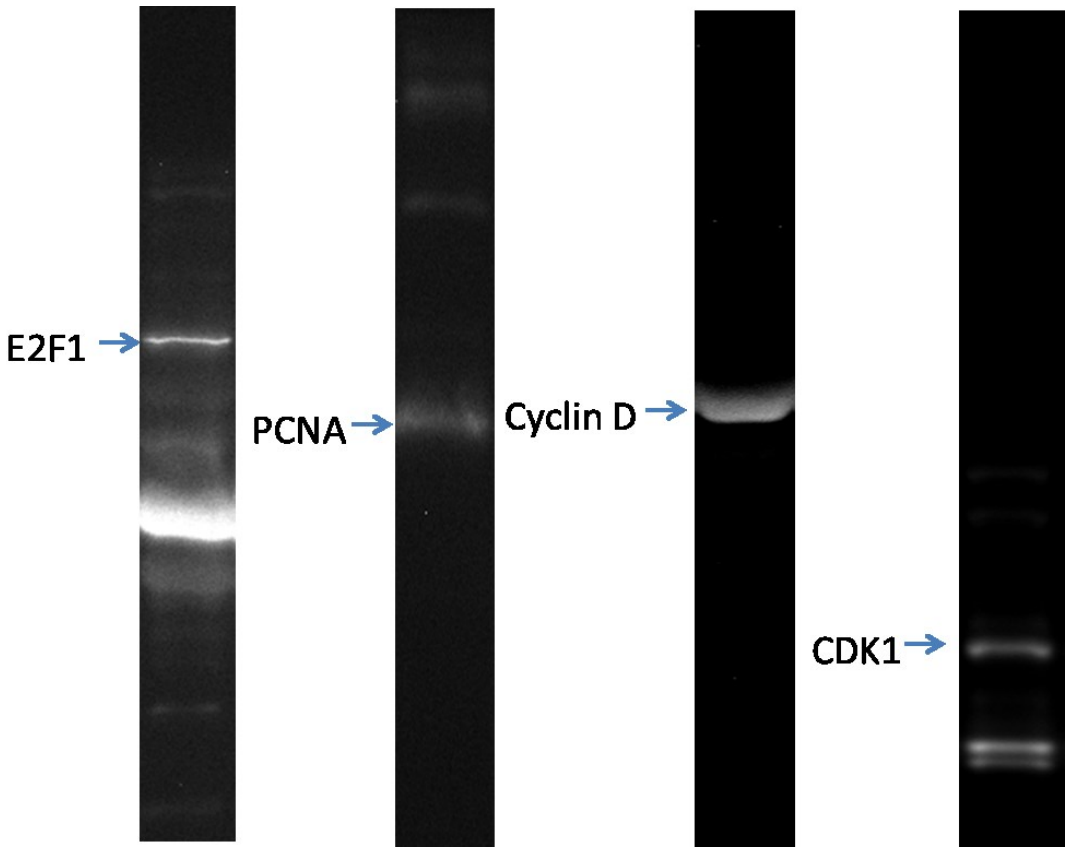

Western Blot Normalization Appendices

Analytical Biochemistry 440 (2013) 186–188

Contents lists available at SciVerse ScienceDirect

Analytical Biochemistry

journal homepage: www.elsevier.com/locate/yabio

Notes & Tips

Stain-Free total protein staining is a superior loading control to β-actin for Western blots

Jennifer E. Gilda [a], Aldrin V. Gomes [a,b,*]

[a] Department of Neurobiology, Physiology, and Behavior, University of California, Davis, CA 95616, USA
[b] Department of Physiology and Membrane Biology, University of California, Davis, CA 95616, USA

ARTICLE INFO

Article history:
Received 22 April 2013
Received in revised form 20 May 2013
Accepted 23 May 2013
Available online 6 June 2013

Keywords:
Stain Free
Ponceau S
β-Actin
Western blotting
Nitrocellulose

ABSTRACT

Semi-quantification of proteins using Western blots typically involves normalization against housekeeping genes such as β-actin. More recently, Ponceau S and Coomassie blue staining have both been shown to be suitable alternatives to housekeeping genes as loading controls. Stain-Free total protein staining offers the advantage of no staining or destaining steps. Evaluation of the use of Stain-Free staining as an alternative to β-actin or the protein stain Ponceau S showed that Stain-Free staining was superior to β-actin and as good as or better than Ponceau S staining as a loading control for Western blots.

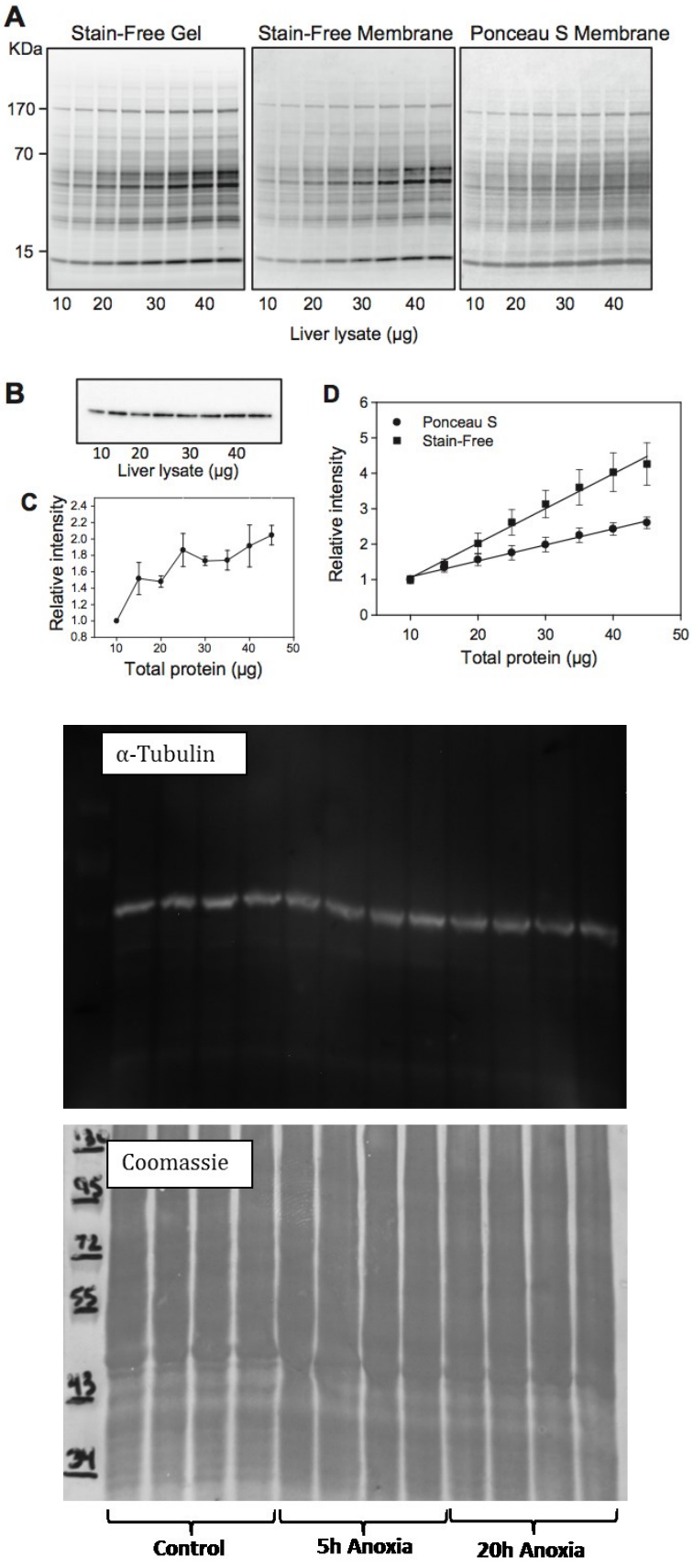
A
Stain-Free Gel
Stain-Free Membrane
Ponceau S Membrane
KDa
170
70
15
10 20 30 40
10 20 30 40
10 20 30 40
Liver lysate (µg)
B
10 20 30 40
Liver lysate (µg)
C
Relative intensity
Total protein (µg)
D
Ponceau S
Stain-Free
Relative intensity
Total protein (µg)
α-Tubulin
Coomassie
Control
5h Anoxia
20h Anoxia

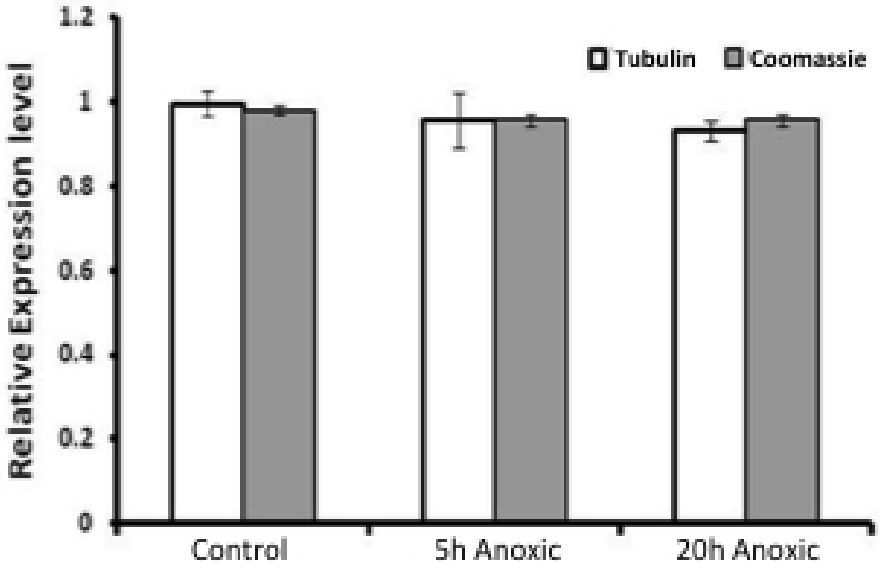

	Tubulin	Coomassie
Control vs. 20h Anoxic	0.563	0.291
Control vs. 5h Anoxic	0.133	0.200
20h Anoxic vs. 5h Anoxic	0.683	0.999

	Control	5h Anoxic	20h Anoxia
Tubulin vs. Coomassie	0.592	0.985	0.440